

Epigenetic Regulation of Reactive Oxygen Species-induced
Tumor Progression in Hepatocellular Carcinoma



A Dissertation Submitted in Partial Fulfillment of the Requirements
for the Degree of Doctor of Philosophy in Medical Biochemistry
Department of Biochemistry
FACULTY OF MEDICINE
Chulalongkorn University
Academic Year 2021
Copyright of Chulalongkorn University

การควบคุมเหนือระบบพันธุกรรมต่อการดำเนิน โรคมะเร็งตับที่ถูกกระตุ้น โดย
อนุพันธ์ออกซิเจนที่ว่องไว



วิทยานิพนธ์นี้เป็นส่วนหนึ่งของการศึกษาตามหลักสูตรปริญญาวิทยาศาสตรดุษฎีบัณฑิต
สาขาวิชาชีวเคมีทางการแพทย์ ภาควิชาชีวเคมี
คณะแพทยศาสตร์ จุฬาลงกรณ์มหาวิทยาลัย
ปีการศึกษา 2564
ลิขสิทธิ์ของจุฬาลงกรณ์มหาวิทยาลัย

สุดจิรา โพธิ์เย็น : การควบคุมเหนือระบบพันธุกรรมต่อการดำเนินโรคมะเร็งตับที่ถูกกระตุ้นโดย อนุพันธ์ออกซิเจนที่ว่องไว.
(Epigenetic Regulation of Reactive Oxygen Species-induced Tumor
Progression in Hepatocellular Carcinoma) อ.ที่ปรึกษาหลัก : ศศ. ดร.ชาอุชัย บุญหล้า, อ.ที่ปรึกษา
ร่วม : ศศ. ดร.เกศิชา จินดาทิพย์

ภาวะเครียดจากออกซิเดชัน คือ ภาวะความไม่สมดุลระหว่างสารต้านอนุมูลอิสระและอนุพันธ์อิสระที่ว่องไว โดยเฉพาะ อนุพันธ์ออกซิเจนที่ว่องไว ปริมาณการสร้างอนุพันธ์ออกซิเจนที่ว่องไวเกี่ยวข้องกับการเกิดโรคเรื้อรังหลายชนิดรวมทั้งโรคมะเร็ง การดำเนินของโรคมะเร็งสามารถเกิดผ่านทั้งทางกระบวนการพันธุกรรมและเหนือพันธุกรรม การเปลี่ยนแปลงโปรตีนฮิสโตนที่บริเวณหางของ โปรตีนฮิสโตน เป็นหนึ่งในกระบวนการควบคุมเหนือพันธุกรรมที่มีความเกี่ยวข้องกับการดำเนินของโรคมะเร็ง มีการศึกษาพบว่า อนุพันธ์ออกซิเจนที่ว่องไวสามารถกระตุ้นให้เกิดการเปลี่ยนแปลงโปรตีนฮิสโตนได้ในมะเร็งหลายชนิด แต่ความสัมพันธ์ระหว่าง เปลี่ยนแปลงโปรตีนฮิสโตนโดยเฉพาะการเปลี่ยนแปลงที่หมู่เมทิลกับการเปลี่ยนแปลงการแสดงออกของยีนที่ถูกเหนี่ยวนำด้วยอนุพันธ์ ออกซิเจนที่ว่องไวในมะเร็งตับยังมีการศึกษาไม่มากนัก งานวิจัยนี้จึงต้องการศึกษาผลของอนุพันธ์ออกซิเจนที่ว่องไว (H_2O_2) ต่อการ ดำเนินโรคมะเร็งตับผ่านการเปลี่ยนแปลงโปรตีนฮิสโตนในเซลล์มะเร็งตับ และศึกษาระดับการแสดงออกของฮิสโตน H4K20me3, H3K9me3 และ H3K4me3 ในเนื้อเยื่อมะเร็งตับ การศึกษาพบว่า H_2O_2 กระตุ้นการเกิด Epithelial-mesenchymal transition (EMT) ในเซลล์มะเร็งตับ โดยลดระดับการแสดงออกของยีน E-cadherin และเพิ่มการแสดงออกของยีน α -SMA และ SNAIL รวมทั้งกระตุ้นการเกิด cell migration, cell invasion และ colony formation เมื่อกระตุ้น เซลล์ด้วย H_2O_2 ร่วมกับสารต้านอนุมูลอิสระ พบว่าสามารถลดการเกิด EMT และลดความรุนแรงของมะเร็งได้ โปรตีนฮิสโตน H4K20me3, H3K9me3 และ H3K4me3 รวมทั้งเอนไซม์ที่เกี่ยวข้องกับการเติมหมู่เมทิลมีการแสดงออกเพิ่มขึ้นในภาวะ เครียดจากออกซิเดชัน การทดลองด้วยเทคนิค chromatin immunoprecipitation พบว่าการลดลงของโปรตีนฮิสโตน H4K20me3 เพิ่มการแสดงออกของยีนที่เกี่ยวข้องกับการซ่อมแซม DNA (MRE11, BRCA2, MMS22L และ RBBP8), ยีนที่เกี่ยวข้องกับความยาวของเทโลเมียร์ (DCLRE1B, TERF1 และ TERF2) และยีนในกระบวนการ EMT (SOS1 และ RHOA) การแสดงออกของ RBBP8 เพิ่มขึ้นในเนื้อเยื่อมะเร็งตับ เมื่อเปรียบเทียบกับเนื้อเยื่อที่ไม่ใช่มะเร็งตับ นอกจากนี้ยังพบว่าการแสดงออกของ H4K20me3 เพิ่มขึ้นในเนื้อเยื่อมะเร็งตับเช่นเดียวกัน และการเพิ่มขึ้นของ H4K20me3 มีความสัมพันธ์กับการกลับมาเป็นมะเร็งซ้ำและอัตราการมีชีวิตรอดต่ำ การศึกษานี้สรุปได้ว่า ภาวะเครียดจากออกซิเดชันที่ถูกกระตุ้นด้วย อนุพันธ์ออกซิเจนที่ว่องไวสามารถเหนี่ยวนำให้เกิดการลุกลามของเซลล์มะเร็งตับผ่านกระบวนการเปลี่ยนแปลงโปรตีนฮิสโตน ที่ส่งผลให้ ระดับ EMT และกระบวนการซ่อมแซม DNA เพิ่มขึ้น และระดับ H4K20me3 ที่เพิ่มขึ้นในผู้ป่วยมะเร็งตับสัมพันธ์กับการมี ชีวิตรอดที่สั้นลงด้วย ดังนั้น การเปลี่ยนแปลงโปรตีนฮิสโตนที่ตำแหน่งหมู่เมทิล โดยเฉพาะ H4K20me3 สามารถนำมาใช้เป็นตัว พยากรณ์โรคมะเร็งตับได้ และน่าจะใช้เป็นเป้าหมายในการรักษาโรคมะเร็งตับได้ในอนาคต

สาขาวิชา ชีวเคมีทางการแพทย์
ปีการศึกษา 2564

ลายมือชื่อนิสิต
ลายมือชื่อ อ.ที่ปรึกษาหลัก
ลายมือชื่อ อ.ที่ปรึกษาร่วม

5874768730 : MAJOR MEDICAL BIOCHEMISTRY

KEYWORD: Hepatocellular carcinoma Epigenetics Histone modifications ROS
Oxidative stress Tumor progression

Suchittra Phoyen : Epigenetic Regulation of Reactive Oxygen Species-induced
Tumor Progression in Hepatocellular Carcinoma. Advisor: Asst. Prof.
CHANCHAI BOONLA, Ph.D. Co-advisor: Asst. Prof. DEPICHA JINDATIP,
Ph.D.

Oxidative stress is a consequence of an imbalance of antioxidants and reactive species. The most common form of reactive species is derived from oxygen, called reactive oxygen species (ROS). ROS involve in pathogenesis of several diseases including cancers. Cancer genesis and progression are contributed through both genetic and epigenetic mechanisms. Histone modification, a post-translational modification at histone tails, is one of the epigenetic mechanisms known to participate in carcinogenesis and tumor progression. Although the ROS-induced histone modification alteration has been demonstrated in some cancers, the change in histone methylation and gene expression by ROS in hepatocellular carcinoma (HCC) is scarcely reported. This study aimed to investigate the effect of ROS on tumor progression via histone modification in HCC cell lines. Expression of inactive chromatin (H4K20me3, H3K9me3) and active chromatin (H3K4me3) marks and their clinical significance were also investigated. The result showed that ROS promoted epithelial-mesenchymal transition (EMT) in HCC cells, indicated by reduced expression of E-cadherin, and enhanced expression of α -SMA and SNAIL. Cell migration, invasion, and colony formation were higher in HCC cells treated with ROS than the untreated controls. Co-treatment with antioxidant attenuated oxidative stress, inhibited EMT and decreased tumor progressivity in HCC cells exposed to H₂O₂. H4K20me3, H3K9me3, H3K4me3 and histone methyltransferases (SUV420H2, SUV39H1 and SMYD3) was upregulated in H₂O₂-treated HCC cells compared with the untreated controls. Chromatin immunoprecipitation-sequencing demonstrated that alteration of histone methylation (H4K20me3 and H3K4me3) by ROS was associated with upregulation of genes involved in DNA repair pathway (MRE11, BRCA1, MMS22L and RBBP8), telomere maintenance (DCLRE1B, TERF1 and TERF2), and EMT pathway (SOS1 and RHOA) in HCC cells. The transcript expression of MRE11, BRCA1, MMS22L, RBBP8, DCLRE1B, TERF1 and TERF2 in HCC cells were increased following the H₂O₂ treatment. RBBP8 was selected to validate in the human HCC tissues, and it was overexpressed in the HCC tissues compared with the non-cancerous liver tissues. Expression of H4K20me3 was also higher in HCC tissues than the non-cancerous tissues. Elevated expression of H4K20me3 was associated with tumor recurrence and poor survival in HCC patients. In conclusion, ROS-induced oxidative stress promoted HCC progression through chromatin remodeling that subsequently upregulated genes related to EMT and DNA repairing pathways. H4K20me3 was upregulated in the HCC tissues, and its

Field of Study: Medical Biochemistry
Academic Year: 2021

Student's Signature
Advisor's Signature
Co-advisor's Signature

ACKNOWLEDGEMENTS

First of all, I would like to express my special thanks to my advisor, Asst. Prof. Chanchai Boonla, for guiding my study and research, encouraging me to improve myself, and supporting in my PhD study. Besides, I would like to thank my thesis co-advisor and thesis committees for your knowledge and guidance to my thesis.

I had a grateful year with Translational Oncology of Solid Tumors Team at Experimental and Clinical Research Center, Charité Universitätsmedizin Berlin and Max-Delbrück-Center for Molecular Medicine, Berlin, Germany. I would like to extend my gratitude to Prof. Ulrike Stein and all the lab members to give me a wonderful chance in research and life experience.

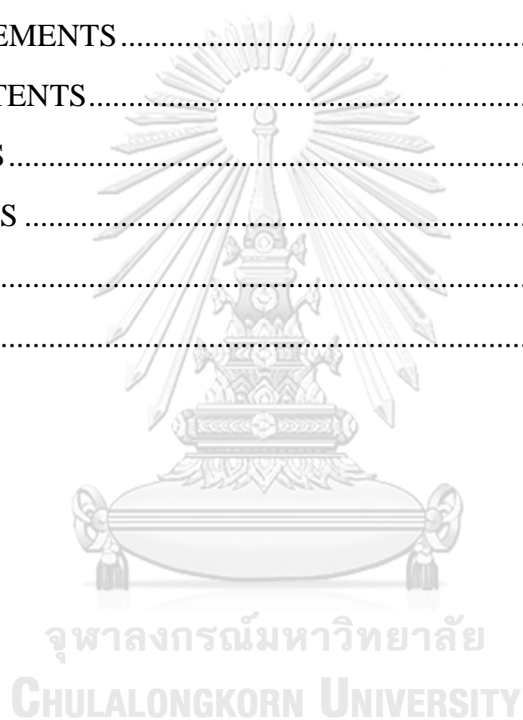
I cannot achieve my PhD study without funding support. Therefore, I would like to thank RGJ scholarship for the educational funding and the research grant from the 90th Anniversary of Chulalongkorn University Scholarship.

Finally, my special thanks are extended to my beloved friends, family, R806 lab members, and my fellow students in medical biochemistry program. I could pass through the struggling time because of my wholehearted support.

Suchittra Phoyen

TABLE OF CONTENTS

	Page
.....	iii
ABSTRACT (THAI)	iii
.....	iv
ABSTRACT (ENGLISH)	iv
ACKNOWLEDGEMENTS	v
TABLE OF CONTENTS	vi
LIST OF TABLES	vii
LIST OF FIGURES	viii
REFERENCES	113
VITA	115



LIST OF TABLES

	Page
Table 1 Primers used for qRT-PCR analysis	25
Table 2 Primers used for relative telomere length qPCR analysis.....	28
Table 3 16-point scale scoring criteria used for histone methylation IHC score calculation.....	36
Table 4 Biological processes of genes less enriched for H4K20me3 in HCC cells following H ₂ O ₂ treatment	56
Table 5 KEGG pathways of genes less enriched for H4K20me3 in HCC cells following H ₂ O ₂ treatment	57
Table 6 Biological processes of genes highly enriched for H3K4me3 in H ₂ O ₂ -treated HCC cells.....	66
Table 7 KEGG pathway of genes highly enriched H3K4me3 in H ₂ O ₂ -treated HCC cells	68
Table 8 Demographic and clinical data of the HCC patients.....	74

LIST OF FIGURES

	Page
Figure 1 Hypothesis	5
Figure 2 Basics of reactive oxygen species (ROS).....	8
Figure 3 Inducers and scavengers of reactive oxygen species (ROS) generation	9
Figure 4 The production and effects of ROS in human cancers.....	11
Figure 5 The pattern of histone modifications on histone tails.....	13
Figure 6 The histone modifications are mediated by histone modifying enzymes.....	14
Figure 7 Development of hepatocellular carcinoma (HCC).....	17
Figure 8 The experimental workflow	21
Figure 9 Cell viability of HepG2 (A) and Huh7 (B) treated with various concentrations of H ₂ O ₂	38
Figure 10 Cell viability of HCC cells following the tocopherol acetate (TA) treatment	38
Figure 11 Intracellular ROS production in HCC cells measured by DCFH-DA assay	39
Figure 12 Protein carbonyl content in HCC cells following the H ₂ O ₂ treatment	40
Figure 13 The mRNA expression of NRF2 in HCC cells following the H ₂ O ₂ treatment.	41
Figure 14 The mRNA expression of NQO1 in HCC cells following H ₂ O ₂ treatment	41
Figure 15 Total antioxidant capacity in HCC cells following H ₂ O ₂ treatment measured by DPPH assay.	42
Figure 16 The mRNA expression of E-cadherin in HCC cells following H ₂ O ₂ treatment.	43
Figure 17 The mRNA expression of α -SMA in HCC cells following H ₂ O ₂ treatment	44
Figure 18 Cell migration in HCC cells measured by transwell assay.....	45
Figure 19 Cell invasion in HCC cells measured by Boyden chamber assay	46
Figure 20 Colony number in HCC cells measured by clonogenic assay	47

Figure 21 The expression of histone methylations following H ₂ O ₂ treatment in HCC cells measured by western blot analysis.	48
Figure 22 Histone methyltransferase enzyme mRNA expression in HCC cells treated with H ₂ O ₂	49
Figure 23 Number and location of the identified protein-coding genes enriched for H4K20me3 in HCC cells under oxidative stress condition.	51
Figure 24 Number and location of the identified protein-coding genes enriched for H3K4me3 in HCC cells under oxidative stress condition.	52
Figure 25 The number of genes enriched for H4K20me3 in HCC cells treated with H ₂ O ₂ compared with the untreated control.	54
Figure 26 Biological process of genes less enriched for H4K20me3 in H ₂ O ₂ -treated HCC cells.	55
Figure 27 Expression of genes related to DNA repair in H ₂ O ₂ -treated HCC cells measured by qRT-PCR.	59
Figure 28 Expression of genes related to DNA repair in H ₂ O ₂ -treated HCC cells measured by qRT-PCR.	60
Figure 29 p21 and p53 mRNA expression in HCC cells following H ₂ O ₂ treatment measured by qRT-PCR.	60
Figure 30 DCLRE1B and shelterin complexes mRNA expression and relative telomere length in HCC cells following H ₂ O ₂ treatment.	62
Figure 31 The number of genes enriched for H3K4me3 in HCC cells treated with H ₂ O ₂ compared with the untreated control.	64
Figure 32 Biological process of genes more enriched for H3K4me3 in H ₂ O ₂ -treated HCC cells.	65
Figure 33 SOS1, JNK2, c-Jun and MMP9 mRNA expressions in HCC cells following H ₂ O ₂ treatment.	70
Figure 34 RHOA, ROCK1, LIMK2 and radixin mRNA expressions in HCC cells following H ₂ O ₂ treatment.	71
Figure 35 SMAD2 and SMAD3 mRNA expression in HCC cells following H ₂ O ₂ treatment.	72
Figure 36 SNAIL mRNA expression in HCC cells following H ₂ O ₂ treatment.	72
Figure 37 H4K20me3 enrichment peaks over the RBBP8 gene in HCC cells compared between H ₂ O ₂ treatment and untreated control.	73

Figure 38 H&E staining of HCC and noncancerous liver tissues.....	76
Figure 39 H4K20me3 expression in HCC tissues	77
Figure 40 H4K20me3 expression in HCC tissues compared with noncancerous liver	78
Figure 41 Kaplan-Meier curve analysis of H4K20me3 expression and tumor relapse in HCC patients.....	79
Figure 42 Kaplan-Meier curve analysis of H4K20me3 expression and overall survival in HCC patients.....	79
Figure 43 H3K9me3 expression in HCC tissues	80
Figure 44 H3K9me3 expression in HCC tissues compared with noncancerous tissues.	81
Figure 45 H3K4me3 expression in HCC tissues	82
Figure 46 H3K4me3 expression in HCC tissues compared with noncancerous tissues.	83
Figure 47 RBBP8 expression in HCC tissues.....	84
Figure 48 RBBP8 expression in HCC tissues quantitatively compared with noncancerous tissues.....	85

Chapter 1

Introduction

Background and rationales

Cancer is a neoplastic disease that acquires many functional capabilities during the multistep carcinogenesis and progression in order to allow cancer cells to survive, proliferate and spread (1). Genomic instability and tumor-promoting inflammation are two enabling characteristics commonly found in all cancers. One of the best known factors to activate inflammatory response in tumor is oxidative stress (2). Furthermore, oxidative stress is recognized to be a critical factor that contributes to genomic instability through both genetic and epigenetic mechanisms in cancer.

Oxidative stress is defined as an overproduction of reactive species, which are mainly derived from oxygen and called reactive oxygen species (ROS), and/or reduction of antioxidant content in cells that consequently causes cellular damage, injury and eventually death. ROS are byproduct from oxidative metabolism including oxidative phosphorylation and inflammatory reactions, and it also can be produced by ionization and UV radiation (2, 3). ROS contribute to the initiation and subsequent progression of several chronic diseases including Alzheimer's disease, cardiovascular disease, and especially, cancers (4). Recently, we immunohistochemically demonstrated that oxidative stress was increased in cancerous tissues of patients with hepatocellular carcinoma (HCC) and bladder cancer when compared with their non-cancerous tissues. Also, we showed that oxidative stress enhanced the tumor aggressiveness in both HCC and bladder cancer cell lines (5, 6). It is well recognized that ROS induce DNA damage leading to DNA lesions, and ROS also promote cell proliferation and survival. ROS can trigger cellular signaling pathways to regulate many cellular processes such as mutation and repair, proliferation, and apoptosis (7). Furthermore, ROS promote progression of cancers through many pathways such as cell migration and invasion, epithelial-mesenchymal transition (EMT), expression of matrix metalloproteinases (MMPs) and autophagy(8, 9). Additionally, ROS promote cancer progression via both genetic and epigenetic mechanism (10).

Epigenetics refer to the study of heritable changes and reversible mechanism in regulation of gene expression through DNA methylation, histone modifications and non-coding RNAs without altering DNA sequence (11). The altered epigenetic is common feature found in all cancers that further cause aberration of gene function and expression eventually leading to cancer initiation and progression (12). Alteration of histone modifications has been demonstrated in various cancers, for examples, esophageal cancer, prostate cancer, breast cancer, colorectal cancer, pancreatic cancer and HCC (13-19). Chemical modifications of histone protein, e.g., histone acetylation and histone methylation, regulate gene expression via remodeling of chromatin structure. In general, histone acetylation causes active or open chromatin formation that favors gene expression (turning genes on). In contrast, histone deacetylation initiates the formation of inactive chromatin or heterochromatin that further represses or silences gene expression (turning genes off). For histone methylation, a common chromatin mark for active chromatin formation is H3K4me₃, whereas common chromatin marks for heterochromatin formation are H3K9me₃, H3K27me₃ and H4K20me₃ (20). Histone modification is also involved in initiating and regulating the DNA damage response (DDR) (21, 22). Furthermore, histone modifications and histone modifying enzymes vitally participate in the EMT process (23, 24). The epigenetic regulation is a dynamic and reversible process largely depending upon external stimuli, and oxidative stress is one of the important stimuli (5, 25-28) (10). Several lines of evidence suggest the cause-and-effect relationship between oxidative stress and histone modifications (29-31). However, the mechanism of how ROS or oxidative stress alters the histone modification in HCC is not fully understood.

HCC is a heterogenous liver cancer. It is the one of the most common cancers worldwide including in Thailand. The incident and mortality rate of HCC in Thailand is high in both males and females (32). There are several risk factors related to HCC development including cirrhosis, chronic hepatitis virus infection, alcoholic consumption and non-alcoholic liver disease (33). The current treatments for HCC patients are surgical resection, chemoembolization, ablation and photo beam therapy depending on the cancer stages (34). HCC is usually diagnosed at the late stage and the treatments are less effective. Therefore, insight into molecular mechanism of HCC

development needs to be elucidated in order to pave the way to develop the more effective diagnostic and therapeutic tools for this life-threatening cancer.

Histone modification has been explored in HCC. The histone modifications were globally altered in HCC (13, 35), and the alteration of histone modifying enzymes was associated with hepatocarcinogenesis (14, 36). The results from previous studies strongly suggested that changes in global histone modification and histone modifying enzyme led to HCC progression. However, the mechanistic factor that influences histone changes in HCC has not been investigated yet. We hypothesize that ROS contribute to the progression of HCC through induction of histone modification changes to turn on genes that require for aggressive phenotypes and turn off genes that do not require for tumor progression.

In this study, we aimed to investigate the effect of ROS on progression of HCC cells through histone modification regulation. Profiles of genes associated with active chromatin formation and those genes associated with inactive chromatin formation in HCC cell lines following the ROS treatment were identified using chromatin immunoprecipitation (ChIP)-sequencing technique. Candidate genes were selected and validated the transcript expression using qRT-PCR analysis. One selected gene (RBBP8) and histone marks (H4K20me3, H3K9me3 and H3K4me3) were further immunohistochemically validated in human HCC tissues. Association of clinicopathological parameters with expression of H4K20me3. were evaluated. The present findings provided the more understanding of the mechanism of ROS-induced HCC progression through histone methylation.

Keywords

Hepatocellular carcinoma, ROS, Oxidative stress, Epigenetics, H4K20me3, RBBP8, Tumor progression

Research questions

1. Whether ROS altered histone methylation and promoted tumor progression in HCC cell lines?
2. What were the profiles of genes associated with active and inactive chromatin marks in ROS-treated HCC cells?
3. What were the expression levels of selected candidate genes validated in HCC cell lines and HCC tissues obtained from HCC patients?

Objectives

1. To investigate the effect of H₂O₂ (as ROS representative) on tumor progression in HCC cell lines.
2. To investigate the effect of H₂O₂ on histone methylation changes in HCC cell lines.
3. To identify genes related to cancer progression and altered chromatin structures (H4K20me₃ vs. H3K4me₃) in HCC cells induced by H₂O₂ using ChIP-sequencing.
4. To validate the expression of selected candidate genes in HCC cell lines and HCC tissues obtained from HCC patients.
5. To investigate expression of inactive (H4K20me₃ and H3K9me₃) and active (H3K4me₃) histone marks in HCC tissues obtained from HCC patients and evaluate their clinical significance.

Hypothesis

We hypothesize that the ROS promoted HCC progression through epigenetic regulation. ROS altered the remodeling of chromatin in HCC cells causing change in gene expression profile to turn on genes required for tumor progression. Our hypothesis is shown in figure 1.

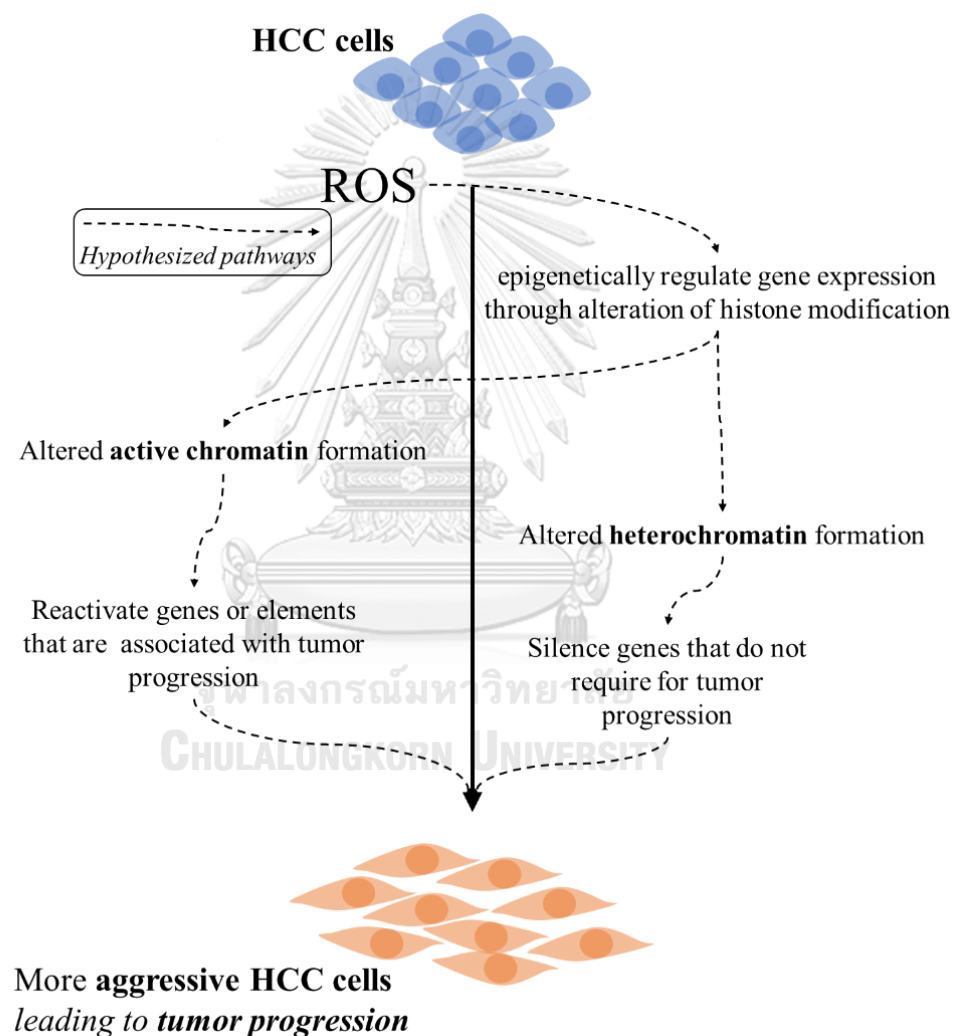


Figure 1 Hypothesis

Ethical consideration

A part of this research was performed in human HCC tissues. Therefore, the research protocol was reviewed and approved by the Institutional Ethics Committees, Faculty of Medicine, Chulalongkorn University (IRB No. 286/62).

Benefits and applications

1. The mechanistic insight into how ROS induced HCC progression via the alteration of histone modification and chromatin remodeling was established.
2. The expression profile of genes that were associated with active vs. inactive chromatin marks in ROS-induced aggressive HCC cells were delineated.
3. Expression levels and clinical significance of chromatin marks, particularly H4K20me3, and selected protein (RBBP8) in human HCC tissues were obtained.
4. Antioxidant intervention was suggested to attenuate oxidative stress and inhibit the ROS-induced HCC progression.

Chapter 2

Literature review

Oxidative stress; generation of ROS and defensive systems

Oxidative stress is defined as an imbalance between the generation of free radical and the elimination systems of protective mechanism by antioxidants leading to cellular injury, as a result of damage of cellular biomolecules by reactive species. Reactive oxygen species (ROS) are an abundance reactive species in the cells, and they are natural byproducts of oxidative metabolism including oxidative phosphorylation, and inflammatory reactions. It is also produced by exogenous sources such as UV radiation and ionization (2, 3). However, production of ROS arise through multiple processes depending on cells and tissue types (37).

The important ROS derived by molecular oxygen includes free oxygen radicals such as superoxide anion ($O_2^{\bullet -}$), hydroxyl radical (OH^{\bullet}) and nitric oxide (NO), and non-radical ROS, for instances, hydrogen peroxide (H_2O_2), organic hydroperoxides and hypochloride. In cells, $O_2^{\bullet -}$ is primarily produced in mitochondria and by NADPH oxidase enzyme. It contains an unpaired electron that can be converts to H_2O_2 by superoxide dismutase (SOD). H_2O_2 can be reduced to H_2O and O_2 by two main antioxidant mechanisms, catalase and glutathione system. On the other side, H_2O_2 can be converted to OH^{\bullet} , which is highly reactive, and it is capable of oxidizing nucleic acids, lipids and proteins to cause oxidative damage leading to cellular injury and finally cell death (Figure 2) (38).

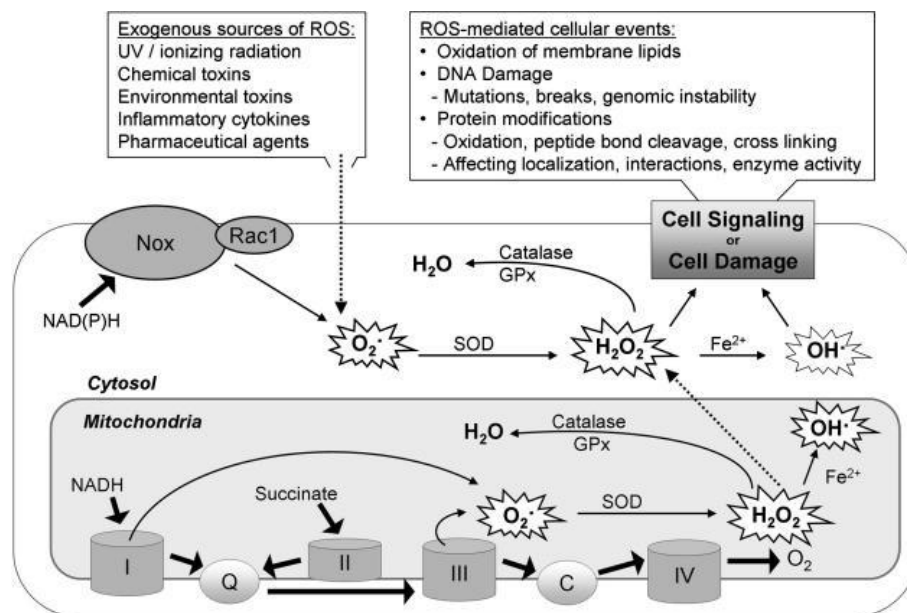


Figure 2 Basics of reactive oxygen species (ROS) including superoxide anion ($O_2^{\bullet-}$), hydrogen peroxide (H_2O_2) and hydroxyl radical (OH^{\bullet}) and intracellular ROS generation (38) The balance between ROS production and elimination has been linked to the several biological processes and diseases. Under normal physiological conditions, ROS is continuously produced into the cells, but generation of ROS is regulated by ROS scavenging mechanisms. ROS scavengers can attack to ROS to inhibit the oxidation of free radicals. When ROS are excessive and accumulated, oxidative stress and disadvantage effects arise causing oxidative damage to cellular components such as nucleic acids, lipids and proteins. To moderate the excessive ROS and attenuate the harmful effects of ROS, cellular defensive mechanisms are taken place to help and protect development pathological conditions. The defensive mechanisms divide into two groups, enzymatic molecules and non-enzymatic molecules. Enzymatic molecules include SOD, catalase, glutathione peroxidase (GPX) and glutathione reductase (GR), whereas the other group, non-enzymatic molecules, composes of glutathione, peroxiredoxin (PRX), thioredoxin (TRX), vitamin C and vitamin E (2, 37, 39) (Figure 3).

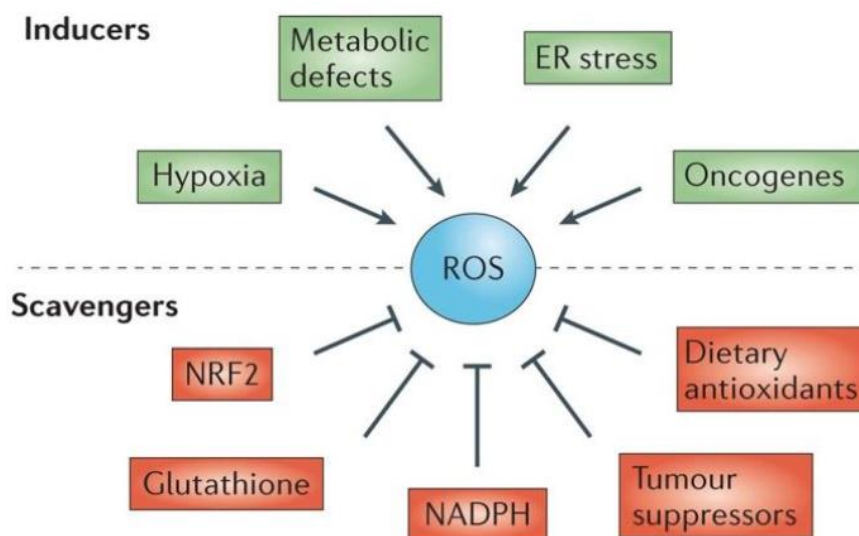


Figure 3 Inducers and scavengers of reactive oxygen species (ROS) generation (7)

Both enzymatic and non-enzymatic scavenging systems are responsible for balancing ROS and preventing the formation of oxidative lesion. Once lesion formed, the second line of defensive system is to fix the lesion, mostly oxidized DNA, through repaired programming or to degrade them, mostly oxidized proteins, through proteasome and turnover processes. The signaling pathway that regulates cytoprotective response to ROS are nuclear factor erythroid 2-related factor 2 (NRF2), nuclear factor-kB (NF-kB), and hypoxia inducible factor-1 (HIF-1) and) which lead to the increased expression of antioxidant molecules such as SOD, catalase, thioredoxin and the GSH antioxidants (4). Under long-term exposure of ROS, the ROS-scavenging system is exhausted, and oxidative stress is set. Moreover, sustained stress causes more ROS production and more deleterious to cell structure and functions. Therefore, increasing of oxidative damage to DNA, proteins and lipids, together with loss of antioxidants cause initiation and subsequent progression of various diseases including aging, Alzheimer's disease, cardiovascular disease and cancers (2, 4).

The implication of ROS in cancers

In cancer cells, ROS are continuously and persistently produced higher than normal cells (2). Regarding to literature, high level of ROS was demonstrated in many cancers including lung cancer (25), breast cancer (28), prostate cancer (27), ovarian cancer (28), bladder cancer (5) and HCC (6, 26, 40). ROS play an important role in all stages of cancer development including initiation, promotion and progression. Several studies have investigated whether ROS are oncogenic or tumor suppressive. At low to moderate levels, ROS may be associated with tumor formation either by acting as signaling molecules or promoting the mutation of genomic DNA. In contrast, at high levels, ROS enhance cell death and severe cellular damage. Cancer cells need high amount of ATP to support high rate of cell proliferation leading to accumulation of ROS in cancer cells. However, cancer cells can adapt to survive in high level of ROS condition. ROS can also activate cellular signaling pathway that control cellular processes such as mutation, proliferation, and apoptosis. ROS can induce DNA damage leading to DNA lesions, ROS and also promote cell proliferation, survival and resistance to cell death (7). ROS can activate oncogene and inactivate tumor suppressor genes in cancer cells that leads to cancer progression through the enhancement of malignant phenotypes (41). In addition, ROS are involved in cancer metastasis by regulating many pathways including EMT, expression of MMPs, migration, invasion, angiogenesis and autophagy in tumor region. Therefore, ROS act as mediators to induce carcinogenesis that sustain subsequent progression of cancer and finally, metastasis (Figure 4) (8, 9).

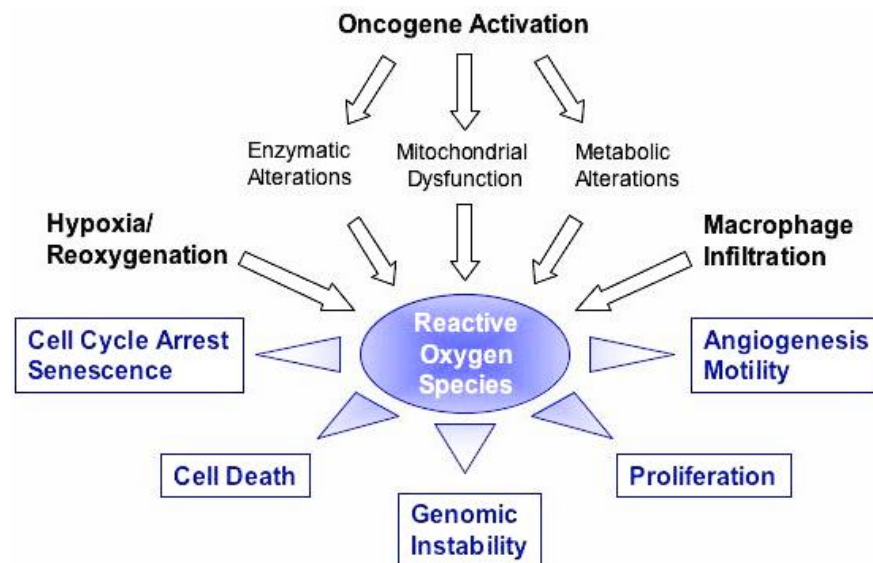


Figure 4 The production and effects of ROS in human cancers (8)

Epigenetics and its alteration in cancer

Epigenetics refer to the study of heritable and reversible changes to regulate the expression of genes without changes in DNA sequences (11). Epigenetic gene patterns play important roles in biological processes including development and maintenance of tissue-specific gene expression pattern in mammals. The key processes responsible for epigenetic regulation are DNA methylation, histone modifications and post-translational gene regulation by non-coding RNAs. Global changes of epigenetic mechanism are considered as the hallmark of cancer. Deregulation of this mechanism leads to aberration of gene function and altered gene expression that is essential for cancer initiation, development and subsequent progression (12).

Histone modification is one type of epigenetic mechanisms which is a covalent post-translational modification to histone proteins. These chemical modifications include methylation, acetylation, phosphorylation, ubiquitination and sumoylation. Histone protein composes of core histone protein and 8 subunits of histone protein H2A, H2B, H3 and H4 and 147 base pairs of DNA-wrapped around the histone which called nucleosome. The sites of histone modification are either N-terminus or C-terminus of histone tails. Histones are modified at many sites and modifications are occurred on specific residues. Additionally, one position can be added more than one modification (20). These

modifications control key cellular processes such as gene transcription, DNA replication and DNA repair. The histone modification patterns have been linked to biological function and they can generate codes to be read by cellular machineries in term of “histone code”, for example H3K18ac refers to acetylation of lysine position 18 on histone H3 and H4K20me3 refers to adding 3 methyl groups to lysine position 20th on histone H4 (42) (Figure 5).

The patterns of histone modifications are associated with chromatin remodeling and gene function. The significance of histone codes is that it can regulate remodeling of chromatin between euchromatin and heterochromatin states. Euchromatin is an accessible chromatin or open chromatin which allows gene to activate transcription. In contrast, heterochromatin is an inaccessible chromatin which is compacted and does not allow transcription to take place, and that leads to transcriptional repression. There are many histone codes that can remodeling of chromatin structure, for instance, H3K18ac and H3K4me3 are euchromatin marks that leads to be active gene expression, whereas H3K9me3, H3K27me3 and H4K20me3 are well known heterochromatin marks, that cause transcriptional repression (43, 44).

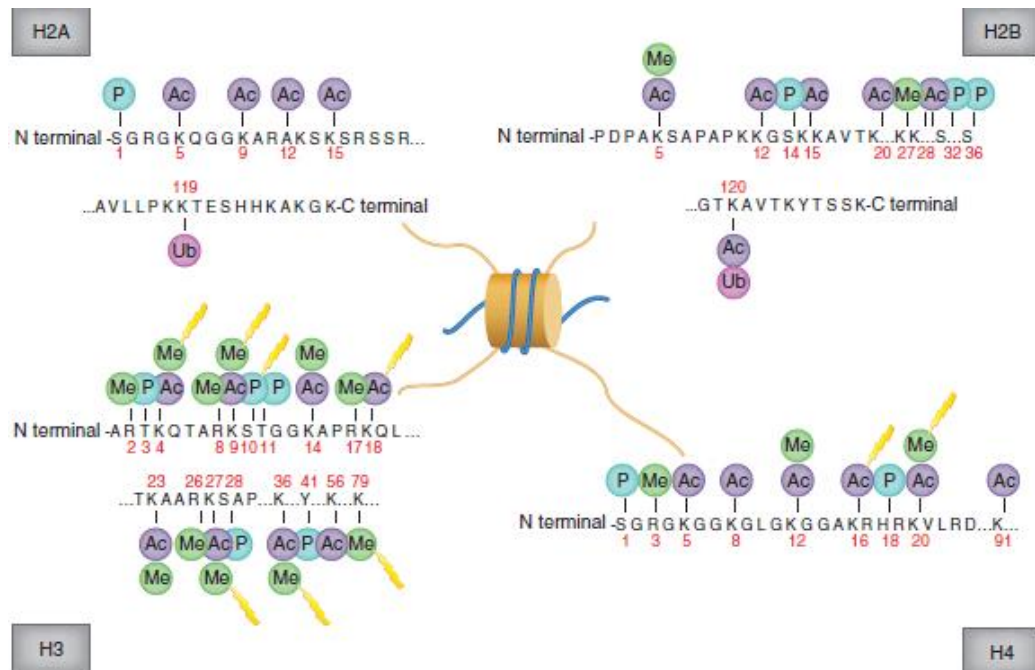


Figure 5 The pattern of histone modifications on histone tails

(Ac= acetylation; Me= methylation; P= phosphorylation) (45)

The effect of histone modifications chromatin remodeling depends on types of modifications. The majority of chemical modifications occurs at lysine, arginine and serine residues, and they takes place on histone tails of H3 and H4 core proteins (46). Histone modifications will be read by epigenetic reader (proteins to read the histone codes) to activate or repress transcription depending on the residues that are be modified. In general, acetylation of lysine residues on histone H3 and H4 relates to open chromatin which leads to transcriptional activation. On the other hand, methylation on lysine residues links to both activation and inactivation of transcription depending on the locations of modified residues and the number of added methyl groups (12, 42). These modifications are mediated by histone modifying enzymes. Histone acetylation or de-acetylation is catalyzed by histone acetyltransferases (HATs, classified as epigenetic writer) and histone deacetylases (HDAC, classified as epigenetic eraser), respectively. The status of histone methylation is evaluated by the balanced action of histone methyltransferases (HMTs, the writer) and histone demethylases (HDMs, the eraser). For example, histone H3

can be tri-methylated by MLL (HMT) at lysine position 4 (H3K4me3) or acetylated by p300 (HAT) at lysine position 18 (H3K18Ac) resulting in euchromatin formation and activation of transcription. In contrast, lysine can be tri-methylated by SUV39H1 (HMT) at position 9 on histone H3 (H3K9me3) or by EZH2 (HMT) at position 27 on histone H3 (H3K27me3) resulting in heterochromatin formation and repression of transcription (47) (Figure 6).

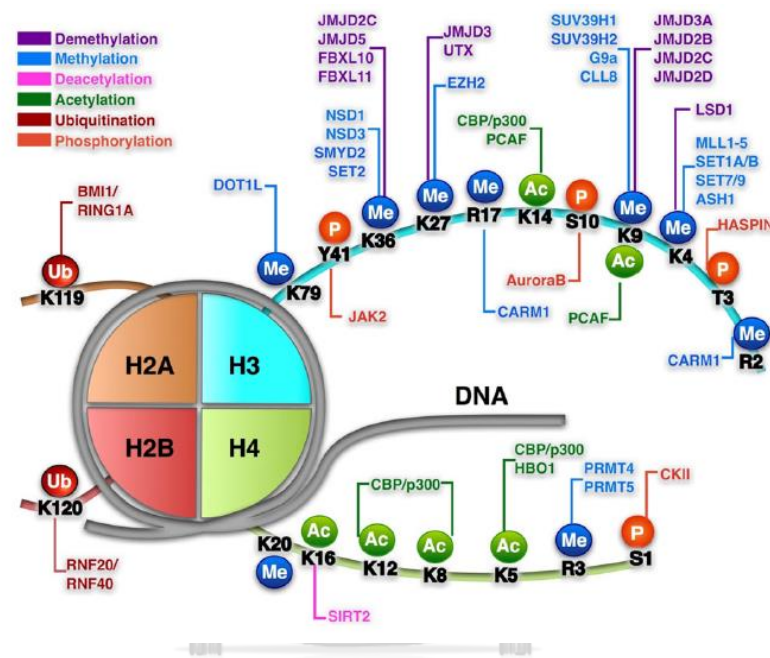


Figure 6 The histone modifications are mediated by histone modifying enzymes (47)

Histone modification involves in all stages of carcinogenesis, including initiation, progression and metastasis (12). The aberration of histone modification patterns is known to associate with a large number of human malignancies. Consistent with this notion, the alteration of histone modifying enzyme disturbs the patterns and levels of histone marks and consequently deregulate the control of chromatin-related processes leading to tumorigenesis and development of cancer (20). There have been many studies demonstrated the aberration of histone modification patterns and histone modifying enzymes in cancers.

H4K20me3, a marker of constitutive heterochromatin, is associated with the silencing of genes during the development of many cancer types. H4K20me3 was

appeared to be decreased in cancer cells (48). Additionally, decreased H4K20me3 can be used as a marker of poor prognosis in patients with breast and bladder cancers (18, 49). In contrast, elevated H4K20me3 was found in colon cancer tissues and it was prognostic in early stage of colon cancer (50). H3K9me3, a constitutive repressive chromatin mark, is concentrated at the pericentric and centric heterochromatin. Induction of H3K9 methylation are important to maintain DNA methylation for gene silencing in colorectal cancer (16). Recent study exhibited that H3K9me3 was increased in bladder cancer tissues relative to adjacent non-cancerous tissues (51). H3K4me3 is commonly associated with the activator of transcription of nearby genes. Moreover, it is highly enriched at active promoters near transcription site and common use as a histone mark in epigenetic studies to identify active gene promoters (52). H3K9me3 and H3K4me3 expression was higher in colon tissues than non-tumor tissues and this was related to short patient survival (50). These evidences indicate that alteration of histone is a common epigenetic feature in cancers, and it is suggested to be essential during development of cancers. Studies of mechanistic regulation of histone modification and its reversibility could be a novel target for developing epigenetic drugs for cancer treatment (53).

Cause-and-effect relationship between oxidative stress and histone modifications

Oxidative stress plays an important role in carcinogenesis and progression via epigenetic alterations (10). Oxidative stress can alter the chromatin remodeling either by influencing of chromatin structure or affecting the histone modifying enzymes (10). Alveolar epithelial cells (A549) exposed to H₂O₂ and cigarette smoking condensate (CSC) led to increased histone acetylation on histone H4 by activating HAT activity and disrupting HDAC activity (30). Nui et al demonstrated that oxidative stress inducing by H₂O₂ in human bronchial epithelial cells inhibits JmjC-domain-containing histone demethylases leading to increase overall levels of histone methylation, especially for H3K4me3, H3K9me3 and H3K27me3 marks. Conversely, oxidative decreased levels of histone acetylation, e.g., H3K9ac and H4K8ac (31). Chronic H₂O₂ exposure in human kidney epithelial (HK-2) cells showed that expression of HDAC1 and HMT1 were significantly increased, while HAT1 was significantly decreased.

Additionally, they showed that expression of these histone modifying enzymes were associated with decreased histone acetylation marks (H3K4ac and H3K9ac), and increased histone methylation marks (H3K4me3 and H3K27me3) (29). Our group recently reported that increased H3K9me3 and its recognized protein, HP1 α , in bladder cancer tissues were positively correlated with oxidative stress levels (51). These evidences indicate once again that oxidative stress is critically involved in histone modification patterns in various cancers.

The involvement of oxidative stress in hepatocellular carcinoma

Since global incidence and mortality rate, HCC is progressively increasing, it is interesting to investigate the mechanism insight of hepatocarcinogenesis and HCC progression. HCC is a heterogeneous liver cancer ranking as the sixth most common type of the human cancer. It is the second cause of death from cancer worldwide, after lung cancer. The estimated new cases of HCC are nearly 782,000 in 2012 worldwide. The global age standardized incident rate (ARS) is 554 and 228 cases per 100,000 persons in males and females, respectively. The incidence of HCC is the fifth in male and the ninth in female worldwide. There are approximately 745,000 deaths from HCC occurred in 2012 (54). In Thailand, the incidence of HCC is increasing and it is one of the most common cancers in both males and females. It is the third rank as a cause of death in males, while it is the fifth leading cause of death in females (32).

Main risk factors of HCC are well known including cirrhosis, chronic viral hepatitis infection, alcoholic liver disease, non-alcoholic fatty liver disease. Additionally, older age, male gender, obesity, type 2 diabetes and smoking are also associated with increased risk for HCC development (33, 55).

HCC development is a multistep process which is characterized by different morphological changes of liver starting from forming of dysplastic nodules, then developing of early HCC and finally evolving to advanced stage of HCC. Chronic liver damage from etiological risk factors changes normal liver to cirrhosis leading to tumor initiation. Primary liver cancers (PLCs) are induced by tumor microenvironment that transforms normal liver cells and begins to develop early stage of HCC. Accumulation

of abnormal liver cells continuously change the stage of cancer and finally proceed to malignant stage and metastasis of HCC as shown in Figure 7 (56).

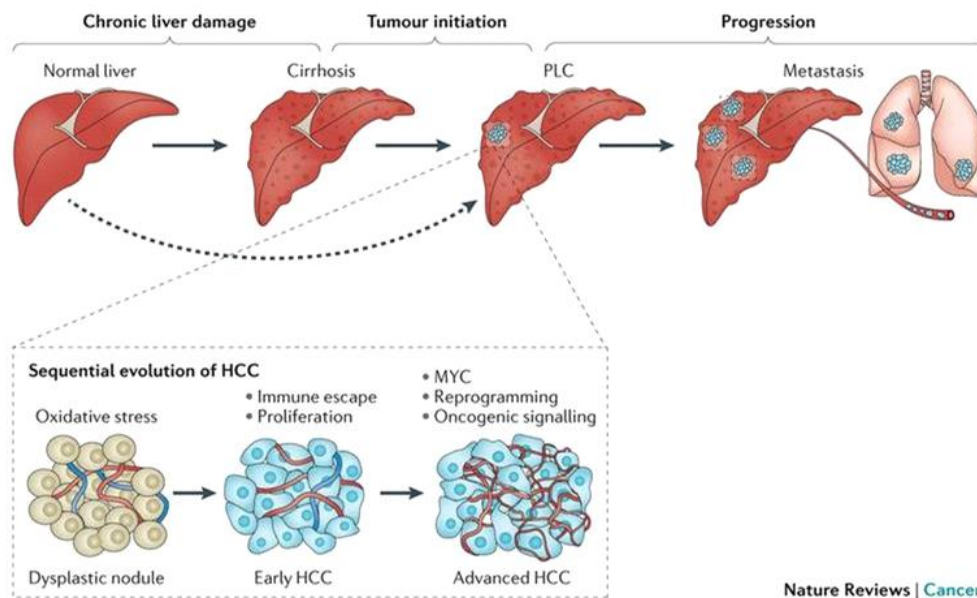


Figure 7 Development of hepatocellular carcinoma (HCC) (56)

Unfortunately, HCC is often diagnosed at the late stage when all treatment options are least effective. For patients with advanced stage, medical treatments including chemotherapy, chemoembolization, ablation and proton beam therapy, remain disappointing. Moreover, most of patients present with tumor recurrence that progress to the advanced stage of HCC. Currently, curative treatments for HCC are surgical resection and liver transplantation, which is a recommended therapy for the early stage. For patients with intermediated and advanced stage are recommended for transarterial chemoembolization (TACE) and tyrosine kinase inhibitor or sorafenib, respectively (34).

Oxidative stress has been implicated in HCC development. ROS play a crucial role in HCC pathogenesis and progression. The several studies have investigated the level of oxidative stress in HCC. Increased expression of oxidative stress biomarkers (oxidative DNA and protein damages) was observed in HCC tissues (6, 26, 40). In Thai patients with HCC, we found increased level of oxidative DNA lesion in cancerous

liver tissues compared to non-cancerous tissues (6, 40), emphasizing, the roles of ROS in HCC. Oxidative DNA damage is known to increase chromosomal alteration that is associated with cell transformation and leads to HCC development (57). Oxidative stress enhances telomerase activity in HCC cells, and it is related to increased proliferative activity and apoptotic resistance in HCC tissues (58). ROS also activate MAPKs, which is associated with cell growth and transformation. Hepatitis C infection is associated with activated ERK, a conventional MAPK, in human HCC tissues (59). Recent study reports that elevated oxidative stress, indicated by increased 8-OHdG and NRF2, leads to HCC progression in *in vitro* experiment (6). The correlation between ROS and EMT has been demonstrated, and it is shown that the EMT in HCC cells was induced through PI3K/AKT pathway activation (60). There is evidence that shown that ROS can regulate autophagy pathway to promote HCC development as well. The sustained accumulation of ROS triggered autophagy leading to increase survival of HCC cells (61). Recently, sorafenib, the drug that has been approved for treatment of late stage HCC is shown to inhibit tumor progression by reduction of MMP expression and repression of MEK-ERK signaling that leads to decreased EMT, cell migration and invasion (62). These evidences strongly support the active involvement of oxidative stress in HCC development and progression.

The alteration of histone modifications in hepatocellular carcinoma

The aberration of histone modification, chromatin structure and histone modifying enzymes, result in activation of oncogenes or inactivation of tumor suppressor genes which contribute to HCC genesis and progression. Several studies show the findings that histone modification is altered in HCC. Elevated levels of H3K9me3 and SUV39H1 (enzyme to produce H3K9me3) are associated with HCC development and progression (14). The overexpression of SETDB1, a histone H3K9 methyltransferase, induces cell proliferation, migration and EMT in HCC cells by interacting with Tiam1 (63). The increased expression of H3K27me3 is significantly correlated with vascular invasion in HCC (13). In the same way, overexpression of EZH2, a histone methyltransferase for H3K27me3, was found in HCC, and it is contributed to malignant transformation and poor prognosis (64). Expression of

H3K4me3 and its histone modifying enzyme (SMYD3) increased in HCC cell lines and tumor tissues, and high expression of H3K4me3 is correlated with short overall survival (35). Deacetylation of H3K18ac by SIRT7 contributes to HCC progression and high level of SIRT7 is related to poor overall survival (65). The P300/CBP-associated factor, one type of HAT, has a low expression in HCC, and it is demonstrated to inhibit HCC tumorigenesis both *in vitro* and *in vivo* (36). Moreover, several EMT transcription factors epigenetically regulate E-cadherin expression. Snail recruits LSD1 to demethylate H3K4me2 and mediates the transcriptional repression of E-cadherin (66). HDAC inhibitors are shown specifically induce apoptosis in hepatoma cells, but not in primary hepatocytes, and this result supports potential clinical application of HDAC inhibitors in treatment of HCC (67). Increasing evidences suggest that histone modification changes together with the aberrant expression of histone modifying enzymes are involving in development of HCC. However, the molecular mechanism and factors triggering the alteration of histone modifications in HCC have not been intensively investigated yet. As mention above, not only HCC carcinogenesis the elevation of ROS also implicates to the progression of HCC. Therefore, in this study, we think that oxidative stress is one of potential factors that alters the chemical modification of histones and contributes critically to HCC progression.

Chapter 3

Research Methodology

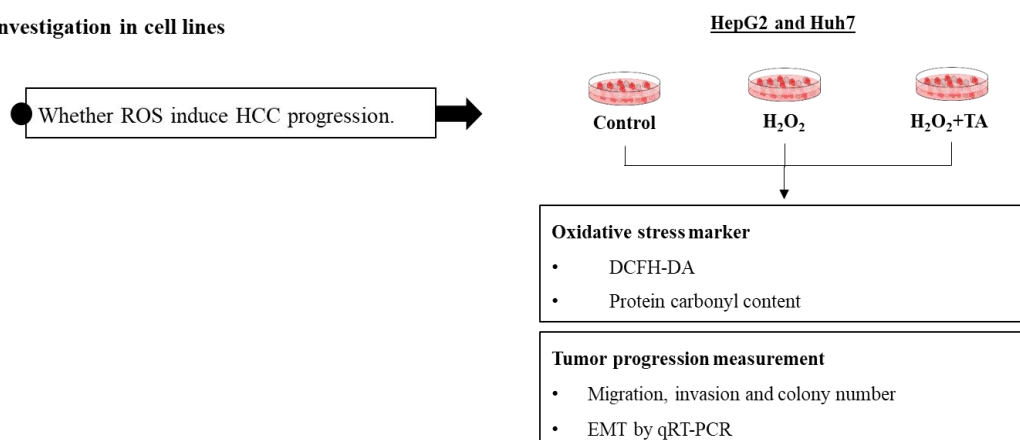
Study design

The whole study divided into two parts. The first part is an *in vitro* experimental analytical study in cell culture model to investigate the effect of ROS on HCC progression and elucidate the mechanism of ROS-induced tumor progression through histone modification changes. The second part is a cross-sectional observational analytical study in human HCC tissues to investigate the expression of genes that are epigenetically regulated and associated with ROS induced HCC progression.

Experimental design and workflow

The schematic workflow of the proposed study is shown in Figure 8. It is divided into 2 stages, first is to confirm the effect of ROS on increasing tumor progressive phenotype and altering histone modification pattern and identify the HCC progression-associated genes that are a result of ROS-induced chromatin remodeling, and the second to verify expression of the candidate proteins in human HCC tissues.

I. Investigation in cell lines



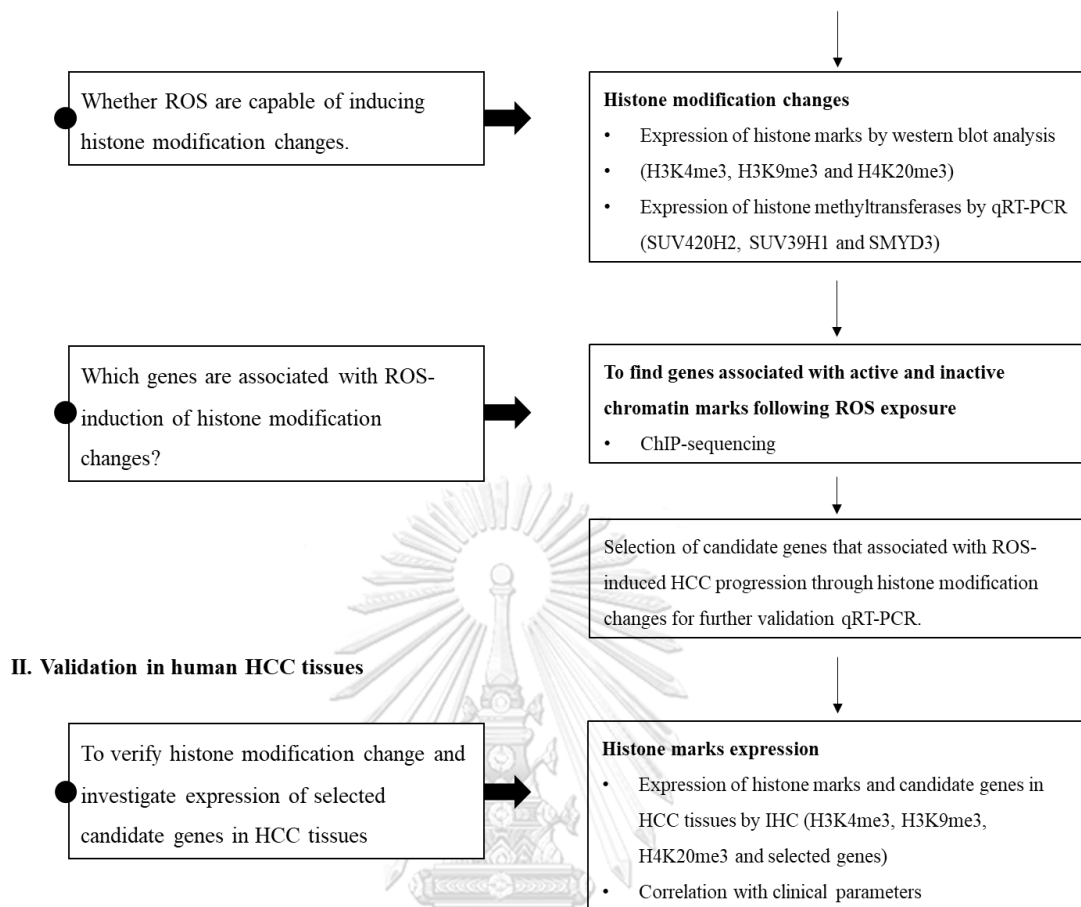


Figure 8 The experimental workflow

DCFH-DA = dichloro-dihydro-fluorescein diacetate, IHC = immunohistochemical staining, and ChIP-sequencing = chromatin immunoprecipitation sequencing

Cell culture experiment

Human liver cancer cells, HepG2 and Huh7, were obtained from Center of Excellence in Immunology and Immune-mediated diseases. HepG2 cells are hepatoma cell line whereas Huh7 cells are hepatocarcinoma cell line. The cells were maintained in Dulbecco's Modified Eagle Medium (DMEM), high glucose without sodium pyruvate (Hyclone, USA) containing 10% fetal bovine serum (FBS) (Hyclone, USA) and 1% non-essential amino acid (Gibco, USA) at 37°C in a humidified atmosphere containing 5% CO₂. The cell conditions were divided into 3 groups including untreated

control, hydrogen peroxide (H₂O₂), and H₂O₂ co-treatment with tocopheryl acetate (TA) in serum free medium.

Cell viability assay

To find the optimal concentration of H₂O₂ and TA, 5,000 cells/well were seeded into 96-well plate and were treated by various concentrations of H₂O₂ (10, 20, 30, 40, 50, 60, 70, 80, 100, and 200 μM) and TA (150, 300, 600, 1,200, and 2,400 μM). After 24-hour treatment, cells were incubated with 0.5 mg/mL of 3-(4,5-dimethylthiazol-2-yl)-2,5-diphenyltetrazolium bromide (MTT) (Invitrogen, USA) at 37°C for 1 hours. Formazan which is MTT product was dissolved in dimethyl sulfoxide (DMSO) and the absorbance was measured at 570 nm using microplate reader Tecan Infinite®200 Pro. Cell viability was calculated following this equation:

$$\% \text{ Cell viability} = \left\{ \frac{\text{OD}_{\text{treatment}}}{\text{OD}_{\text{control}}} \right\} \times 100$$

Oxidative stress biomarker measurement

Dichloro-dihydro-fluorescein diacetate (DCFH-DA) assay

DCFH-DA assay is a method for intracellular ROS detection by a fluorometric probe. DCFH-DA (non-fluorescent) is entered into the cells and converted into DCFH by cellular esterase. DCFH is converted into DCF (fluorescent) by intracellular ROS. To measure intracellular ROS following H₂O₂ and TA treatment, 10,000 cells/well were seeded in 96-well black plate, cultured overnight, and then incubated with media containing 0.5 mM DCFH-DA (Sigma Aldrich, USA) at 37°C for 30 minutes. After washing with phosphate buffer saline (PBS), H₂O₂ and TA was added, and the fluorescent intensity (excitation at 480 nm and emission at 535 nm) was immediately measured at initial time (T₀) and 60 minutes later (T₆₀). Arbitrary fluorescent unit (AFU) that proportionally reflects amount of ROS generated in cells was calculated following this equation (68);

$$\text{Arbitrary fluorescent unit (AFU)} = \frac{\text{Fluorescent intensity at T60}}{\text{Fluorescent intensity at T0}}$$

Protein carbonyl assay

Protein carbonyl assay is a method to detect the carbonyl group in amino acids which are oxidized by ROS. Extracted protein from each cell culture condition was incubated with 10 mM 2, 4-dinitrophenylhydrazin (DNPH) (TCI, Japan) for 1 hour in dark at room temperature. Then, cold 20% trichloroacetic acid (TCA) (Merck Millipore, USA) was added and solution was incubated for 10 minutes on ice. The pellet was collected by centrifugation at 10,000xg, 4°C for 15 minutes. Ethanol: ethyl acetate (ratio 1:1 V/V) (Merck Millipore, USA) was added to wash pellet followed by centrifugation at 10,000xg, 4°C for 20 minutes and discarded supernatant. The pellet was incubated in 6 M guanidine chloride (GdmCl) (Sigma Aldrich, USA) at 60°C for 30 minutes to dissolve the pellet. The solution was measured absorbance at 375 nm to calculate the protein carbonyl level following this equation (68):

$$\text{Protein carbonyl (nmol/mg protein)} = \frac{\text{Absorbance}_{375} \times 45.459 \text{ (nmol/L)}}{\text{Total protein concentration (mg/mL)}}$$

จุฬาลงกรณ์มหาวิทยาลัย
CHULALONGKORN UNIVERSITY

Total antioxidant capacity (TAC) measurement

TAC was measured using 2,2-diphenyl-1-picrylhydrazyl (DPPH) (Sigma Aldrich, USA) method. Absorbance of DPPH (freshly prepared in 80% methanol) at 517 nm was adjusted to 0.650 ± 0.020 prior to use. Five microliters of samples or water (blank) were added to 295 μ L of DPPH solution and mixed well. The mixture was incubated at room temperature for 30 min in dark. Absorption (A) at 517 was measured using microplate reader. Percentage of antioxidant activity (%AA) of each sample was calculated from: $\%AA = ((A_{\text{blank}} - A_{\text{sample}}) / A_{\text{blank}}) \times 100$. Vitamin C standard with known concentration (0, 0.25, 0.5 and 1 mM) was used to generate a standard curve (%AA vs.

vitamin C concentration). TAC of each sample was derived from standard curve and expressed as vitamin C equivalent antioxidant capacity (VCEAC).

RNA extraction and qRT-PCR analysis from cell culture

Total RNA was extracted from HepG2 and Huh7 cells using GF-1 total RNA extraction kit (Vivantis, Malaysia) according to the manufacturer's instructions. Cell pellet of each condition was collected and washed with PBS. The lysate was resuspended in lysis buffer and then the solution was transferred to the homogenized column. After centrifugation, the flow-through fraction was collected and 80% ethanol at the equal volume was added in the flow-through solution followed by centrifugation at 10,000xg for 1 minute. To precipitate RNA, flow-through solution was transferred into RNA binding column, centrifuged at 10,000xg for 1 minute and washed with wash buffer. To eliminate genomic DNA contaminant, all RNA samples were incubated with DNase I for 15 minutes at room temperature and centrifuged at 10,000xg for 1 minute. RNA was washed with wash buffer twice and RNAase-free water was added directly onto the membrane to elute and collected RNA sample by centrifugation.

The total RNA concentration was measured using Nanodrop Spectrophotometer. cDNA was synthesized from RNA sample by TaqMan™ Reverse Transcription kit (Thermo Scientific, USA) using 1 µg of RNA template. The expression level of interested genes was performed on QuantStudio™ 6 Real-Time PCR system. qRT-PCR was performed using SYBR Green PCR Master Mix (Biotechrabbit, Germany) and primers were shown in table 1. The relative amount of the target RNA was calculated by $2^{-\Delta\Delta CT}$ method and normalized against an endogenous control, glyceraldehyde 3-phosphate dehydrogenase (GAPDH).

Table 1 Primers used for qRT-PCR analysis

Primers	Sequences	Annealing temperature (°C)
NRF2	F: 5'-ACACGGTCCACAGCTCATC-3' R: 5'-TGCCTCCAAGTATGTCAATA-3'	60 (69)
NQO1	F: 5'-GAAGAGCACTGATCGTACTGGC-3' R: 5'-GGATACTGAAAGTTCGCAGGG-3'	60 (69)
SUV420H2	F: 5'-GGCCCGCTACTTCCAGAG-3' R: 5'-GCAGGATGGTAAAGCCACTT-3'	58 (18)
SUV39H1	F: 5'-GTCATGGAGTACGTGGGAGAG-3' R: 5'-CCTGACGGTCGTAGATCTGG-3'	60 (14)
SMYD3	F: 5'-TTCCCGATATCAACATCTACCAG-3' R: 5'-AGTGTGTGACCTCAATAAGGCAT-3'	60 (70)
E-cadherin	F: 5'-TGAGTGTCCCCCGGTATCTT-3' R: 5'-GAATCATAAGGCGGGGCTGT-3'	60 (71)
α -SMA	F: 5'-CCCTTGAGAAGAGTTACGAGTTG-3' R: 5'-ATGATGCTGTTGTAGGTGGTTTC-3'	60 (71)
MRE11	F: 5'-TAGCATCTCAGCAGCAACCA-3' R: 5'-TTTAAAGGCTCTTCTCTTTGAGAC-3'	58 (72)
TP53BP1	F: 5'-AGCAGGAGCTGGCTATATCCTTGA-3' R: 5'-GACAATGCTGATCCGCAATTAGAA-3'	58 (73)
RBBP8	F: 5'-ATTTGGCACTCTGGTGAGGG-3' R: 5'-GGACAGGTCAAATACCGCCT-3'	60
MMS22L	F: 5'-TGAGCGGGAATCTCTTCACA-3' R: 5'-AGCTGTCAGTCAGGAACGTC-3'	60
TONSL	F: 5'-ACCTGGGAGACTTTTTGGCT-3' R: 5'-CCCTAGCTGCTCACAGATGA-3'	60
DCLER1B	F: 5'-ATTGCTCTGCTGGGCTCTTT-3' R: 5'-CCAGTGGGATCTTCTCCACG-3'	60

BRCA1	F: 5'-GGGCCACACGATTTGACGGA-3' R: 5'-GAGCAGCAGCTGGACTCTGG-3'	60 (74)
BRCA2	F: 5'-TCCACACCTGTCTCAGCCCA-3' R: 5'-GCCACAACCTCCTTGGTGGCT-3'	58 (74)
p53	F: 5'-CCTCAGCATCTTATCCGAGTGG-3' R: 5'-TGGATGGTGGTACAGTCAGAGC-3'	58 (75)
p21	F: 5'-CCTGTCACTGTCTTGTACCCT-3' R: 5'-GCGTTTGGAGTGGTAGAAATCT-3'	58 (75)
TERF1	F: 5'-GCTGTTTGTATGGAAAATGGC-3' R: 5'-CCGCTGCCTTCATTAGAAAG-3'	60 (76)
TERF2	F: 5'-GACCTTCCAGCAGAAGATGCT-3' R: 5'-GTTGGAGGATTCCGTAGCTG-3'	60 (76)
POT1	F: 5'-TCAGATGTTATCTGTCAATCAGAACCT-3' R: 5'-TGTTGACATCTTCTACCTCGTATAATGA-3'	60 (76)
SOS1	F: 5'-GAGTGAATCTGCATGTCGGTT-3' R: 5'-CTCTCATGTTTGGCTCCTACAC-3'	58 (77)
JNK2	F: 5'-TACGTGGTGACACGGTACTACC-3' R: 5'-CACAACCTTTCACCAGCTCTCC-3'	58 (78)
c-Jun	F: 5'-CAGGTGGCACAGCTTAAACA-3' R: 5'-GTTTGCAACTGCTGCGTTAG-3'	58 (79)
MMP9	F: 5'-CTTTGGACACGCACGAC-3' R: 5'-CCACCTGGTTCAACTCAC-3'	58 (80)
RHOA	F: 5'-CTCATAGTCTTCAGCAAGGACCAGTT-3' R: 5'-ATCATTCCTGAAGATCCTTCTTATT-3'	58 (81)
ROCK1	F: 5'-TGAGGTTAGGGCGAAATGGT-3' R: 5'-AATCGGGTACAACCTGGTGCT-3'	58 (82)
LIMK2	F: 5'-GGGTGAAGATGTCTGGAG-3' R: 5'-TCGTTGACAGTCCTGTACC-3'	58 (83)
Radixin	F: 5'-GAATTTGCCATTCAGCCCAATA-3' R: 5'-GCCATGTAGAATAACCTTTGCTGTC-3'	58 (84)
SMAD2	F: 5'-CCGACACACCGAGATCCTAAC-3'	58

	R: 5'-GAGGTGGCGTTTCTGGAATATAA-3'	(85)
SMAD3	F: 5'-TGGACGCAGGTTCTCCAAAC-3'	58
	R: 5'-CCGGCTCGCAGTAGGTAAC-3'	(85)
SNAIL	F: 5'-CACTATGCCGCGCTCTTC-3'	58
	R: 5'-GGTCGTAGGGCTGCTGGAA-3'	
GAPDH	F: 5'- CAAGGTCACCATGACAACCTTG-3'	58
	R: 5'- GTCCACCACCCTGTTGCTGTAG-3'	

DNA extraction from HCC cells and qPCR for relative telomere length

Total DNA was extracted from HepG2 and Huh7 cells using GF-1 DNA extraction kit (Vivantis, Malaysia) according to the manufacture's instruction. To prepare working buffer TB and elution buffer, both of them were heated at 65°C until using. Briefly, cell pellet of each condition was collected after 72-treatment and washed with PBS. Lysate was completely resuspended in PBS. To break cells, proteinase K, lysis enhancer, and preheated buffer TB were added to lysate resuspension, then mixed by vortexing. After incubation at 65°C, 10 minutes, absolute ethanol were added into resuspension, and mix immediately by pipetting. Resuspension was transfer to column, centrifuged at 5,000xg, 1 minute, and discard flow through. To wash column, column was washed by washing buffer 2 times, and then column was dried by centrifugation at 10,000xg, 1 minute. Column was transferred to 1.5 microcentrifuge tube, added preheated elution buffer, and finally centrifuged at 5,000xg, 1 minute. DNA was stored at -20°C for further qPCR analysis.

DNA concentration was measured using Nanodrop Spectrophotometer. The expression of interested genes was used 3.12 ng of DNA concentration and primers were shown in table 2. qPCR was performed using SYBR Green PCR Master Mix (Biotechrabbit, Germany) and QuantStudio™ 6 Real-Time PCR system. The relative amount of the target DNA was calculated by $2^{-\Delta\Delta CT}$ method and normalized against to 36B4 gene as an endogenous control.

Table 2 Primers used for relative telomere length qPCR analysis

Primers	Sequences	Annealing temperature (°C)
Telomere	F: 5'-CGGTTTGTGGTTGGGTTTGGGTTT GGGTTTGGGTTTGGGTT-3' R: 5'-GGCTTGCCTTACCCTTACCCTTA CCCTTACCCTTACCCT-3'	54 (76)
36B4	F: 5'-CAGCAAGTGGGAAGGTGTAATCC-3' R: 5'-CCCATTCTATCATCAACGGGTACAA-3'	54 (76)

Whole protein extraction from cell culture

After 72-treatment, cells were washed by cold PBS and cell lysates were collected after centrifugation at 1,000xg for 4 minutes. To break cells, cell lysate was resuspended in RIPA buffer containing 1Xprotease inhibitor cocktail (#78429, Thermo Scientific, USA) and incubated on ice for 30 minutes. Cells were vortexed every 10 minutes for completely lyse. Cells were centrifuged at 10,000xg, 4°C for 10 minutes and then supernatant was transferred into a new 1.5 mL microcentrifuge tube and concentration of the extracted protein sample was determined by BCA method.

Histone protein extraction from cell culture

After treatment, cells were washed by cold PBS and cell lysates were collected after centrifugation at 1,000 rpm for 4 minutes. Cell lysates were resuspended in ice-cold hypotonic lysis buffer containing 1Xprotease inhibitor cocktail (#78429, Thermo Scientific, USA), 1 mM phenylmethylsulfonylfluorid (PMSF) and 1 mM dithiothreitol (DTT), and solution was rotated with rotating shaker at 4°C for 1 hour. After centrifugation, pellet intact nuclei were collected and resuspended in sulfuric acid (H₂SO₄) very well by rotating with shaker at 4°C overnight. To remove nuclear debris,

the suspension was centrifuged at 14,800xg, 4°C for 20 minutes and supernatant was transferred into a new 1.5 mL microcentrifuge tube. To precipitate histone proteins, ice-cold 100% TCA was added drop by drop, repeatedly mixed by inverting, and incubated the obtained milky solution on ice for 30 minutes. To collect histone pellet, cell pellet was centrifuged at 14,800xg, 4°C for 20 minutes. Histone pellet was collected carefully and washed twice with 100% acetone without disrupting the pellet. Removing supernatant carefully, histone pellet was allowed to dry for 20 minutes at room temperature. Histone pellet was dissolved in distilled water and concentration of the histone protein was measured by BCA method.

BCA assay for protein concentration determination

Total protein and histone protein concentration were measured by Pierce™ BCA Protein Assay Kit (#23225, Thermo Scientific, USA). To estimate concentration of protein, 25 µL of cell lysate from each cell culture condition was mixed with 200 µL of BCA reagent (reagent A: reagent B ratio 196 µL: 4 µL) and incubated at 37°C for 30 minutes. Bovine serum albumin (BSA) at 0.25, 0.5, 0.75, 1.0, 1.5 and 2 mg/mL were used as protein standards. The absorbance was measured at 562 nm by microplate reader Tecan Infinite®200 Pro. The standard curve was created by Microsoft Excel for protein concentration calculation.

Western blot analysis

For sample preparation, 1 µg of extracted histone protein of each sample was mixed with loading buffer and incubated at 95°C for 10 minutes to denature structure of protein. The denatured protein was loaded into the wells of 12% gel of SDS-PAGE and electrophoresed by at 100 volts for 20 minutes followed by 200 volts for 1 hour. The separating proteins were then transferred to PVDF membrane using Turbo transfer machine for 5 minutes. The membranes were incubated with 5% skimmed milk (Sigma Aldrich, USA) in TBS-T for 1 hour at room temperature for blocking of non-specific binding, and then incubated with primary antibodies (**1:10,000 H4K20me3 (ab9053, Abcam, UK)**, **1:25,000 H3K9me3 (ab8898, Abcam, UK)** and **1:25,000 H3K4me3**

(ab8580, Abcam, UK), 1:1000 Histone H4 (#2935, Cell Signaling, USA) and 1:25000 Histone H3 (#14269, Cell Signaling, USA) as internal controls) at 4°C overnight. After washing with TBS-T for 10 minutes 3 times, membrane was incubated with HRP-conjugated secondary antibodies (anti-rabbit IgG #7074, Cell Signaling, USA, and anti-mouse IgG #81-6520, ZyMax™, USA) at room temperature for 1 hour, and then washed with TBS-T. Chemiluminescent substrate was applied to membrane and specific immunocomplex SuperSignal™ West Femto Maximum Sensitivity Substrate (#34095, Thermo Scientific, USA) was visualized under the chemiluminescent imager.

Transwell assay for cell migration study

After HepG2 and Huh7 cells were treatment for 72 hours, then 5×10^4 cells in 100 μ L DMEM without FBS were seeded into 96-transwell chambers with a pore size of 8 μ m. Two hundred and seventy-five μ L of fresh medium with 10% FBS was added to the bottom chamber. After 24-hour incubation, cells that had migrated to the lower chamber were trypsinized and transferred into medium with FBS. One hundred microliters of resuspended solution were incubated with 25 μ L CellTiter-Glo® (Promega) at room temperature for 10 minutes. Luciferase activity was measured by laminator using Tecan infinite®200 PRO.

Boyden Chamber Transwell assay for cell invasion study

Transwell assay is used to examine the motility and invasion activity of the cells. This method can quantify the number of the invaded cells. The transwell device is divided into two parts, upper and lower parts. At beginning, transwell chambers (upper part) containing 8- μ m-pore-size membranes with matrix gel were rehydrated in media with serum for 1 hour at 37°C. Then, cells (approximately 2×10^5 cells for HepG2 and 4×10^5 cells for Huh7) in serum-free media were added to the upper compartment of the transwell chambers. Media supplemented with 10% FBS was added to the lower chamber to function as chemoattractant. The upper compartment

is then inserted into the lower chamber and incubated for 24 hours to allow the cells invade through matrix proteins to the other side of membrane. After 24 hours, non-invaded cells in the upper compartment were removed using a cotton-tipped swab. Invaded cells at the lower side of membrane were fixed with 10% paraformaldehyde for 10 minutes, and stained with 1% crystal violet in 2% ethanol. Finally, invaded cells were photographed and counted under microscope.

Clonogenic assay for cell survival study

Clonogenic assay is used to evaluate cell survival assay based on the ability of single cells to grow into colony. After 72-hour treatment, 1×10^3 and 2×10^3 cells (HepG2 and Huh7, respectively) per well were seeded into 6-well plate and grown in media with 10% FBS at 37 °C with CO₂ (10 days for HepG2 and 14 days for Huh7). After media removing, cells were fixed and stained with FixNStain solution containing 4% formaldehyde and 0.1% crystal violet for 10 minutes. Cells were washed with tap water and allowed them dry at room temperature. Cells were photographed and counted using AlphaView SA software.

Chromatin immunoprecipitation (ChIP)

Chromatin immunoprecipitation or ChIP is a powerful method to identify genome-wide DNA binding sites for transcription factors and the other proteins. According to the manufacture of Magna ChIP™ HiSen Chromatin Immunoprecipitation Kit (Merck Millipore, USA), approximately 5×10^6 cells were required for each condition. After 72-hour treatment, cells were fixed with 1% formaldehyde for 10 minutes at room temperature. To quench excess for excess formaldehyde, cells were incubated with glycine for 5 minutes at room temperature, placed dish on ice and washed with PBS containing protease inhibitor cocktail twice. Cells were scraped in PBS containing protease inhibitor cocktail, transferred into a new 1.5 mL microcentrifuge tube and centrifuged at 800xg, 4°C for 5 minutes. Then, Cell pellet was collected and resuspended in nuclei isolation buffer containing protease

inhibitor cocktail. Cell suspension was incubated on ice for 15 minutes, vortexed every 5 minutes and centrifuged at 800xg, 4°C for 5 minutes. Chromatin pellet was collected followed by resuspending in SCW buffer containing protease inhibitor, and then chromatin was sheared by sonication. The expected size of sheared cross-linked DNA bp was 200-1000 bp. Five nanograms of sheared chromatin was incubated with Protein A/G Magnetic Beads in SCW buffer and 3 µg of primary antibodies at 4°C overnight with rotating shaker. Primary antibodies included **H4K20me3 (ab9053, Abcam, UK)** and **H3K4me3 (ab8580, Abcam, UK)**. After washing with SCW buffer containing protease inhibitor cocktail 3 times, the beads were resuspended in low stringency buffer containing protease inhibitor cocktail and transferred into a new tube. The solution was resuspended in ChIP elution buffer and chromatin was eluted from magnetic beads. Then, chromatin was treated with Proteinase K at 65°C for 2 hours and then at 95°C for 15 minutes to purify DNA. Purified ChIP DNA was transferred into a new tube and prepared for further sequencing.

TruSeq ChIP-Seq Protocol

To start the protocol with end repair procedure, 10 ng of ChIP-DNA were mixed with Resuspension Buffer and End Repair Mix solution, then placed the tubes on the pre-heated thermal cycler at 30°C for 30 minutes. End-Repaired DNA was incubated with well-mixed AMPure XP beads at room temperature for 5 minutes and placed the tube on magnetic stand for 5 minutes. Beads were resuspended in 80% ethanol without disrobing the beads, incubated for 30 seconds, and removed supernatant twice. Beads were dried and resuspended in Resuspension Buffer. After incubation, the tubes were placed on magnetic stand and supernatant were transferred into the new tube. The next step is adenylated 3' ends. DNA was mixed with Resuspension Buffer and A-Tailing Mix to each tube. Tubes were placed on pre-programmed thermal cycler following pre-heat lid option and set to 100°C, 37°C for 30 minutes, 70°C for 5minutes and hold at 4°C, and proceeded immediately to ligate adapters. DNA solution was incubated with Resuspension Buffer, Ligation Mix and RNA Adaptor at 30°C for 10 minutes, and removed tubes from thermal cycler. Stop Ligation Buffer and AMPure XP beads and

adapter ligated dsDNA were added and incubated for 5 minutes. Pellet was collected and washed with 80% ethanol twice. Dried bead was resuspended in Resuspension Buffer and placed on magnetic stand. 50 μ L of supernatant were incubated with AMPure beads and washed with 80% ethanol for 2 times. Then, beads were dried and resuspended in Resuspension Buffer, and 20 μ L of supernatant were prepared for enrich DNA fragmentation. Supernatant was mixed with PCR Primer Cocktail to the adapter ligated ds cDNA and PCR Master Mix following this programmed thermal cyclers; 98°C for 30 seconds, 18 cycles of : 98°C 10 minutes, 60°C 30 seconds and 72°C 30 seconds, 72°C for 5 minutes, and hold at 4°C. After that PCR product were mixed with AMPure XP beads with gently pipetting 10 times and placed the tubes on magnetic stand. After washing with 80% ethanol twice, dried beads were dissolved in Resuspend Buffer and 17 μ L of supernatant were collected into a fresh PCR tube. Finally, to validate library, the concentration of DNA was measured using the Qubit HS Assay, and run a Bioanalyzer DNA1000 Chip. Data from ChIP-seq were analyzed using PiGx ChIPseq analysis.

Gene Ontology (GO) and KEGG pathway data analysis

Gene Ontology or GO is the international standard classification of gene function. The selected genes were classified via GO analysis. KEGG pathway is a database of pathway maps representing the molecular interaction, reaction and relation networks. Online tool DAVID (<https://david.ncifcrf.gov/>) was employed for GO analysis and KEGG pathway. Important biological functions were enriched via significance analysis. Genes were classified using p value < 0.05 and fold enrichment > 1.5 in both GO and KEGG pathway analysis.

Sample population for immunohistochemical study

The number of HCC tissue was calculated that based on the prevalence of H3K9me3 in HCC in previous study (13).

$$n = \frac{Z^2 P(1-P)}{d^2}$$

n = number of samples

Z = level of confidence at 95% CI (1.96)

P = prevalence rate

d = proportion of sampling error which is 10% confidence limit

$$n = \frac{(1.96)^2 \times 0.548 (1-0.548)}{(0.1)^2}$$

$$n = 95.3$$

Therefore, total number of HCC tissues was approximately 95 cases for immunohistochemical study.

จุฬาลงกรณ์มหาวิทยาลัย
CHULALONGKORN UNIVERSITY

Paraffin-embedded HCC tissues

Cancer liver tissues were obtained from patients with HCC at King Chulalongkorn Memorial Hospital admitted to the hospital between 2009 to 2015. The HCC tissues and clinical data of patients were collected and archived (n=100) by Prof. Nuttiya Hirankarn and Prof. Pisit Tangkitvanich. Inclusion and exclusion criteria were shown below;

Inclusion criteria

1. Both males and females aged over 18 years old
2. Diagnosed as HCC patients with histological proof

Exclusion criteria

1. Pregnant HCC patients
2. Other cancers

Immunohistochemical staining

To detect expression of antigens of interest in tissues, immunohistochemical (IHC) staining was performed. Initially, the tissue sections were deparaffinized and rehydrated with xylene, and ethanol with concentration ranking from high to low concentration (100%, 95%, 80% and 75%) and finally soaked in distilled water. Antigen retrieval was performed in sodium citrate buffer (pH 6.0) and then sections were washed by PBS-T (1XPBS, 100 μ L/L TritonX-100) for 5 minutes and distilled water 5 minutes, respectively. Endogenous peroxidase was inactivated by incubation with 0.3% H₂O₂ in distilled water for 30 minutes. Non-specific binding was blocked by incubating in 10% normal goat serum (VECTASTAIN® Elite ABC-HRP kit, PK7200) for 1 hour. Primary antibodies (**1:250 H4K20me3 (ab9053, Abcam, UK), 1:500 H3K9me3 (ab8898, Abcam, UK), 1:500 H3K4me3 (ab8580, Abcam, UK) and 1:150 RBBP8 (ab117722, Abcam, UK)**) were applied and incubated at 4 °C, overnight. After incubation, sections were washed by PBS-T for 3 times for 3 minutes each. Secondary antibody conjugated with horseradish peroxidase (HRP) (VECTASTAIN® Elite ABC-HRP kit, PK7200) was applied and incubated for 1 hour at room temperatures and then sections were washed again by PBS-T for 3 times. Sections were incubated with ABC reagent (VECTASTAIN® Elite ABC-HRP kit, PK7200) for 30 min followed by washing 3 time with PBS-T. For color development, sections were immersed in 0.2% 3, 3'-diaminobenzidine (DAB) with 0.005% H₂O₂ for 3-5 minutes and then rinsed with distilled water. Haematoxylin was used for counterstaining. Finally, stained sections were dehydrated with ethanol starting from at low to high concentrations and mounted with mounting solution. The sections were visualized under light microscope to evaluate the expression level of each antigen.

For relative level of expression, IHC score was calculated from a score of the positive cells multiplied by a score of the intensity level (score shown in table 3), averaged from all of microscopic fields (40x). Therefore, the IHC score ranges from 0 to 16. Adjacent non-cancerous liver tissues obtained from the HCC patients were used as controls to compare the IHC expression level of each antigen.

Table 3 16-point scale scoring criteria used for histone methylation IHC score calculation

Grayscale intensity		Positive cells		
Intensity level		Score	%Positive cells	Score
Histone methylation	RBBP8			
>150-180	>180-200	0	0%	0
>120-150	>150-180	1	>0-25%	1
>90-120	>120-150	2	>25-50%	2
>60-90	>90-120	3	>50-75%	3
30-60	60-90	4	>75-100%	4

Statistical analysis

The data was presented as mean \pm standard deviation (SD). Categorical data were showed as frequency and percentage. Student's t-test or Mann-Whitney test or unpaired t-test was used for comparison of variables between the two independent groups. One-way analysis of variance (ANOVA) was used for three group comparisons. Kaplan-Meier curve analysis was used to find the association of H4K20me3 expression with survival data. GraphPad Prism version 9.0 was used for all graphs and calculations. *P-value* < 0.05 was considered as statistically significant.

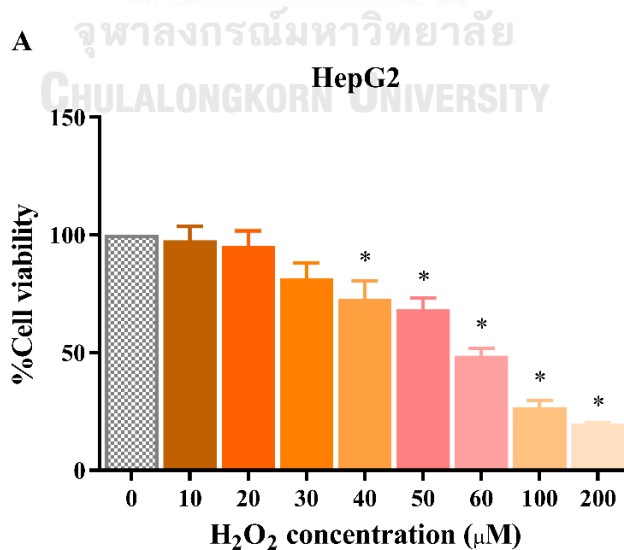
Chapter 4

Results

Cell viability following H₂O₂ treatment in HCC cell lines

To examine the optimal concentrations of hydrogen peroxide (H₂O₂) and tocopherol acetate (TA, acted as antioxidant) treatments in HCC cell lines, HepG2 and Huh7 cells were treated with various concentrations of each testing substance. MTT assay was performed after the 24-h treatment. Subsequently, cell viability (% of control) and inhibitory concentration 50% (IC₅₀) were determined.

Viability of HepG2 and Huh7 cells following the H₂O₂ treatment (10-200 μM for HepG2 and 30-200 μM for Huh7) are shown in figure 9. The viability of HepG2 cells was significantly decreased at 40 μM H₂O₂ treatment compared with the untreated control, but in Huh7 cells it was significantly decreased at 70 μM. The IC₅₀ of H₂O₂ was 58.48 μM for HepG2 cells and 86.05 μM for Huh7 cells. These results indicated that HepG2 cells was more sensitive to H₂O₂ than the Huh7 cells. Nevertheless, the sub-lethal doses of H₂O₂ (30 μM for HepG2 and 60 μM for Huh7) were used for the further experiments.



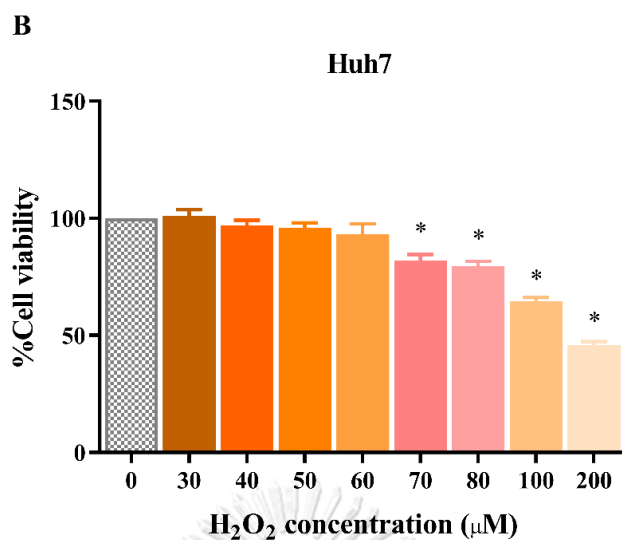


Figure 9 Cell viability of HepG2 (A) and Huh7 (B) treated with various concentrations of H₂O₂. For further experiments, sub-lethal doses of 30 μM and 60 μM were selected for HepG2 and Huh7, respectively. (* p<0.05 vs. control)

The cytotoxicity of TA was evaluated. As shown in figure 10, TA at concentration varied from 150-2400 μM showed no toxicity to both HepG2 and Huh7 cells. However, 600 μM TA was selected for the further H₂O₂ co-treatment experiment.

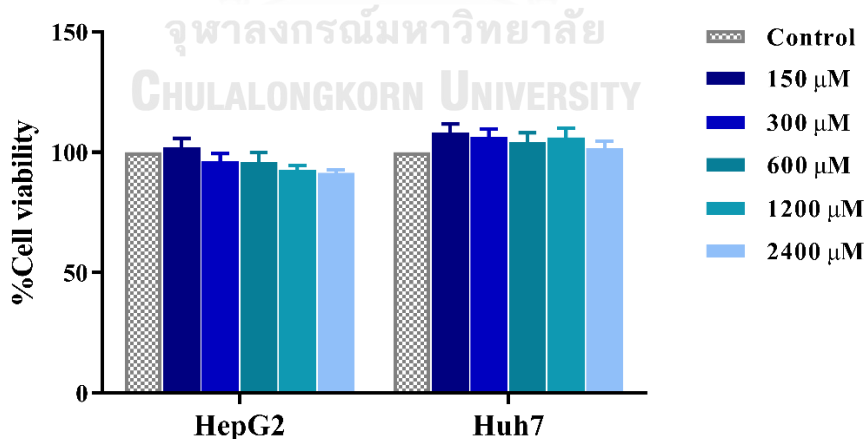


Figure 10 Cell viability of HCC cells following the tocopherol acetate (TA) treatment TA at concentrations between 150 and 2400 μM was not significantly toxic to HepG2 and Huh7 cells.

H₂O₂ induced oxidative stress in HCC cell lines

To induce the oxidative stress in HCC cell lines, HepG2 and huh7 were treated with the sub-toxic doses of H₂O₂ for 72 h. Co-treatment with TA, antioxidant, was investigated as an inhibitory model. DCFH-DA and protein carbonyl content were measured as oxidative stress markers.

The level of intracellular ROS measured by the DCFH-DA assay showed that the arbitrary fluorescent unit (AFU, indicated the amount of ROS production in the cells) in cells treated with H₂O₂ alone, 30 μ M in HepG2 and 60 μ M in Huh7, was significantly increased compared with the untreated control (Figure 11). In contrast, the AFU was significantly decreased in cells co-treated with 600 μ M TA compared with the cells treated with H₂O₂. These results indicated that H₂O₂ at sub-toxic concentrations could induce the production of intracellular ROS both in HepG2 and Huh7 cells, and TA antioxidant could reduce the intracellular ROS production induced by H₂O₂.

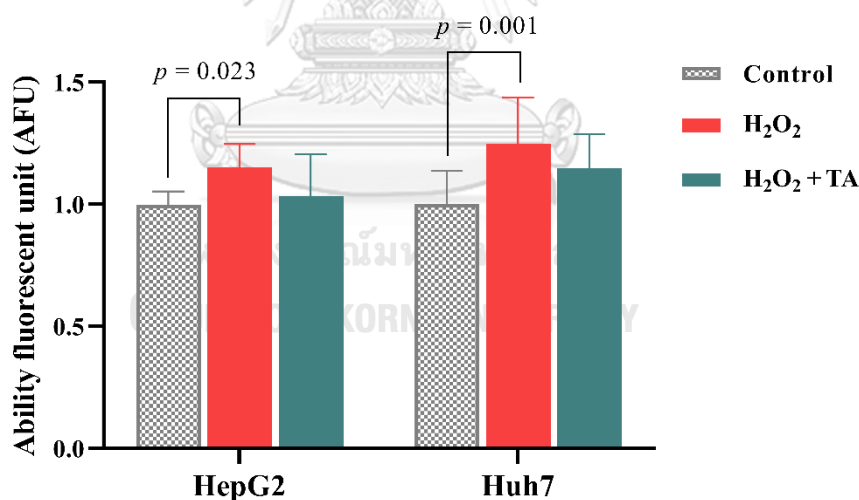


Figure 11 Intracellular ROS production in HCC cells measured by DCFH-DA assay

The intracellular ROS production was significantly increased following the H₂O₂ treatment, but it was significantly reduced by the antioxidant (TA) co-treatment.

The level of protein carbonyl content was significantly increased in H₂O₂-treated HepG2 and Huh7 cells compared with the untreated control (Figure 12). After co-treatment with TA, the protein carbonyl content was significantly decreased in HepG2, but not Huh7 cells, relative to the H₂O₂ treatment. These results demonstrated that H₂O₂ at sub-lethal doses could induce oxidative stress. Conversely, co-treatment with antioxidant could prevent the induction of oxidative stress by H₂O₂ in HCC cell lines.

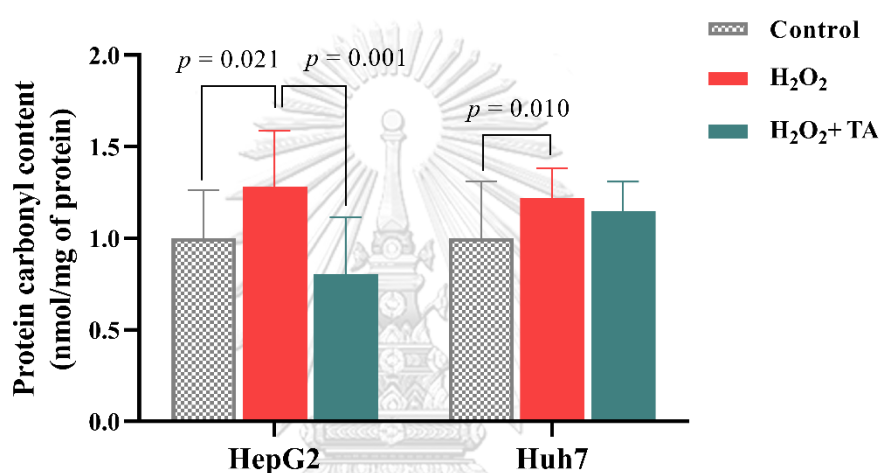


Figure 12 Protein carbonyl content in HCC cells following the H₂O₂ treatment. The protein carbonyl content was significantly increased in cells exposed to H₂O₂, but it was significantly decreased in the co-treatment with TA (in HepG2 cells).

To examine genes that respond to oxidative stress, nuclear factor erythroid 2-related factor 2 (NRF2) and its downstream target, NAD(P)H dehydrogenase quinone 1 (NQO1), were investigated in H₂O₂-treated HCC cell lines. NRF2 transcript expression was up-regulated in HepG2 and Huh7 treated with H₂O₂ compared with the untreated control (Figure 13). After co-treatment with TA, NRF2 was down-regulated relative to the H₂O₂ treated cells, and the effect was more pronounced in the Huh7 cells. These results suggest that H₂O₂ at sub-lethal concentration could activate NRF2 mRNA expression, but TA could attenuate NRF2 expression in HCC cell lines.

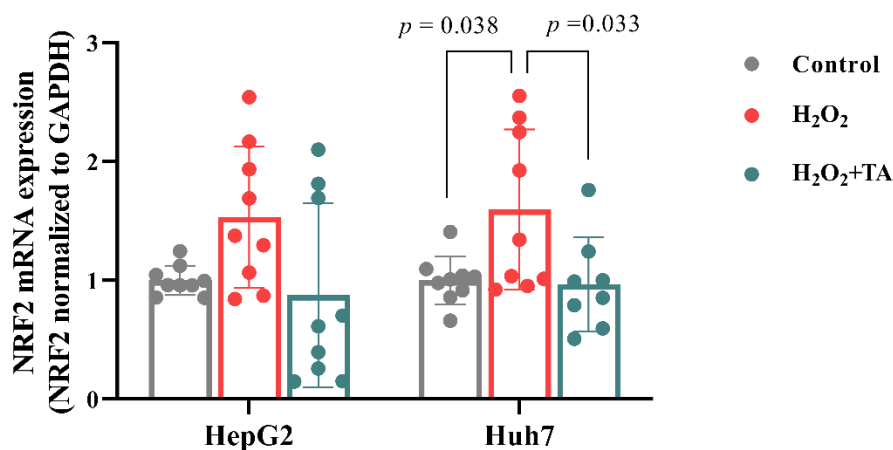


Figure 13 The mRNA expression of NRF2 in HCC cells following the H₂O₂ treatment. NRF2 mRNA expression was increased in cells treated with H₂O₂, but it was decreased in the co-treatment with TA.

NOQ1 mRNA expression was significantly increased in HepG2 and Huh7 cells treated with H₂O₂ compared with the untreated control (Figure 14). After co-treatment with TA, the NOQ1 mRNA expression was decreased in both cells relative to the H₂O₂ treatment. These results suggest that H₂O₂ at sub-lethal concentration could up-regulate the NOQ1 mRNA expression in response to oxidative stress. TA could reduce the NOQ1 mRNA expression in HCC cells exposed to H₂O₂.

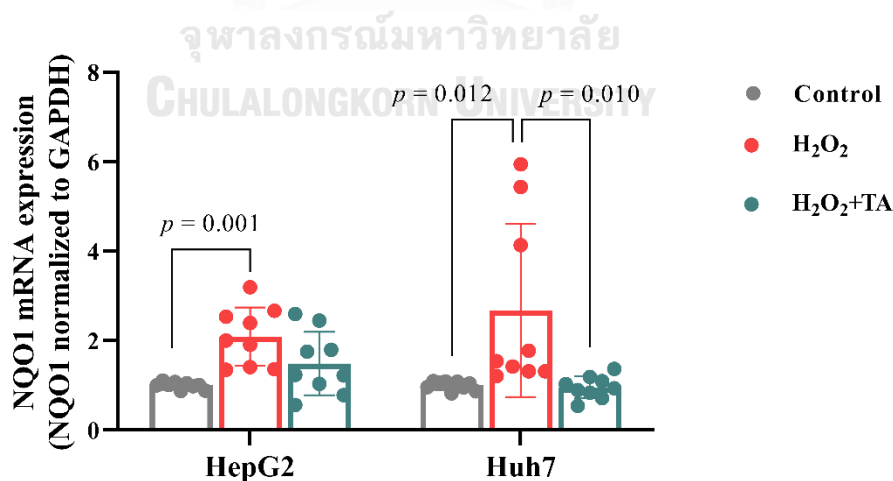


Figure 14 The mRNA expression of NOQ1 in HCC cells following H₂O₂ treatment. NOQ1 mRNA expression was increased in cell treated with H₂O₂, but it was decreased in co-treatment with TA.

DPPH assay was performed for total antioxidant capacity (TAC) measurement in HCC cell lines treated with H₂O₂. The level of TAC was significantly decreased in H₂O₂-treated cells compared with the untreated control (Figure 15). In HepG2 cells, co-treatment with TA at 600 μ M showed a significant increase in TAC level relative to the H₂O₂-treated condition. In Huh7 cells, the TAC level in cells co-treated with TA was slightly increased compared with the H₂O₂ treatment.

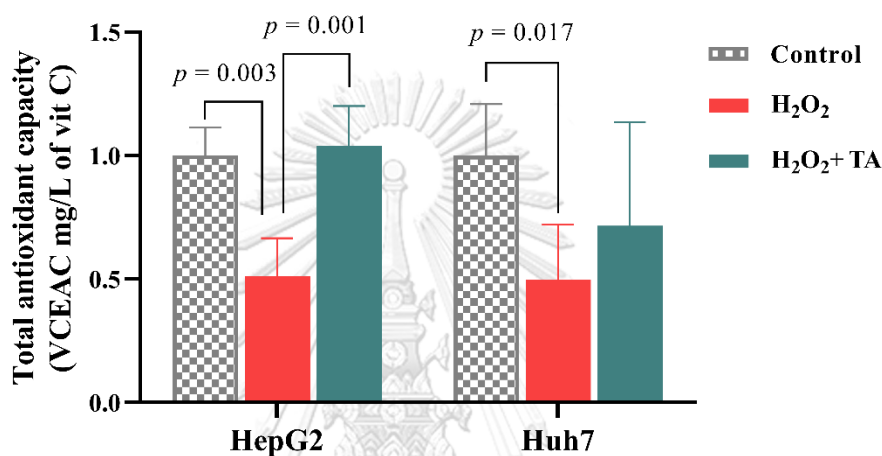


Figure 15 Total antioxidant capacity in HCC cells following H₂O₂ treatment measured by DPPH assay. The total antioxidant was significantly decreased in cells exposed to H₂O₂, but it was increased in the co-treatment with TA.

Oxidative stress promoted epithelial-mesenchymal transition (EMT)

To investigate whether ROS could induce epithelial-mesenchymal transition or EMT in HCC cells, E-cadherin and α -SMA expression were measured in HCC cells treated with H₂O₂ for 72 h. The mRNA expression of E-cadherin was significantly decreased in cells treated with H₂O₂, compared with the untreated control (Figure 16). On the other hand, E-cadherin was significantly increased in cells co-treated with TA relative to the H₂O₂-treated condition.

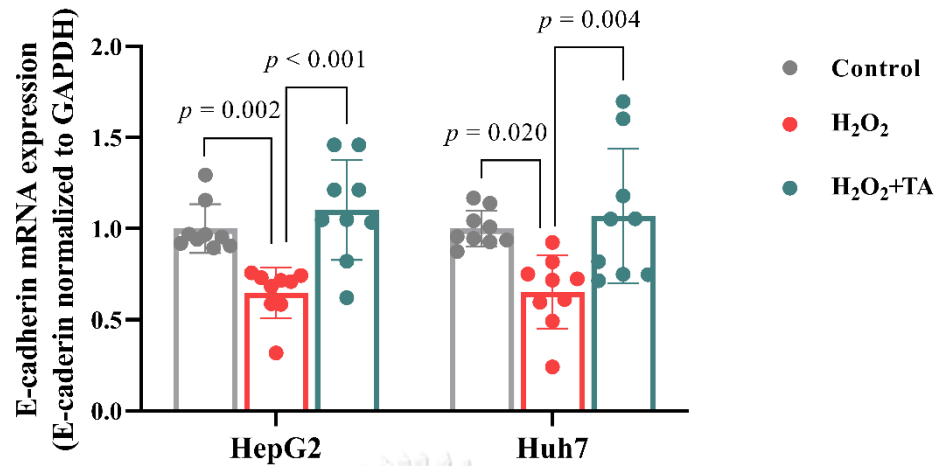


Figure 16 The mRNA expression of E-cadherin in HCC cells following H₂O₂ treatment. E-cadherin mRNA expression was significantly decreased in H₂O₂, but it was significantly increased in co-treatment with TA.

The transcript expression of α -SMA was significantly increased in HepG2 cells treated with H₂O₂ compared with the untreated control (Figure 17). Conversely, α -SMA was slightly decreased in cells co-treated with TA relative to the H₂O₂-treated condition. In Huh7 cells, α -SMA mRNA expression was also significantly increased following the H₂O₂ treatment compared with the untreated control. Co-treatment with TA could decrease α -SMA mRNA expression in H₂O₂-treated Huh7, although it was not statistically significant.

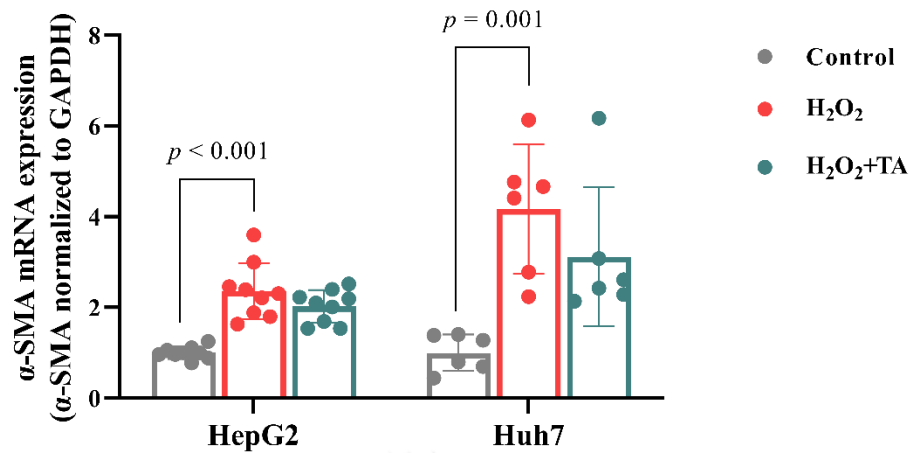


Figure 17 The mRNA expression of α -SMA in HCC cells following H₂O₂ treatment. α -SMA mRNA expression was significantly increased in H₂O₂, but decreased in the co-treatment with TA.

Oxidative stress induced cancer progression in HCC cell lines

To determine aggressiveness of HCC cells induced by H₂O₂, cell migration, invasion and colony formation were performed. HepG2 cells treated with H₂O₂ had significantly higher migrated cells than the untreated control (Figure 18). After co-treatment with TA, the number of migrated cells were lower than the H₂O₂-treated condition, but not statistically significant. In Huh7 cells, cell migration was significantly increased following treatment with H₂O₂ compared with untreated control.

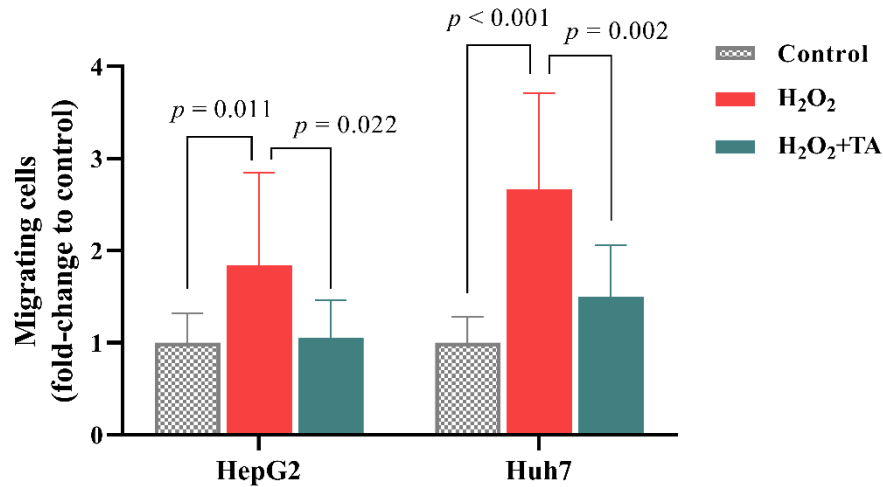
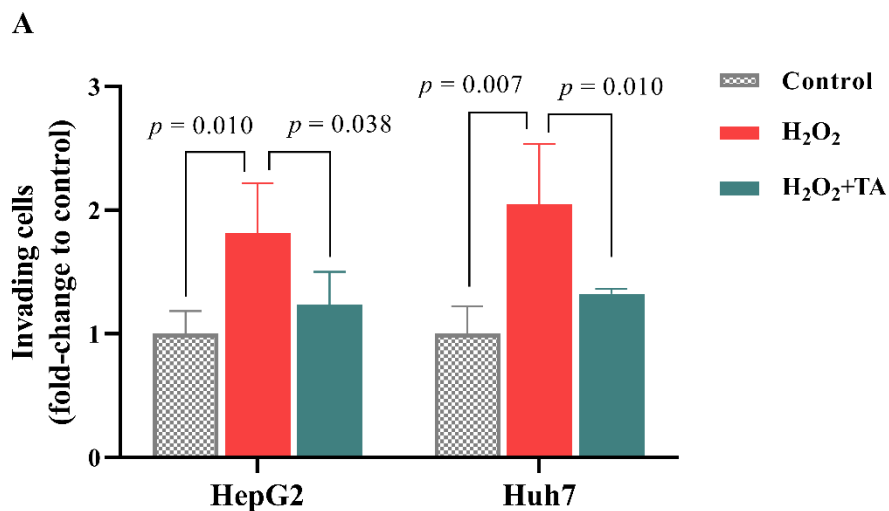


Figure 18 Cell migration in HCC cells measured by transwell assay

Migrating cells were increased in cells exposed to H₂O₂, but it was reduced by the co-treatment with TA.

For cell invasion, HepG2 cells treated with H₂O₂ had number of invaded cells significantly higher than the untreated control (Figure 19). Co-treatment with TA significantly reduced the number of invaded cells relative to the H₂O₂ treatment. In the same way, Huh7 treated with H₂O₂ invaded more than the untreated control. Co-treatment with TA significantly decreased the number of invaded cells compared with the H₂O₂ treatment.



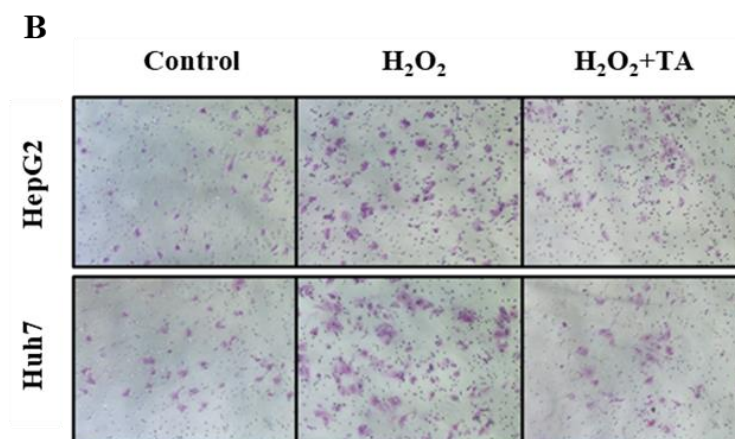


Figure 19 Cell invasion in HCC cells measured by Boyden chamber assay (A) Invading cells were increased in cells treated with H₂O₂, but it was reduced by co-treatment with TA. (B) Micrograph of invading cell in HCC cell lines after crystal violet staining. Invading cells were increased in cells treated with H₂O₂, but it was reduced by co-treatment with TA.

To investigate capability of cell survival and colony formation in HCC cells treated with H₂O₂, the clonogenic assay was carried out. Both HepG2 and Huh7 cells treated with H₂O₂ had significantly higher colony number than the untreated control (Figure 20). Co-treatment with TA significantly decreased the colony number in Huh7 cells, but not HepG2, compared with the H₂O₂ treatment.

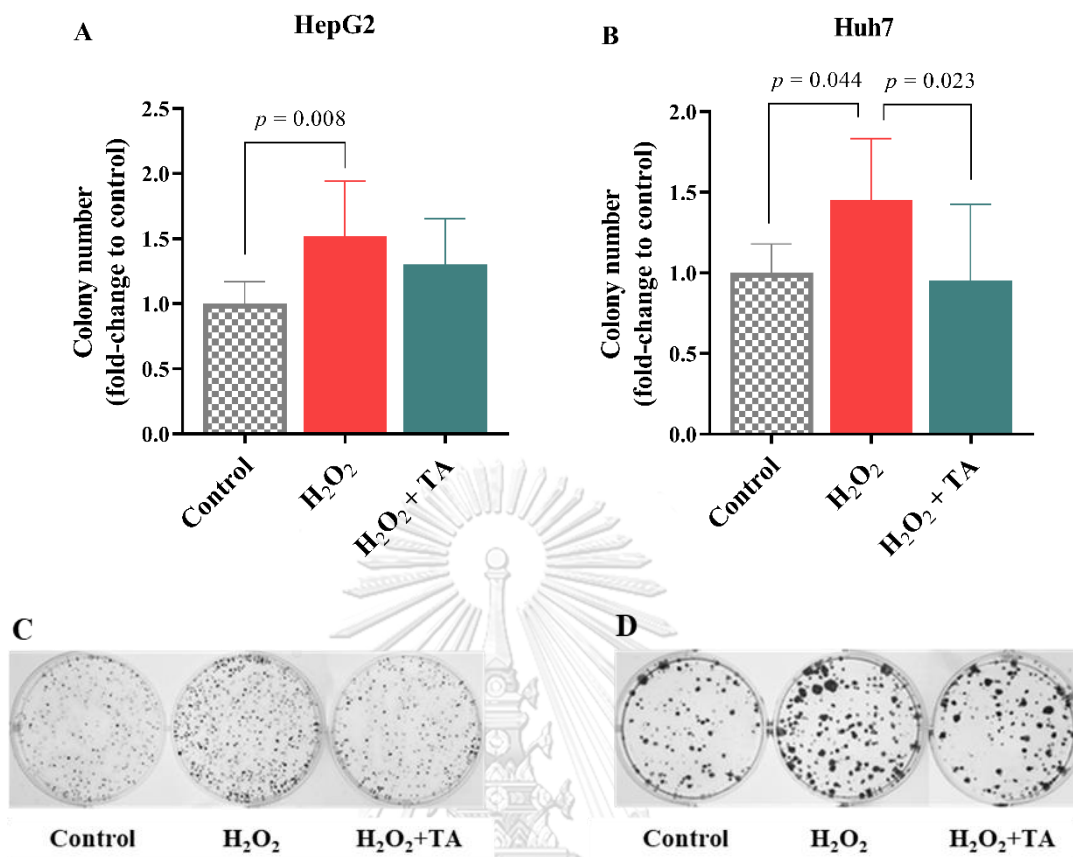
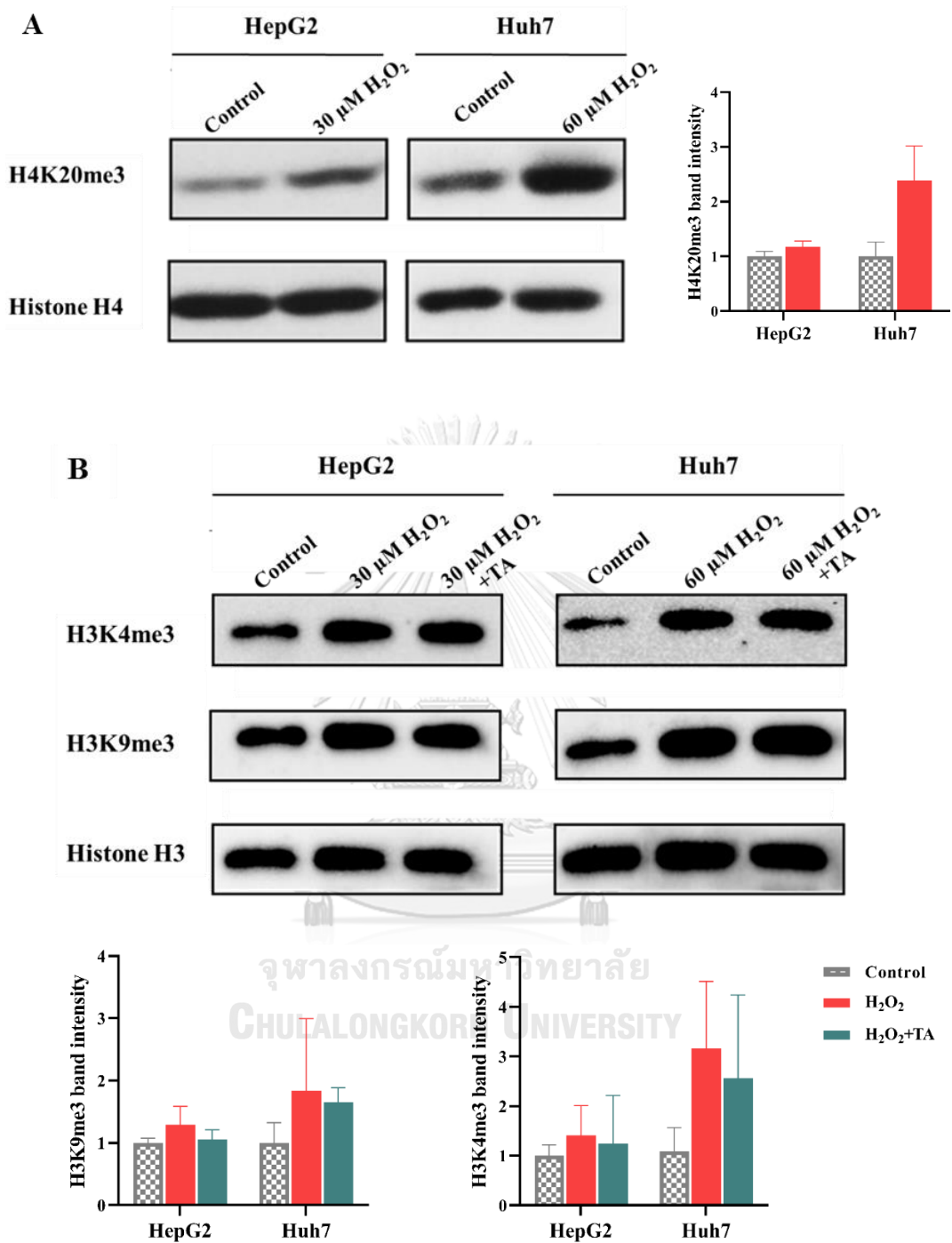


Figure 20 Colony number in HCC cells measured by clonogenic assay (A, B) Number of colonies were increased in cells exposed to H₂O₂, but reduced by co-treatment with TA. (C, D) Micrograph of colony formation number in HCC cells following H₂O₂ treatment.

Oxidative stress altered histone modifications in HCC cell lines

Changes in H4K20me₃, H3K9me₃ and H3K4me₃ expression in HCC cells treated with H₂O₂ were determined using western blot analysis. The results revealed that all of these histone marks were upregulated in both HepG2 and Huh7 cells treated with H₂O₂ compared with the untreated control (Figure 21). The expression of H3K9me₃ and H3K4me₃ were likely attenuated by the co-treatment with TA in both cell lines (Figure 21).



Expression of histone modifying enzyme for each histone mark following H₂O₂ treatment were investigated. The mRNA expression SUV420H2 (for H4K20me₃), SUV39H1 (for H3K9me₃), and SMYD3 (for H3K4me₃) were increased in HepG2 cells treated with H₂O₂ compared with the untreated control (Figure 22). Co-treatment with TA apparently reduced these histone modifying enzymes compared with the H₂O₂ treatment. These results suggested that increased H4K20me₃, H3K9me₃, and H3K4me₃ expression in H₂O₂-treated HCC cells may be caused by increased expression of SUV420H2, SUV39H1, and SMYD3.

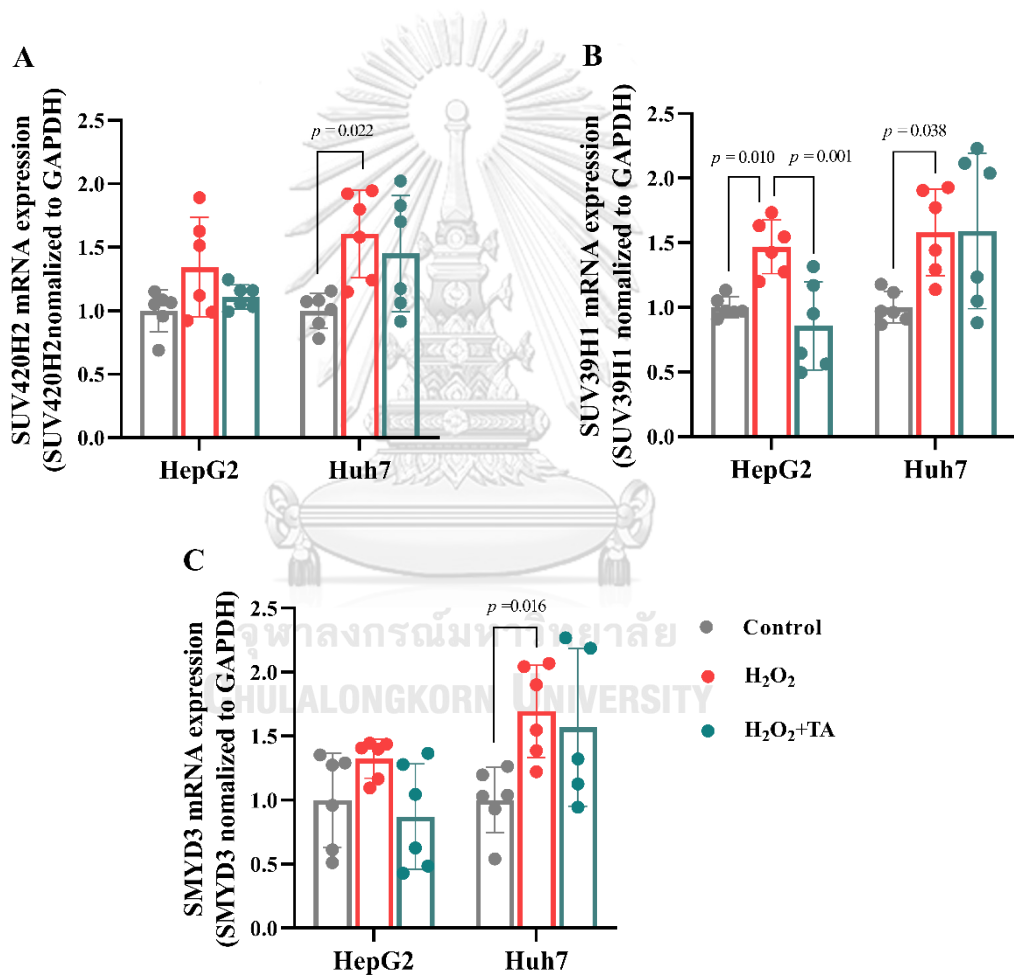


Figure 22 Histone methyltransferase enzyme mRNA expression in HCC cells treated with H₂O₂. The mRNA level of SUV420H2, SUV39H and SMYD3 were generally increased in H₂O₂-treated condition, and co-treatment with TA could attenuate their expression.

Distribution of gene profile in HCC cells by ChIP-seq

ChIP-seq was performed to identify protein-coding genes that were regulated by H4K20me3 and H3K4me3 in HCC cells under the oxidative stress condition. HepG2 cells were treated with 30 μ M H₂O₂ and Huh7 cells were challenged with 60 μ M H₂O₂ for 72 h. According to ChIP-seq data, the profile of protein-coding genes associated with H4K20me3 formation is displayed Figure 23. There were 12,111 protein-coding genes enriched for H4K20me3 in the untreated HepG2 cells. About 44.4% of genes were located at promoter or transcriptional start site (TSS), 29.5% at intron, 12.7% at intergenic, 11.7% at exon, and 1.8% at TTS (transcriptional terminal site). The number of protein-coding genes enriched for H4K20me3 in H₂O₂-treated HepG2 cells were 12,953 genes. Most of these identified sequences were located at the gene promoters (58.8%), and the rest were found in introns (21.7%), intergenic (8.5%), exons (7.5%) and TTS (3.4%). In Huh7 cells, the number of identified protein-coding genes enriched for H4K20me3 in H₂O₂-treated condition and untreated control were 12,081 and 17,895 genes, respectively. In untreated Huh7 cells, about 40.0% of the sequences were found at promoter sites, 33.3% at introns, 13.5% at intergenic, 8.2% at exons, and 5.0% at TTS sites. In H₂O₂-treated Huh7 cells, the identified sequences were located at promoters (40.0%), introns (35.5%), intergenic sequences (12.9%), exons (7.5%), and TTS sites (4.0%).

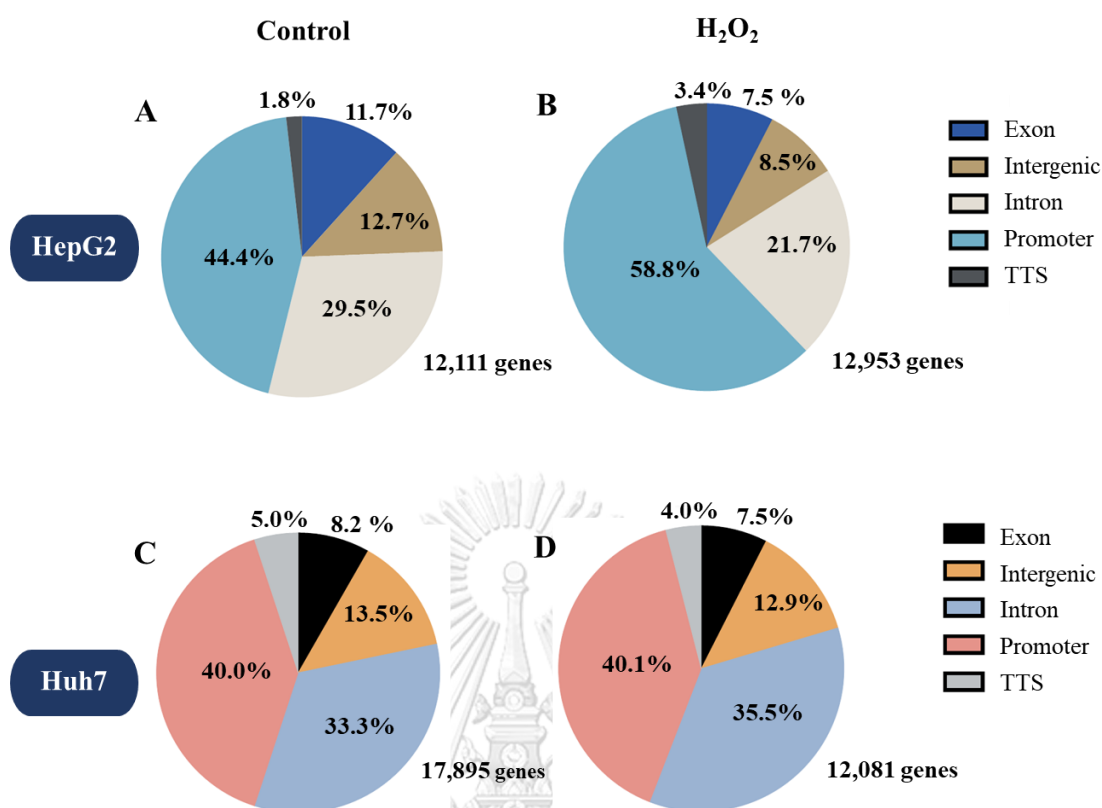


Figure 23 Number and location of the identified protein-coding genes enriched for H4K20me3 in HCC cells under oxidative stress condition. (A) untreated HepG2 cells, (B) H₂O₂-treated HepG2 cells, (C) untreated Huh7 cells, (D) H₂O₂-treated Huh7 cells.

Numbers indicate the percentage of identified genes located at each gene region.

CHULALONGKORN UNIVERSITY

The protein-coding gene profile enriched for H3K4me3 in HepG2 cells exposed to H₂O₂ was elucidated. Similar to H4K20me3, the identified sequences associated with H3K4me3 were found in various locations. The number of genes identified in the H₂O₂-treated and untreated HepG2 cells were 8,513 and 7,808 genes, respectively (Figure 24). The 68.1% of identified sequences in untreated control were located at promoter sites or transcription start sites (TSS), and the rest were found at intron sites (16.3%), exon (7.9%), intergenic (5.6%) and TTS sites (2.1%). In H₂O₂-treated HepG2, more than 60% of the identified sequences were located at promoter sites, 19.8% at intron, 7.8% at exon, 6.1% at intergenic, and 2.3% at TTS. The number of protein-coding genes enriched for H3K4me3 in untreated Huh7 cells were 12,533 genes. Fifty-eight percent

of these identified sequences were found at TSS sites, 21.6% at introns, 9.9% at exons, 7.0% at intergenic, and 3.2% at TTS. In H₂O₂-treated Huh7, 15,953 protein-coding genes were enriched for H3K4me3. These identified sequences were located at promoters (46.9%), introns (25.4%), intergenic (16.6%), exons (7.7%) and TTS (3.1%) (Figure 24).

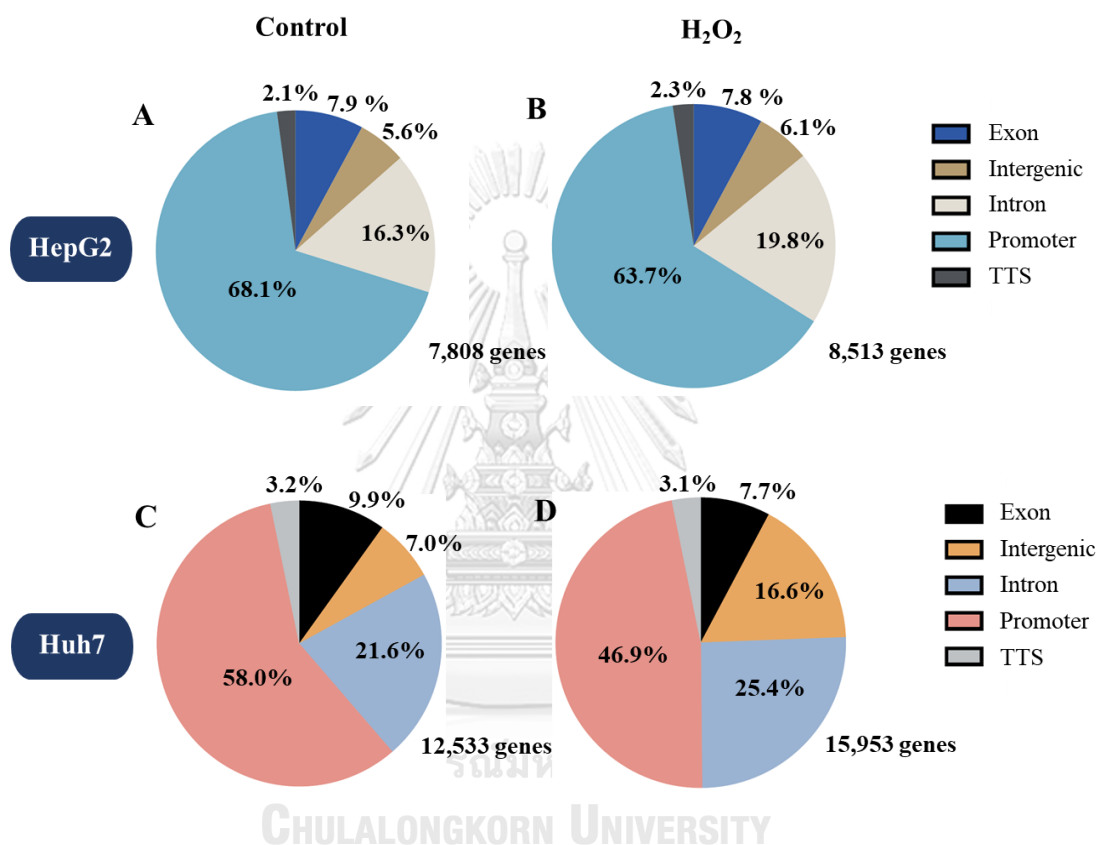


Figure 24 Number and location of the identified protein-coding genes enriched for H3K4me3 in HCC cells under oxidative stress condition. (A) untreated HepG2 cells, (B) H₂O₂-treated HepG2 cells, (C) untreated Huh7 cells, (D) H₂O₂-treated Huh7 cells. Numbers indicate the percentage of identified genes located at each gene region.

The above ChIP-seq data indicated that the enrichments of H4K20me3 and H3K4me3 are mostly located over the gene promoters or TSS. The profiles of genes identified in H₂O₂-treated condition and untreated control in each cell line for each chromatin mark enrichment were then combined, and classified into 3 categories, genes identified only in the untreated control, genes identified only in the H₂O₂ treatment, and common genes identified in both conditions. The total number of common genes enriched for H4K20me3 and found in both untreated control and H₂O₂-treated condition in HepG2 were 10,739, and there were 11,953 genes in Huh7 cells (Figure 25A-B). Subsequently, these two portions of genes were combined to find the common H4K20me3-enriched genes between HepG2 and Huh7 cell lines. We found 8,620 genes that were enriched for H4K20me3 in both HepG2 and Huh7 cells (Figure 25C). The common H4K20me3-enriched genes (found in both H₂O₂ and control conditions) were classified into 3 groups according to the peak score ratio (H₂O₂/control): peak score ratio ≥ 2 (high enrichment), peak score ratio 0.5 – 2 (equal enrichment) and peak score ratio ≤ 0.5 (low enrichment) (Figure 25D). Genes with low enrichment for H4K20me3 were expected to be upregulated under the oxidative stress condition. These common genes with low enrichment for H4K20me3 that were found in both HepG2 and Huh7 were selected and used for further GO and KEGG pathway analysis.

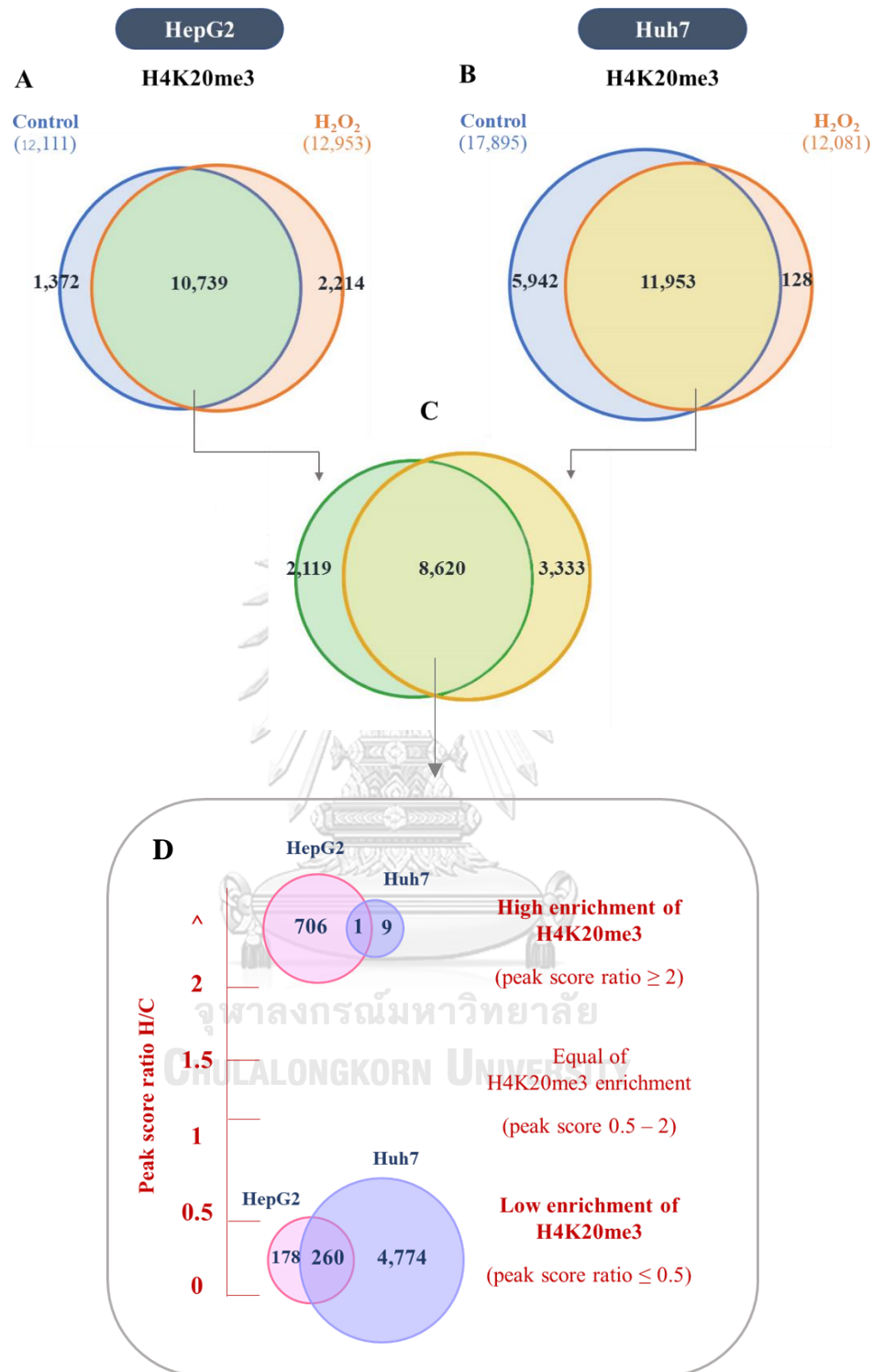


Figure 25 The number of genes enriched for H4K20me3 in HCC cells treated with H₂O₂ compared with the untreated control.

The GO and KEGG pathway were analyzed by the DAVID online program. For the analysis, we selected the common genes enriched for chromatin marks based on their peak score ratios (H₂O₂-to-Control). In case of H4K20me₃, genes with peak score ratio of ≤ 0.5 were selected (genes lowly or less enriched for H4K20me₃ following H₂O₂ treatment). We found that genes less enriched for H4K20me₃ following H₂O₂ treatment were associated with 5 biological processes including double-strand break repair, nucleotide-excision repair, DNA damage response, detection of DNA damage, DNA damage response, signal transduction by p53, and telomere maintenance (Figure 26), and name of each name found in each biological process is displayed in Table 4. Moreover, the KEGG pathway was assessed, and found that 3 pathways were associated with less H4K20me₃ enrichment under oxidative stress condition including base excision repair, homologous recombination, and nucleotide-excision repair (Table 5).

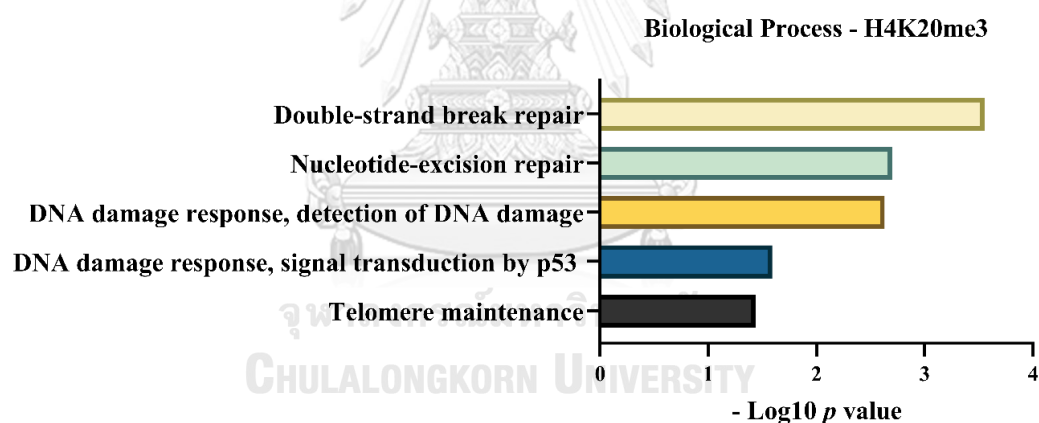


Figure 26 Biological process of genes less enriched for H4K20me₃ in H₂O₂-treated HCC cells. The biological process of the identified genes was related to DNA repair process and telomere maintenance.

Table 4 Biological processes of genes less enriched for H4K20me3 in HCC cells following H₂O₂ treatment

Biological process	P value	Fold enrichment	Gene name
GO:0000724 Double-strand break via homologous recombination	2.80E-04	1.51104	<i>MRE11, PSMD14, AP5Z1, MCM9, NUCKS1, SMC5, SMC6, BRCA2, YY1, SFRI, SWI5, RBBP8, RAD54L, NBN, ZSWIM7, AP5S1, GEN1, POLQ, HELQ, PARP1, RAD21L1, XRCC2, XRCC1, RPA2, LIG3, INO80, SPIDR, PALB2, RAD51B, MMS22L, RAD51, RAD51C, ERCC4, UBE2N, FAN1</i>
GO:006289 Nucleotide-excision repair	0.00201	1.91939	<i>SLC30A9, OGG1, XPA, RPA2, FANCC, GTF2H1, GTF2H2, BRCA2, RAD23B, GTF2H5, DDB2, DDB1, ATXN3, NEIL2, ERCC4, ERCCI, ERCC2, RBBP8, MMS19, NEIL1, FAN1</i>
GO:0042769 DNA damage response, detection of DNA damage	0.00235	1.97778	<i>MRPS26, PCNA, MRPS35, PARP1, UBE2B, RFC1, RFC2, ZBTB32, RPA2, HMGGA2, RBX1, DDB1, POLD3, UBB, USP1, RPS27A, DTL, SOX4, CUL4B</i>
GO:0006977 DNA damage response, signal transduction by p53 class mediator resulting in cell cycle arrest	0.02564	1.51104	<i>PCNA, UBB, PCBP4, E2F1, EP300, SFN, RPS27A, GTSE1, SOX4, NPMI, CNOT6L, CRADD, CNOT10, PPP2R5C, RBL2, CNOT6, TFDPI, CNOT7, TFDP2, CENPJ, CDK2, CDK1, MDM2, MDM4, CNOT8</i>

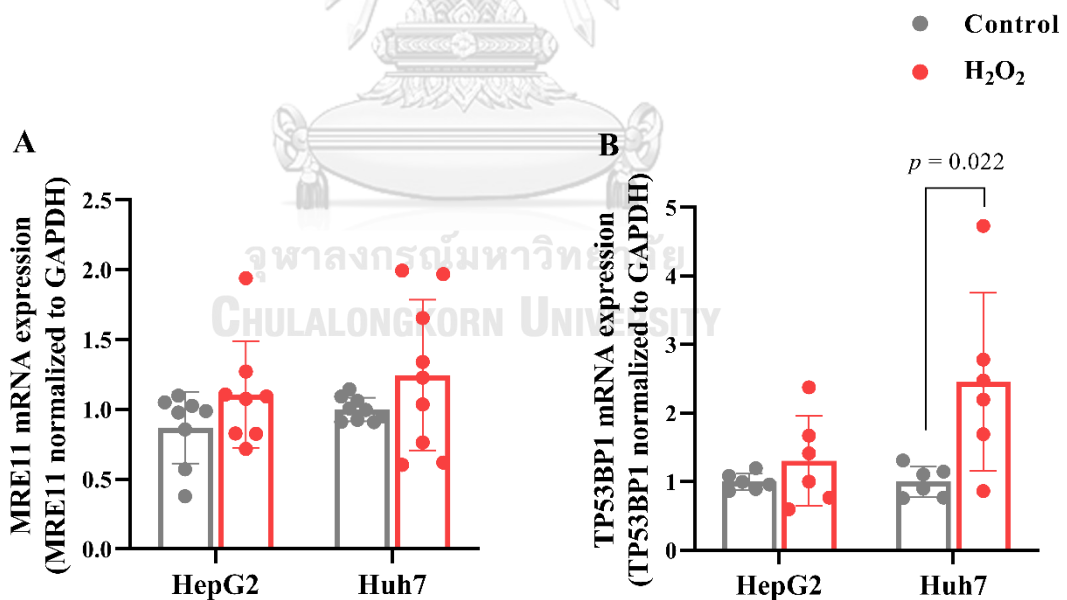
GO:0000723	0.03641	1.6655	<i>DCLRE1B, SMG1, SPI100, XRCC6, STN1, PARP3, PCNA, XRCC5, RPA2, TERF1, TERF2, POLD3, ERCC4, FBXO4, DNA2, NBN</i>
Telomere maintenance			

Table 5 KEGG pathways of genes less enriched for H4K20me3 in HCC cells following H₂O₂ treatment

KEGG Pathway	P value	Fold enrichment	Gene name
hsa03410	0.01699	1.79702	<i>PARP3, PARP4, PCNA, PARP1, OGG1, XRCC1, LIG3, HMGB1, POLE4, POLD3, SMUG1, NEIL2, POLE2, TDG, NEIL1, MUTYH</i>
hsa03440	0.02892	1.78928	<i>TOP3B, MRE11, XRCC2, TOP3A, RPA2, BRCA2, RAD51B, RAD52, POLD3, RAD51, RAD51C, EME1, RAD54L, NBN</i>
Homologous recombination			
hsa03420	0.03077	1.57717	<i>PCNA, RFC1, RFC2, XPA, RPA2, GTF2H1, GTF2H2, RAD23B, GTF2H5, DDB2, RBX1, DDB1, POLE4, POLD3, ERCC4, ERCC1, POLE2, ERCC2, ERCC5, CUL4B</i>
Nucleotide excision repair			

We selected 7 genes related to DNA repair and telomere maintenance (MRE11, BRCA2, RBBP8, MMS22L, DCLRE1B, TERF1, and TERF2) for further validation using qRT-PCR. Transcript expression of these genes were determined in HCC cells treated with H₂O₂ compared with untreated control. Additional genes related to DNA damage and repair (TP53BP1, BRCA1, TONSL, p21 and p53) and telomere maintenance (POT1) were also determined.

Expression of MRE11, TP53BP1, BRCA1 and BRCA2 mRNA was significantly increased in H₂O₂-treated HCC cells (both HepG2 and Huh7) compared with the untreated control (Figure 27). mRNA expression of MMS22L and its complex TONSL were significantly elevated in cells treated with H₂O₂ compared with the untreated cells (Fig 28A-B). RBBP8 mRNA level was significantly upregulated in H₂O₂ treated cells relative to the untreated controls both in HepG2 and Huh7 cells (Figure 28C). p21 and p53 mRNA expression significantly elevated in H₂O₂ treatment group compared with the untreated control group in both HCC cell lines (Figure 29).



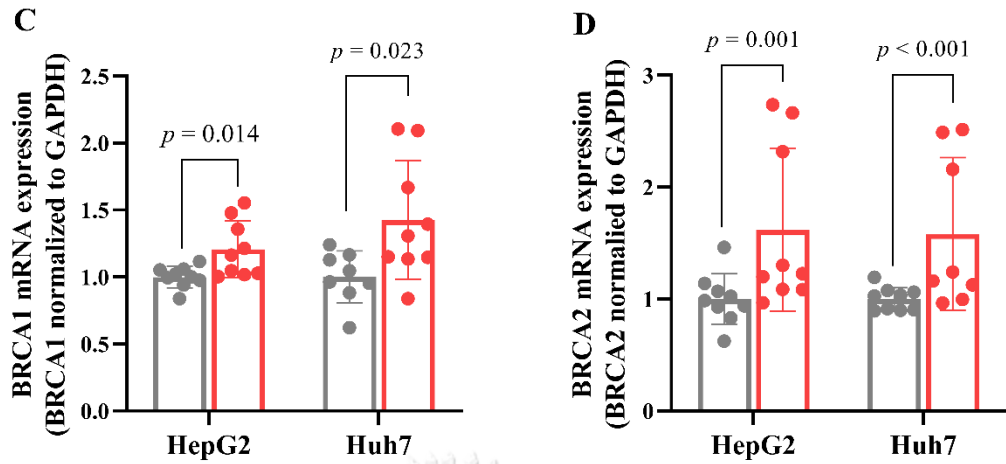
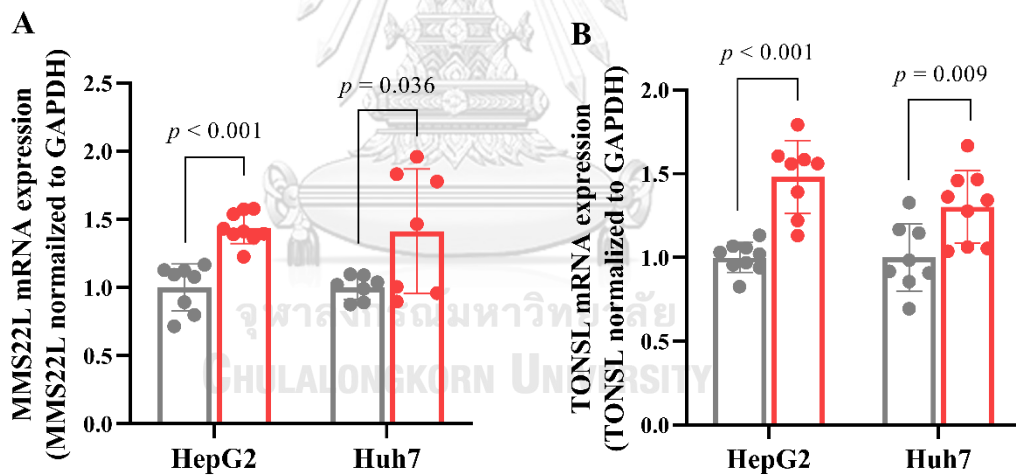


Figure 27 Expression of genes related to DNA repair in H_2O_2 -treated HCC cells measured by qRT-PCR. Expression of MRE11, TP53BP1, BRCA1 and BRCA2 was significantly increased in H_2O_2 treated cells relative to untreated control.



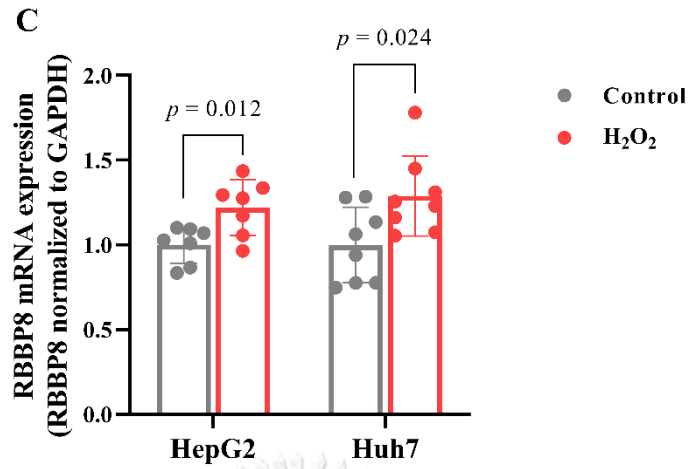


Figure 28 Expression of genes related to DNA repair in H₂O₂-treated HCC cells measured by qRT-PCR. The mRNA expression of MMS22L, TONSL and RBBP8 was significantly increased in H₂O₂ treated cells relative to untreated control.

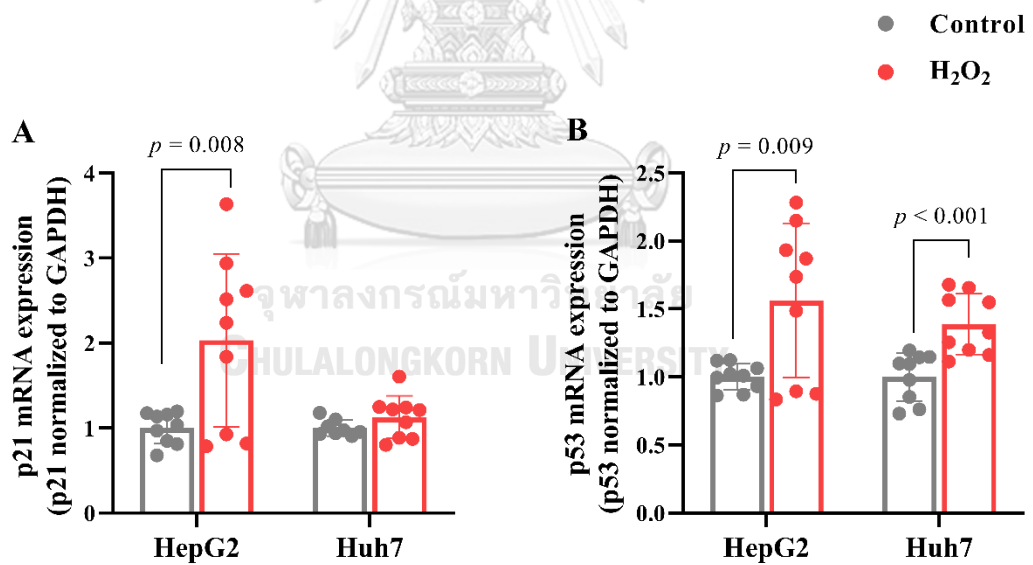
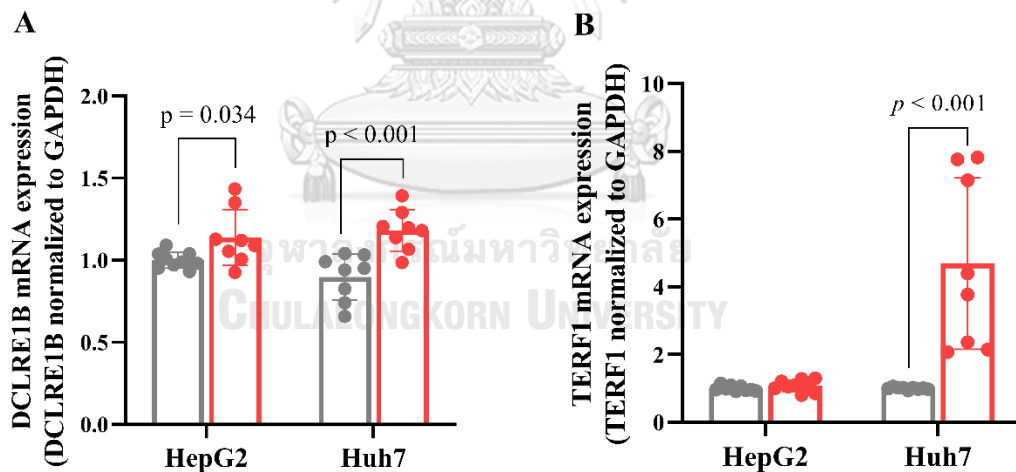


Figure 29 p21 and p53 mRNA expression in HCC cells following H₂O₂ treatment measured by qRT-PCR. Expression of p21 and p53 was significantly increased in H₂O₂ treated cells relative to untreated control.

The genes related to telomere maintenance including DCLRE1B, and shelterin components (TERF1, TERF2, and POT1) were also validated using RT-qPCR. DCLRE1B mRNA expression was significantly increased in cells treated with H₂O₂ compared with untreated controls in both HepG2 and Huh7. TERF1 expression significantly increased only in Huh7 cells treated with H₂O₂ compared with untreated control. TERF2 and POT1 were significantly up-regulated in cells treated with H₂O₂ compared with the untreated controls. In Huh7 cells, TERF1, TERF2 and POT1 mRNA expression in H₂O₂-treated condition were also significantly higher than the untreated control (Figure 30B-D). Furthermore, the relative telomere length was determined. The result showed that the length of telomere was not significantly changed following H₂O₂ treatment compared with untreated control (Figure 30E). Induction of telomere shortening by ROS is well established. These results indicated that oxidative stress induced the expression of genes associated with telomere maintenance that could maintain the telomere length in ROS-treated HCC cells.



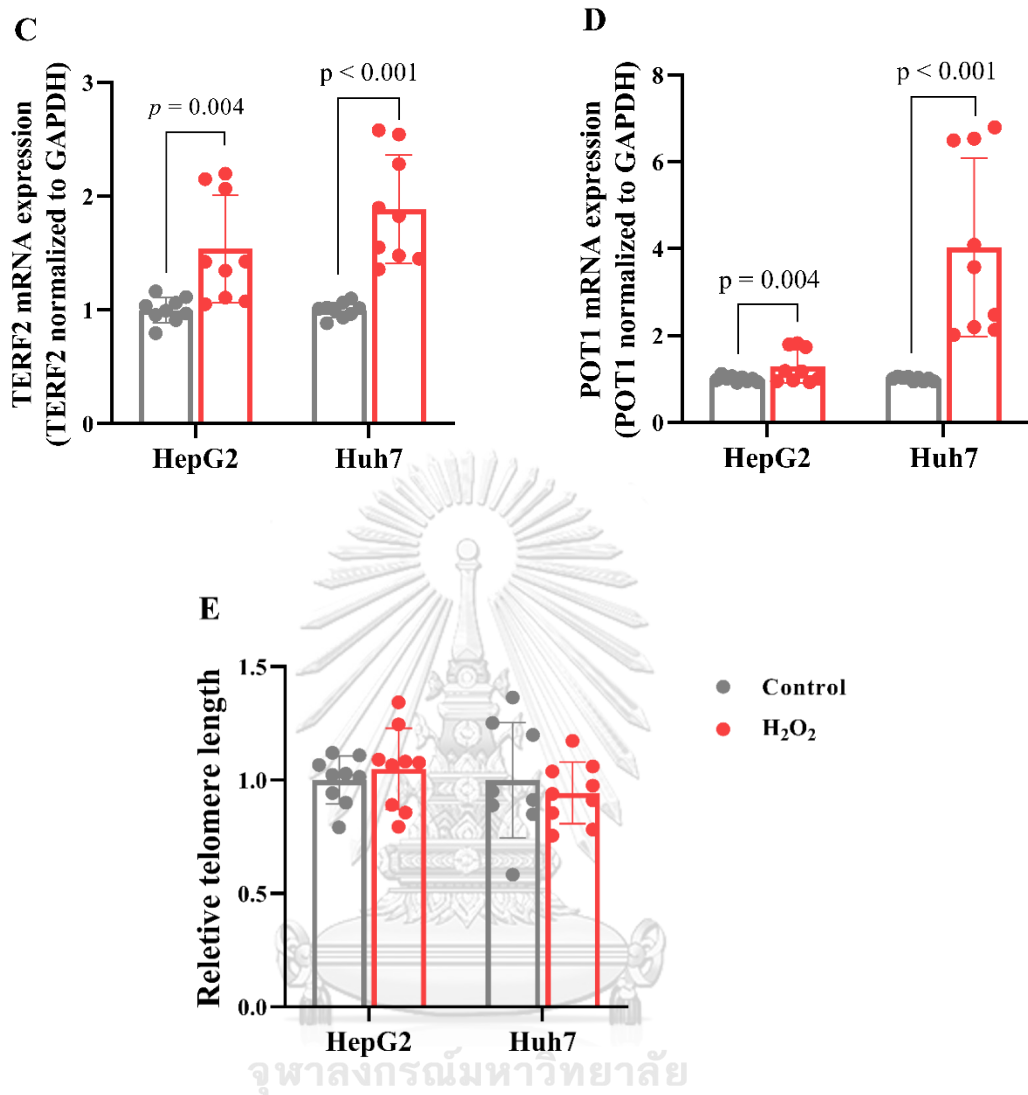


Figure 30 DCLRE1B and shelterin complexes mRNA expression and relative telomere length in HCC cells following H₂O₂ treatment. (A-D) The mRNA expression of DCLRE1B, TERF1, TERF2 and POT1 was increased in H₂O₂ treated cells. (E) Relative telomere length was not significantly different between H₂O₂ treatment and untreated control groups.

We did the same for H3K4me3-enriched genes as shown in Figure 31. The profiles of genes identified in H₂O₂-treated condition and untreated control in each cell line for H3K4me3 enrichment were then combined, and classified into 3 categories, genes identified only in the untreated control, genes identified only in the H₂O₂ treatment, and common genes identified in both conditions. The common genes enriched for H3K4me3 that were found in both untreated control and H₂O₂-treated condition in HepG2 and Huh7 were 6,476 and 9,555 genes, respectively. There were 5,953 H3K4me3-enriched genes commonly found in both cell lines. The common H3K4me3-enriched genes identified in both H₂O₂ and control conditions were categorized into 3 groups according to the peak score ratio (H₂O₂/control): peak score ratio ≥ 2 (high enrichment), peak score ratio 0.5 – 2 (equal enrichment) and peak score ratio ≤ 0.5 (low enrichment) (Figure 31D). Genes with high enrichment for H3K4me3 (active chromatin mark) were expected to be upregulated under the oxidative stress condition. These common genes with high enrichment for H3K4me3 that were found in both HepG2 and Huh7 were selected and used for further GO and KEGG pathway analysis.

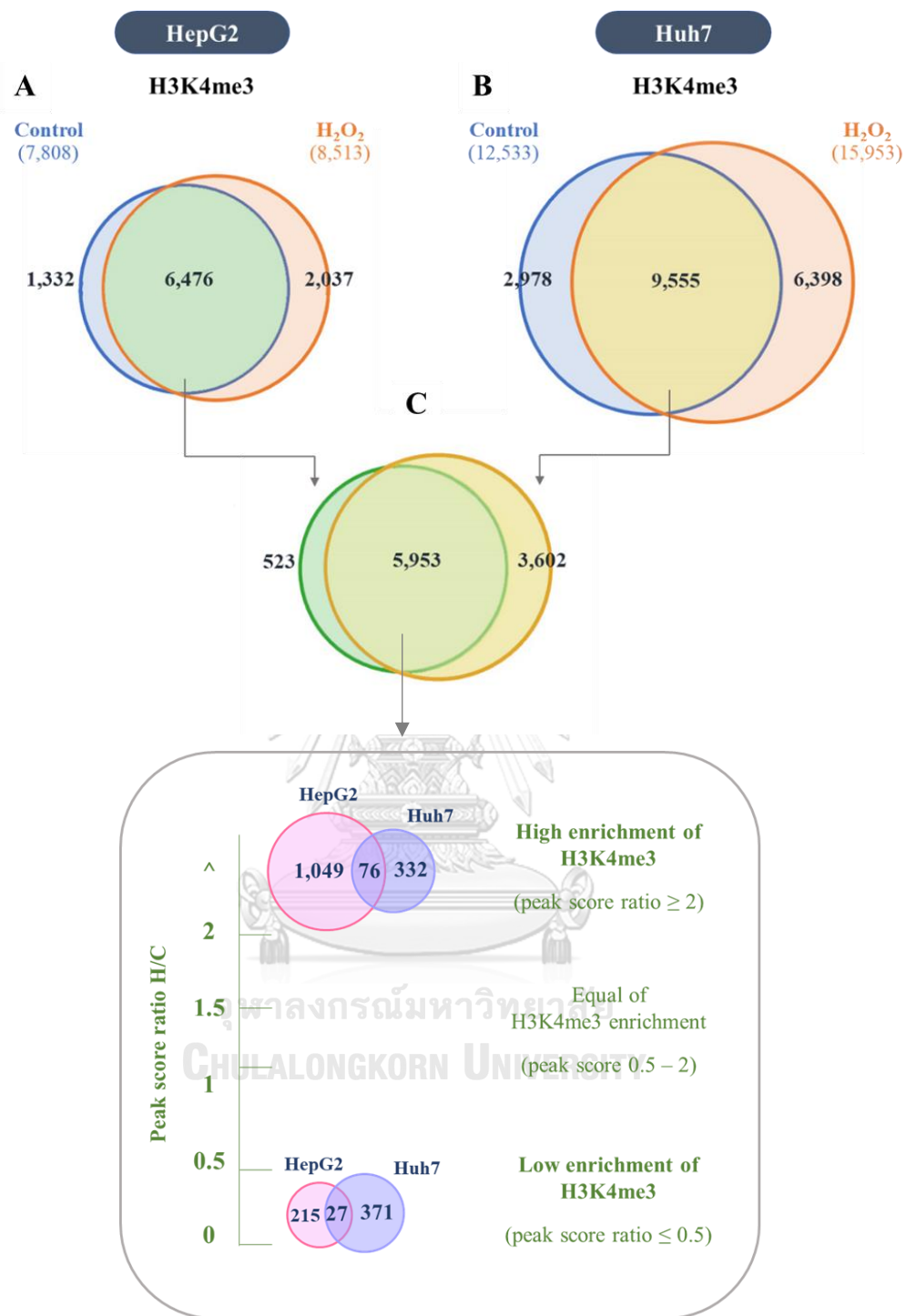


Figure 31 The number of genes enriched for H3K4me3 in HCC cells treated with H₂O₂ compared with the untreated control.

For H3K4me3, genes with peak score ratio of ≥ 2 were selected (genes highly or more enriched for H3K4me3 following H₂O₂ treatment). These selected genes were expected to be up-regulated in the H₂O₂ condition relative to the control. The genes were identified by GO in term of biological process. In ChIP-seq data analysis, genes selected were with $p < 0.05$ and fold enrichment > 1.5 .

Based on ChIP-seq analysis for H3K4me3 mark and the online DAVID program analysis, the genes that were highly or more enriched for H3K4me3 following H₂O₂ treatment were associated with 5 biological processes including positive regulation of GTPase activity, regulation of Rho protein signal transduction, cell-cell adhesion, cytoskeleton organization, and cell migration (Figure 32, Table 6). Moreover, the KEGG pathway results showed that 2 pathways were associated with H3K4me3 enrichment, i.e., tight junction and Wnt signaling pathway (Table 7).

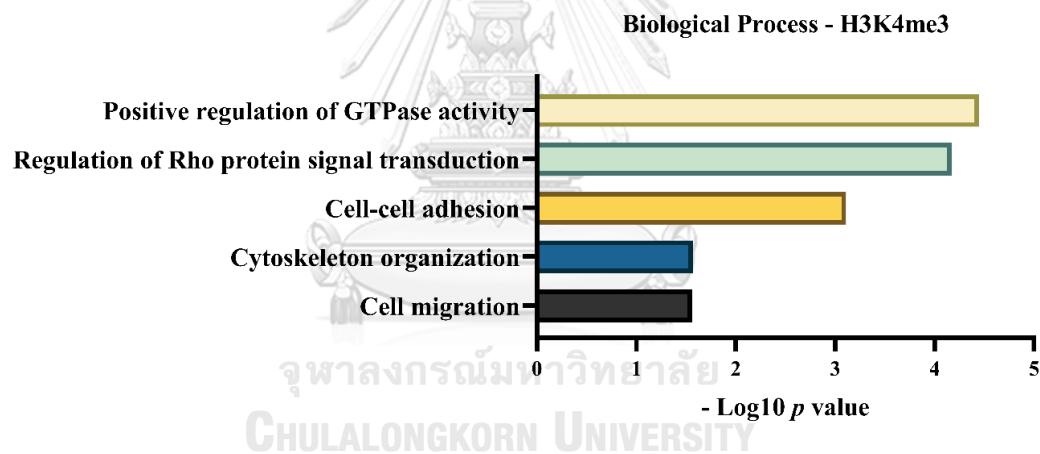


Figure 32 Biological process of genes more enriched for H3K4me3 in H₂O₂-treated HCC cells. The biological process of the identified genes was related to cell migration and cytoskeleton organization signaling.

Table 6 Biological processes of genes highly enriched for H3K4me3 in H₂O₂-treated HCC cells

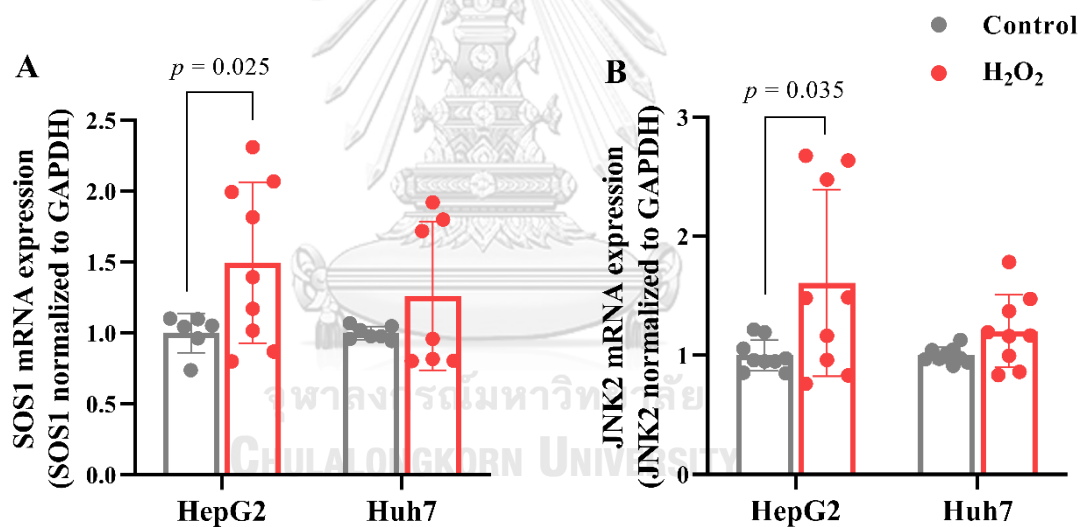
Biological process	P value	Fold enrichment	Gene name
GO:0035023 Regulation of Rho protein signal transduction	6.70E-05	3.023951	<i>PLEKHG3, PLEKHG4, FARP1, ARHGEF12, PLEKHG2, ARHGEF37, ARHGEF39, ARHGEF28, PLEKHG6, KALRN, FGDI, AKAP13, ARHGEF9, DNMBP, FGD6, ARHGEF3, ARHGEF7, SOS1</i>
GO:0043547 Positive regulation of GTPase activity	3.58E-05	1.661835	<i>DENND1B, ERRF1, GDI2, ARRB1, F11R, SIPAIL3, RAPGEFL1, SRGAP2C, AKAP13, ARHGAP40, PSD3, SH3BGR13, DNMI1, SBF2, ARFGF3, AGFG2, NDE1, AGFG1, PLEKHG3, ARHGEF12, RASA4B, PLEKHG2, PLEKHG6, AXIN1, NRG2, AXIN2, ARFGAP2, BTC, ARHGEF9, RABEP2, ARHGEF3, TBC1D24, PREB, PGAM5, ARHGEF7, PLCB1, SOS1, DOCK1, RIN2, LLGL2, HBEGF, ARHGEF28, ARHGAP19, PIK3R2, KALRN, FGDI, INPP5B, ARHGAP21, FGD6, SRGAP2, RALGDS, SRGAP1, CYTH1, SPTBN1, FARP1, GIT2, ARHGEF37, ARHGEF39, ARHGAP29, ARHGAP32, DNMBP, NFI, GRB2, PLXNB1, LAMTOR1, RGL1, SERGEF, CALM2, GTPGP1</i>

GO:0098609	7.81E-04	1.807676	<i>MACF1, LRRC59, HSP90AB1, YWHAB, PARK7, F11R, PPL, CRKL, KLC2, LARPI, PERP, KIF5B, COBLL1, MYO6, EIF4H, TNKS1BP1, LRRFIP1, EMD, ARGLU1, SPTBN1, TMPO, PAK4, CAST, SH3GLB2, SWAP70, CSNK1D, EPS15L1, EEF2, PAICS, YWHAZ, SND1, RAB10, EIF5, RAN, CC2D1A, ADGRL3</i>
Cell-cell adhesion			
GO:0016477	0.027459	1.661415	<i>USP24, LAMA5, TGFB2, PRKCI, BTGI, JUP, ARPC5L, PRKCZ, RHOA, PPP1R9B, EFNA1, ABI2, KCTD13, SDC1, ADAM9, HES1, PLXNB1, DOCK1, CTHRC1, PAK4, NDELI</i>
Cell migration			
GO:0007010	0.02715	1.690407	<i>LAMA5, MACF1, PRKCI, MAST4, MICAL2, PPL, SIPA1L3, FGDI, FGD6, TUBB2A, PCLO, ABI2, TUBB3, ZMYM4, DOCK1, CYLC1, SPTBN1, NECTIN2, CAP2, PAK4</i>
Cytoskeleton organization			

Table 7 KEGG pathway of genes highly enriched H3K4me3 in H₂O₂-treated HCC cells

KEGG Pathway	P value	Fold enrichment	Gene name
hsa04530 Tight junction	0.034643	1.928511	<i>PRKCI, SRC, PRKCE, PPP2R2A, F11R, PRK CZ, RHOA, ACTG1, MYL12B, MYL2, CLDN18, MYH14, LGL2</i>
hsa04310 Wnt signaling pathway	0.036696	1.683416	<i>CREBBP, WNT2B, CTBP1, CUL1, AXIN1, WNT9B, CACYBP, AXIN2, WNT9A, PSEN1, RHOA, RBX1, PPP3CA, FRAT1, FRAT2, PLCB1, BTRC, PRKACA</i>

SOS1 and RHOA their related genes (JNK2, c-Jun, MMP9, ROCK1, LIMK2 and radixin) in the signaling cascades were selected for further mRNA expression validation by qRT-PCR. SOS1 mRNA expression was significantly elevated in H₂O₂ treated HepG2 cells compared with untreated control (Figure 33A). Similarly, SOS1 mRNA expression was significantly increased in H₂O₂ treated Huh7 cells relative to untreated control. JNK2, c-Jun, and MMP9, which are the downstream targets of SOS1, were significantly increased in HepG2 cells treated with H₂O₂ compared with untreated control. In Huh7 cells, JNK2 and c-Jun mRNA expression slightly increased in the H₂O₂ treated condition relative to the untreated control, the mRNA expression of MMP9 significantly increased in the H₂O₂ treatment compared with untreated control (Figure 33B-D). These finding suggested that ROS enhanced SOS1 signaling pathway in HCC cells.



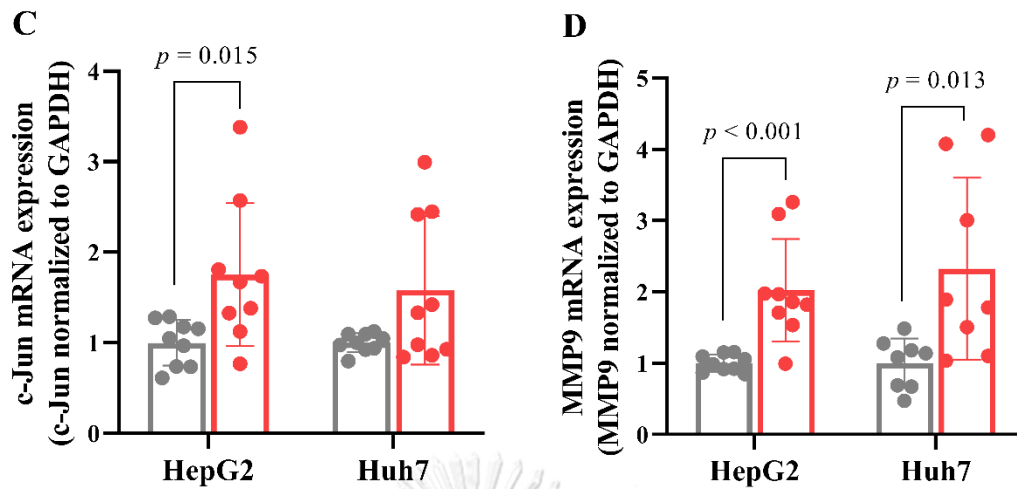


Figure 33 SOS1, JNK2, c-Jun and MMP9 mRNA expressions in HCC cells following H₂O₂ treatment. The mRNA expression of SOS1, JNK2, c-Jun, and MMP9 was increased in H₂O₂ treated cells.

For RHOA and its related genes, the RHOA mRNA expression was significantly upregulated in HepG2 cells treated with H₂O₂ compared with untreated control (Figure 34). RHOA also was significantly upregulated in Huh7 cells treated with H₂O₂ compared with its untreated control. Transcript expression of ROCK1, LIMK2, and radixin, RHOA downstream targets, was significantly increased in cells treated with H₂O₂ relative to the untreated controls both in HepG2 and Huh7 cells (Figure 34). These findings suggested that ROS augmented the RHOA signaling pathway in HCC cells.

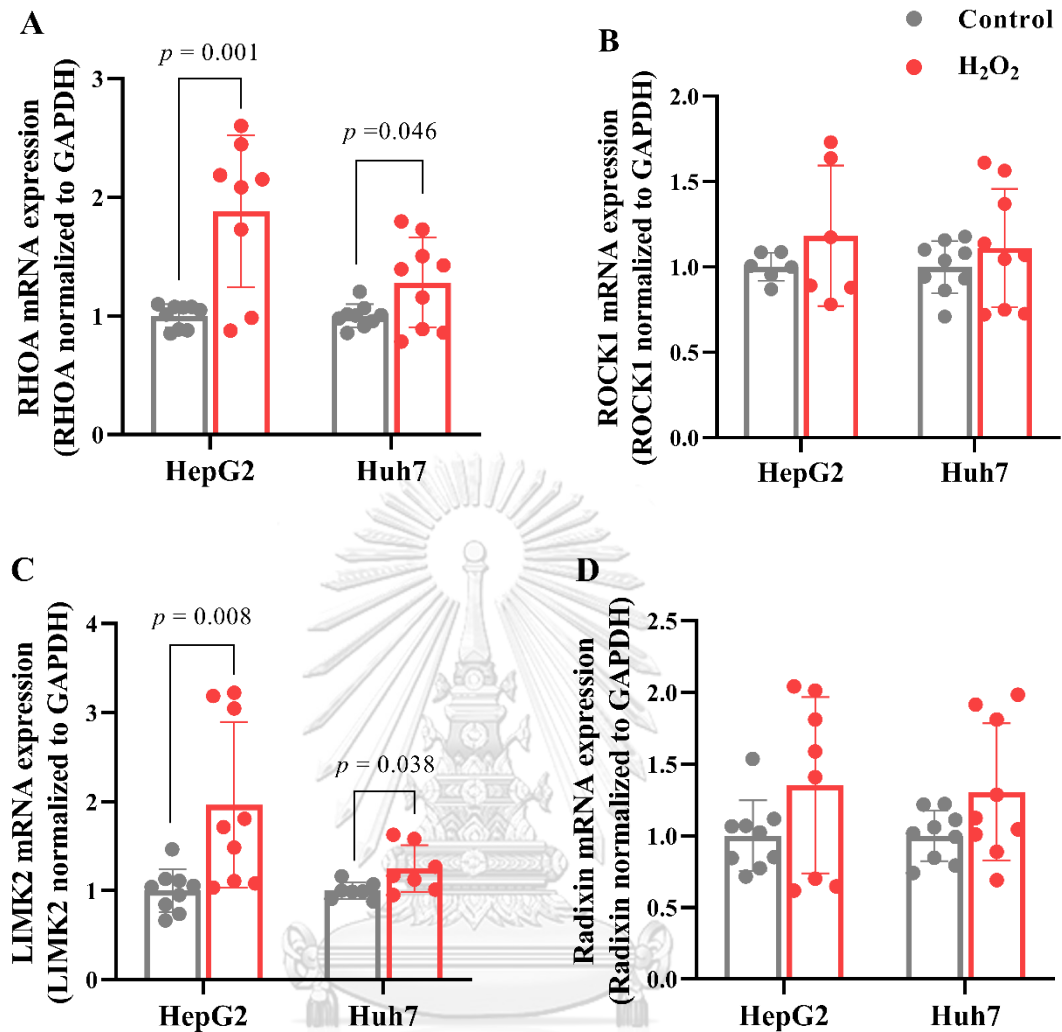


Figure 34 RHOA, ROCK1, LIMK2 and radixin mRNA expressions in HCC cells following H_2O_2 treatment. The mRNA expression of RHOA, ROCK1, LIMK2, and radixin was increased in H_2O_2 treated cells.

SMAD2 and SMAD2 also were evaluated in HepG2 and Huh7 cells. Both SMAD2 and SMAD3 mRNA expression were elevated in H_2O_2 treated cells compared with untreated control both in HepG2 and Huh7 (Figure 35). Furthermore, SNAIL, a mesenchymal maker, was investigated. Results showed that mRNA expression of SNAIL was significantly increased in H_2O_2 treated cells relative to untreated control in both HepG2 and Huh7 cells (Figure 36). These finding suggested that ROS induced the SMAD pathway in HCC cells.

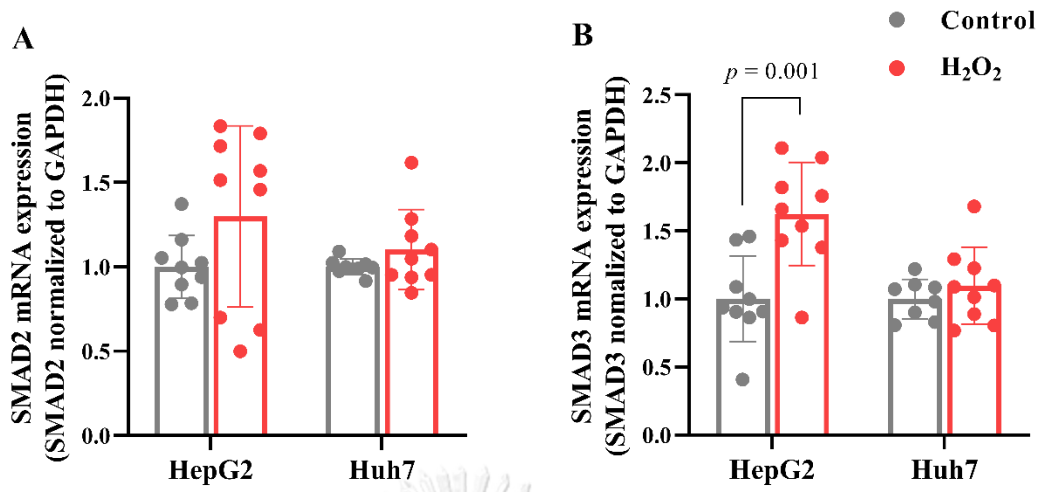


Figure 35 SMAD2 and SMAD3 mRNA expression in HCC cells following H₂O₂ treatment. The mRNA expression of SMAD2 and SMAD3 was increased in H₂O₂ treated cells.

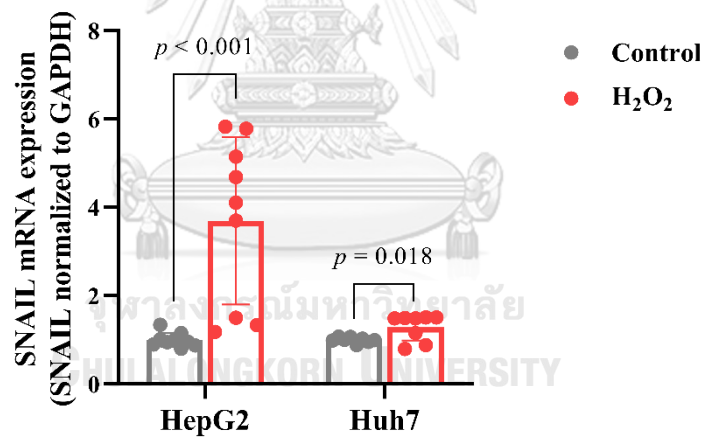


Figure 36 SNAIL mRNA expression in HCC cells following H₂O₂ treatment. The mRNA expression of SNAIL was significantly increased in H₂O₂ treated cells.

Based on the qRT-PCR validation and landscape of H4K20me3 enrichment, RBBP8 was selected as candidate gene for further verification. The *RBBP8* gene was located at chromosome 18. The H4K20me3 enrichment landscape data showed that the H4K20me3 enrichment over *RBBP8*, particularly at the promoter, was relatively lower in H₂O₂ treatment compared with the untreated control in both HepG2 and Huh7 cells (Figure 37).

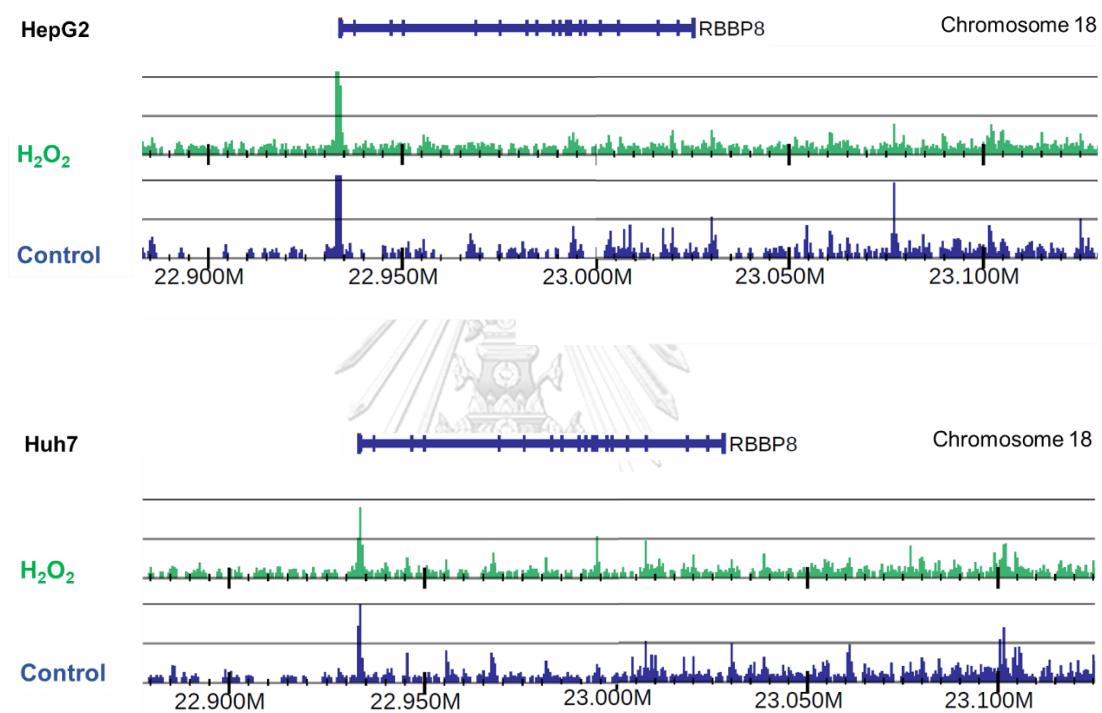


Figure 37 H4K20me3 enrichment peaks over the RBBP8 gene in HCC cells compared between H₂O₂ treatment and untreated control.

Overall enrichment of H4K20me4 on RBBP8 gene relatively lower in H₂O₂ treatment than that in untreated control both in HepG2 (upper panel) and Huh7 (lower panel) cells.

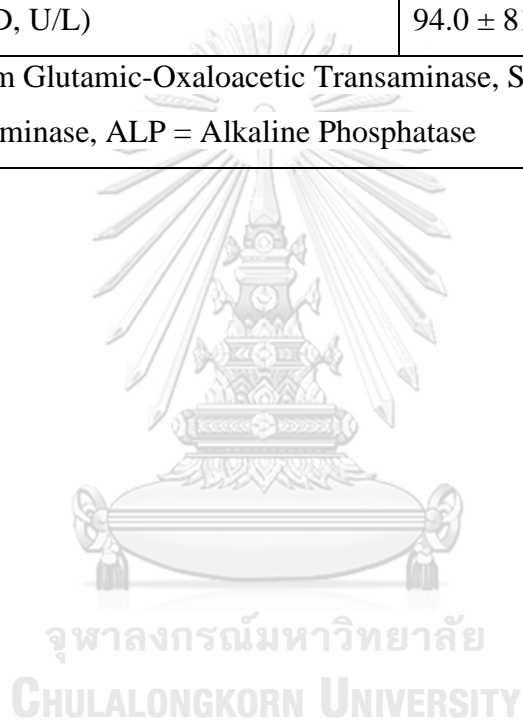
The characteristics of HCC patients

This study was ethically approved by The Institutional Review Board (IRB), Faculty of Medicine, Chulalongkorn University. A total of 100 liver cancer tissues are obtained from patients with HCC at King Chulalongkorn Memorial Hospital admitted to the hospital between 2009 to 2015. As shown in table 8, patients had mean age of 64.0 ± 11.0 years old, and there were 79 (86.0%) males and 13 (14.0%) females. Fifty-one (55.4%) cases of patients were infected with hepatitis B virus, and 12 (13.0%) cases of patients were infected with hepatitis C virus. There were 6 (6.5%) cases of alcoholic disease, whereas 2 (2.2%) cases of nonalcoholic steatohepatitis (NASH). According to characteristics of tumor, 27 (29.3%) were well differentiation, 49 (53.2%) were moderate differentiation, and 16 (17.4%) were poor differentiation.

Table 8 Demographic and clinical data of the HCC patients

Characteristics	Frequency (%)
Total number of patients	92
Average age (mean \pm SD)	64.0 \pm 11.0 years old
Sex:	
• Male	79 (86.0%)
• Female	13 (14.0%)
Hepatitis B infection	51 (55.4%)
Hepatitis C infection	12 (13.0%)
Alcoholic disease	6 (6.5%)
Nonalcoholic steatohepatitis (NASH)	2 (2.2%)
Tumor differentiation	
• Well differentiation	27 (29.3%)
• Moderate differentiation	49 (53.2%)
• Poor differentiation	16 (17.4%)
Cirrhosis (n=75):	
• Yes	46 (61.3%)

• No	29 (38.7%)
Metastasis (n=74):	
• Yes	5 (6.8%)
• No	69 (93.2%)
Total bilirubin (mean \pm SD, mg/dL)	1.9 \pm 4.4
Albumin (mean \pm SD, mg/dL)	3.4 \pm 0.7
SGOT (mean \pm SD, U/L)	357.4 \pm 603.9
SGPT (mean \pm SD, U/L)	269.8 \pm 416.7
ALP (mean \pm SD, U/L)	94.0 \pm 81.1
* SGOT = Serum Glutamic-Oxaloacetic Transaminase, SGPT = Serum Glutamic Pyruvate Transaminase, ALP = Alkaline Phosphatase	



Histological examination of HCC tissues by Haematoxylin and Eosin staining

Haematoxylin and Eosin (H&E) staining was employed in all HCC and non cancerous liver tissues and these stained sections were examined by pathologist. According to H&E assesment, there were 100 cancerous sections and 15 noncancerous sections (Figure 38). These sections were used for further immunohistochemical staining for H4K20me3, H3K9me3, and RBBP8.

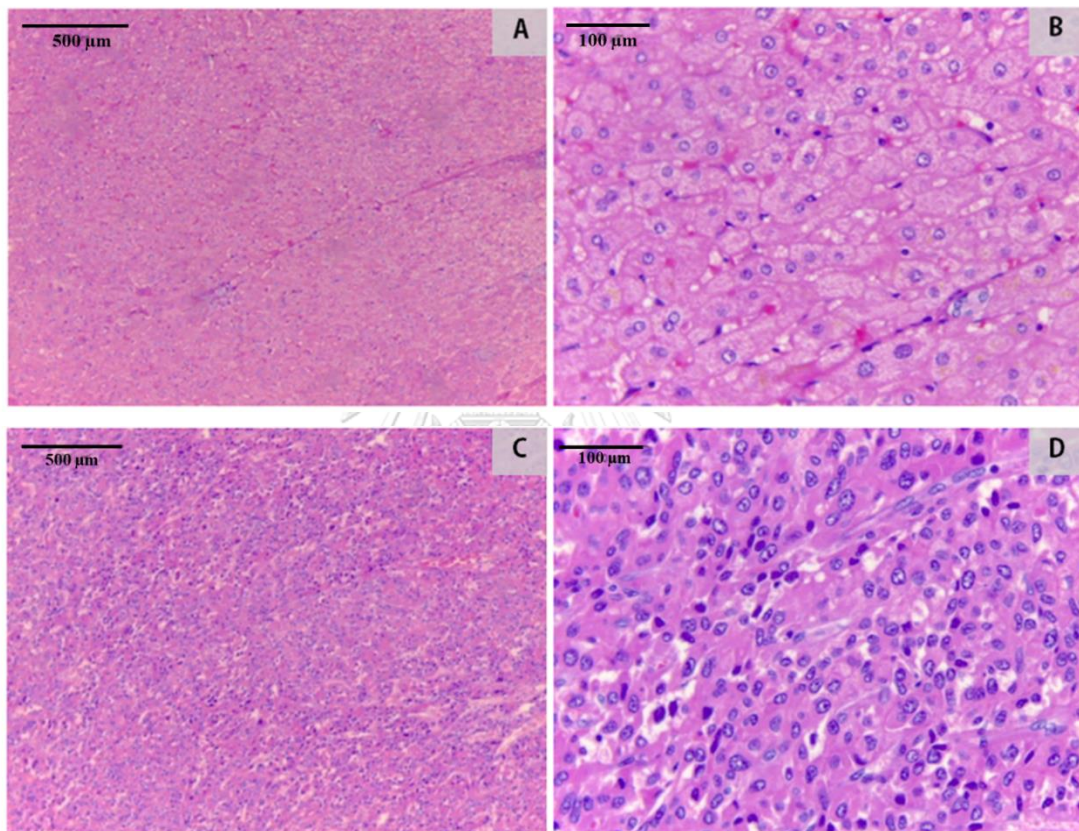


Figure 38 H&E staining of HCC and noncancerous liver tissues
(A) Non cancerous tissues magnification 100x, (B) Noncancerous tissues magnification 400x, (C) HCC tissues magnification 100x, (D) HCC tissues magnification 400x (6)

Histone methylation alteration in HCC tissues

H4K20me3 and H3K9me3 are well-known heterochromatin marks, but H3K4me is known as a euchromatin mark. Expression of these histone methylations were explored in HCC tissues by IHC staining. The expression of H4K20me3 was analysed in 100 HCC tissues and 15 noncancerous tissues. The IHC results showed that the expression of H4K20me3 was significantly increased, expressed predominantly in nuclei, in HCC tissues (IHC score = 9.31 ± 2.18) compared with the noncancerous tissues (IHC score = 7.23 ± 1.06) ($p = 0.0003$) (Figure 39-40). Furthermore, H4K20me3 was also highly positive in sinusoidal cells and neutrophils.

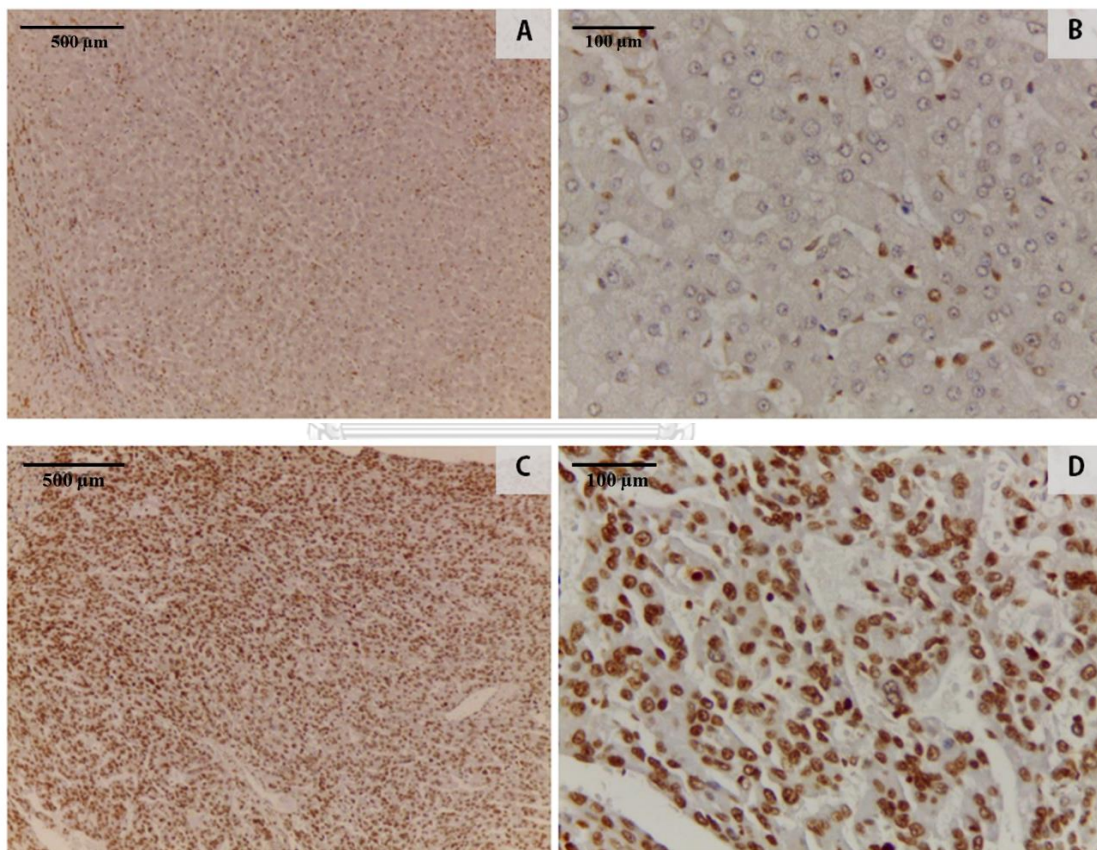


Figure 39 H4K20me3 expression in HCC tissues

H4K20me3 expression in HCC tissues (C, D) was higher than noncancerous liver tissues (A, B). Magnification; 100x (A, C), 400x (B, D)

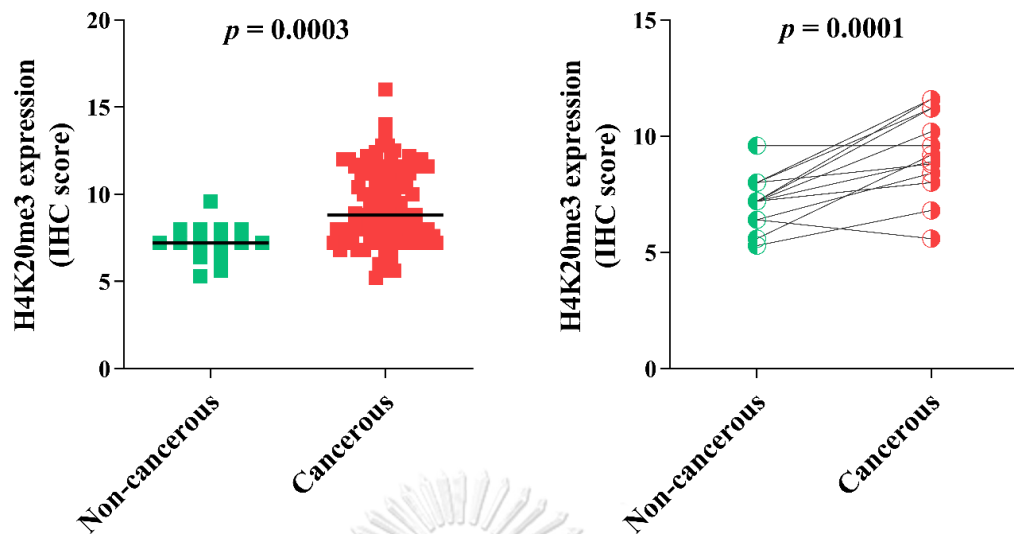


Figure 40 H4K20me3 expression in HCC tissues compared with noncancerous liver tissues. The expression of H4K20me3 was significantly increased in HCC tissues (red) compared with the noncancerous liver tissues (green).

Left; Overall comparison (Mann-Whitney U test),

Right; Paired comparison (Paired t-test)

Furthermore, we explored whether H4K20me3 expression was associated with disease progression in term of tumor relapse and patients' survival. Association of H4K20me3 expression with patient's tumor relapse and survival were evaluated using Kaplan-Meier curve estimator. The relapse data were available for seventy-three patients. Of 73 cases, twenty-one (30%) patients developed tumor relapse. H4K20me3 expression was categorized into high (IHC score ≥ 7.3) and low (IHC score < 7.3). High expression of H4K20me3 was significantly associated with the tumor recurrence ($p = 0.0259$) (Figure 41).

Survival data was obtained from ninety-two patients. H4K20me3 expression was recategorized into high (IHC score ≥ 11) and low (IHC score < 11) expression. High level of H4K20me3 expression was associated with a short survival in HCC patients. Patients with high expression of H4K20me3 had significantly shorter than low expression of H4K20me3 ($p = 0.0306$) (Figure 42). These data suggested that the

elevated H4K20me3 expression was associated with tumor recurrence and poor prognosis in HCC patients.

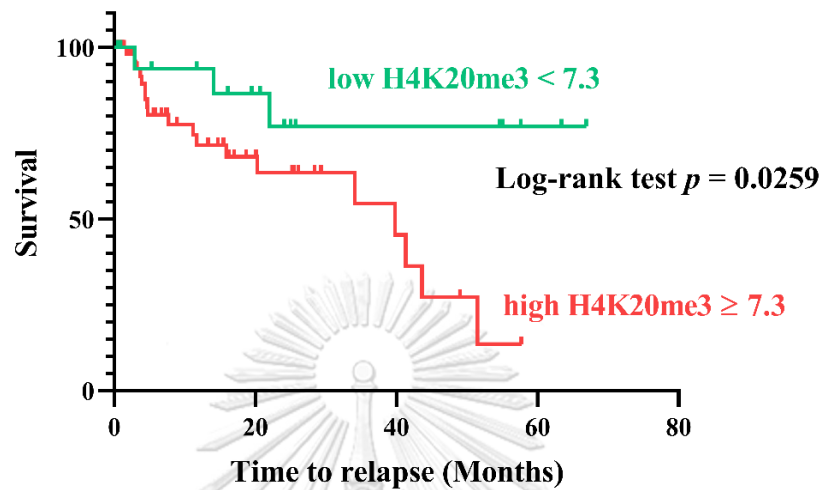


Figure 41 Kaplan-Meier curve analysis of H4K20me3 expression and tumor relapse in HCC patients. Elevated expression of H4K20me3 was significantly associated with tumor relapse (Log-rank test, $p = 0.0259$).

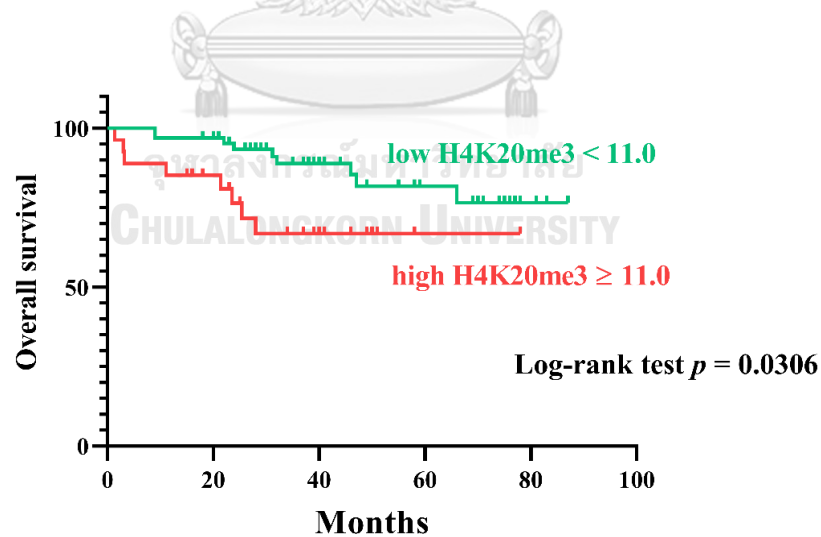


Figure 42 Kaplan-Meier curve analysis of H4K20me3 expression and overall survival in HCC patients. The survival time of patients with high H4K20me3 expression had significantly shorter than those with low H4K20me3 expression (Log-rank test, $p = 0.0306$).

The level expression of H3K9me3 was assessed in 32 HCC tissue sections and 15 noncancerous sections. The IHC results revealed that H3K9me3 was significantly up-regulated, prominently expressed in nuclei, in HCC tissues (IHC score = 10.16 ± 1.74) compared with the noncancerous tissues (IHC score = 7.02 ± 2.45) ($p < 0.0001$) (Figure 43-44).

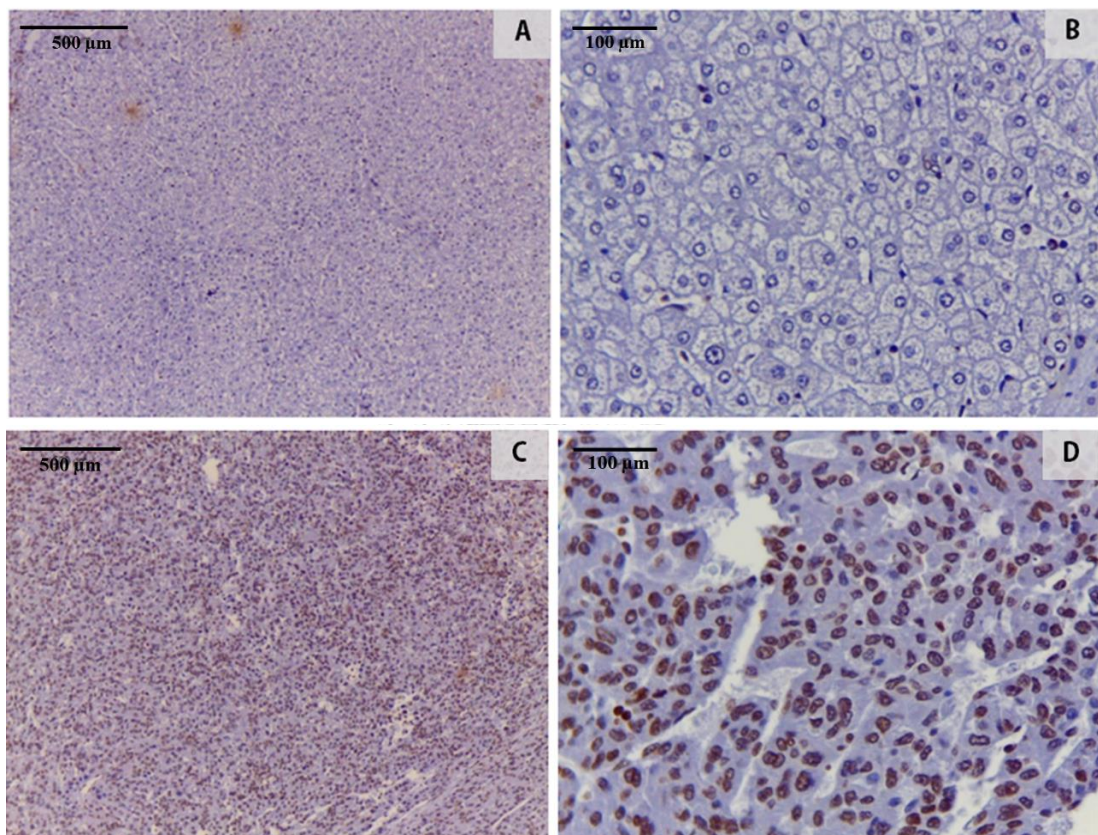


Figure 43 H3K9me3 expression in HCC tissues

H3K9me3 expression in HCC tissues (C, D) was higher than that in the noncancerous tissues (A, B). Magnification; 100x (A, C), 400x (B, D)

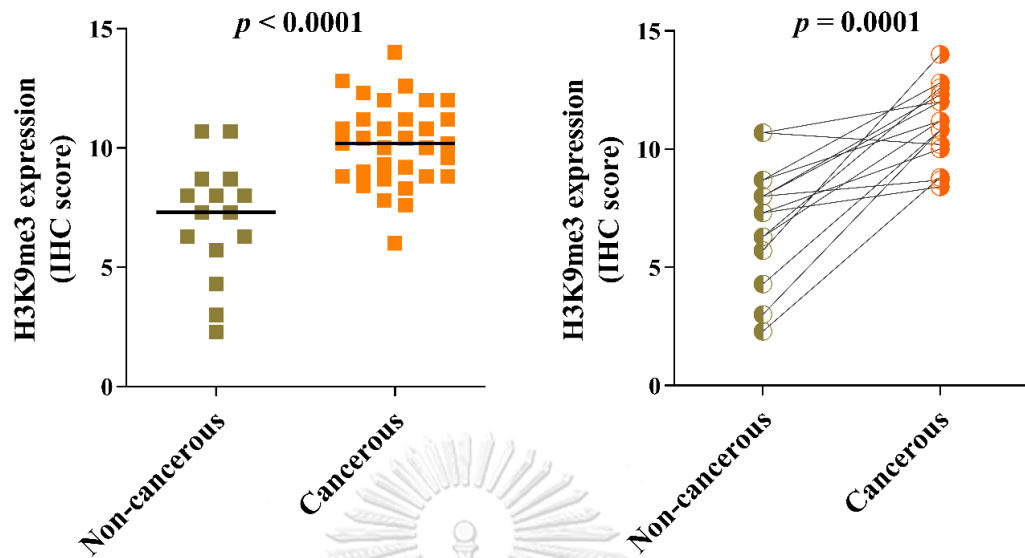


Figure 44 H3K9me3 expression in HCC tissues compared with noncancerous tissues. The expression of H3K9me3 was significantly increased in HCC tissues (orange) compared with the noncancerous tissues (dark green).

Left; Overall comparison (Mann-Whitney U test)

Right; Paired comparison (Paired *t*-test)

Expression of H3K4me3 was evaluated in 31 HCC tissues and 15 noncancerous tissues. The IHC results showed that H3K4me3 expression was significantly increased, mainly labelled in nuclei, in HCC tissues (IHC score = 9.38 ± 1.64) compared with the noncancerous tissues (IHC score = 4.48 ± 2.65) ($p < 0.0001$) (Figure 45-46). According to the present IHC results, histone methylations, specifically H4K20me3, H3K9me3 and H3K4me3, were upregulated in human HCC tissues.

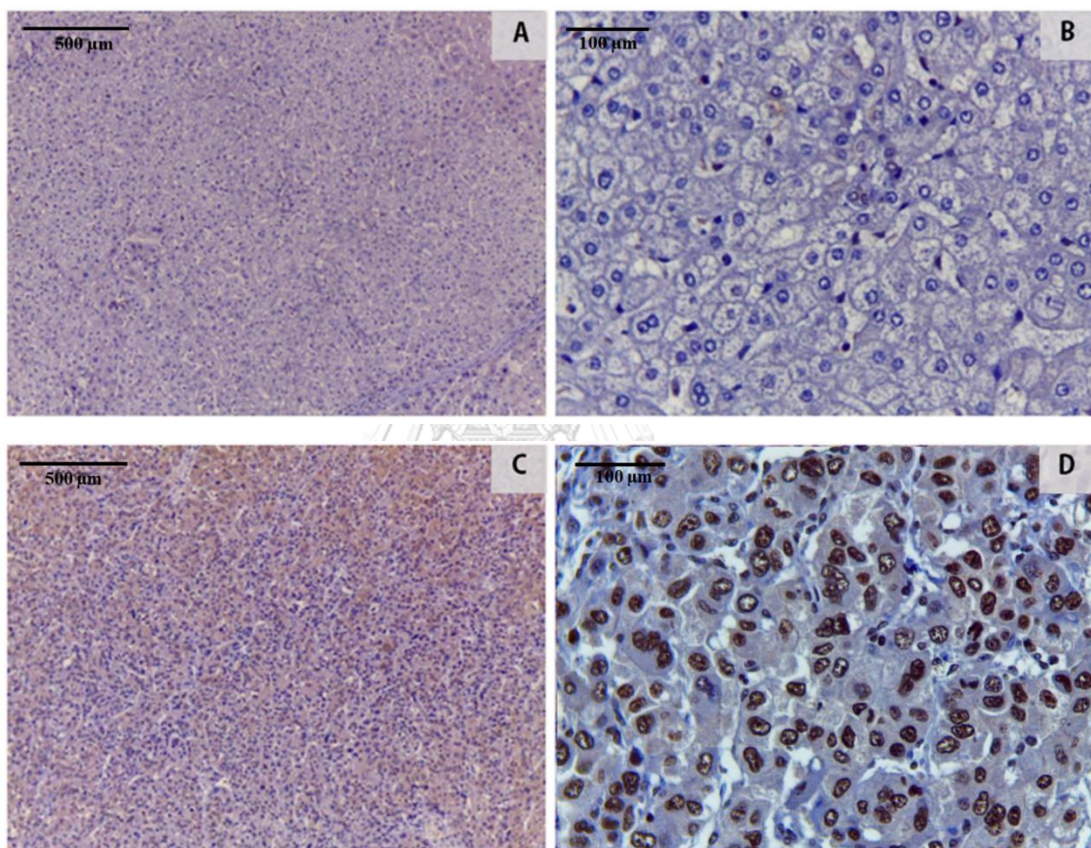


Figure 45 H3K4me3 expression in HCC tissues

H3K4me3 expression in HCC tissues (C, D) was higher than in noncancerous tissues (A, B). Magnification; 100x (A, C), 400x (B, D)

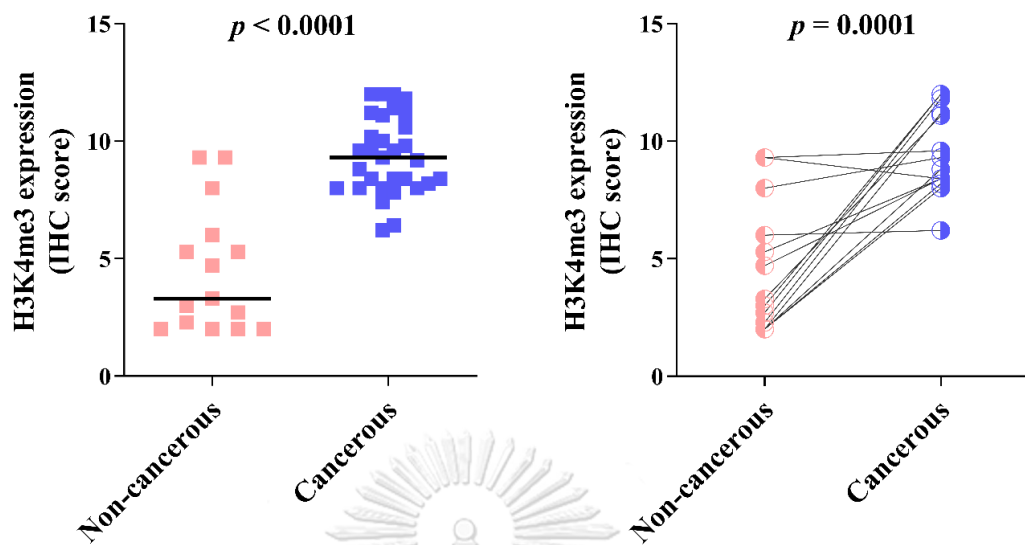


Figure 46 H3K4me3 expression in HCC tissues compared with noncancerous tissues. The expression of H3K4me3 was significantly increased in HCC tissues (purple) compared with noncancerous tissues (pink).

Left; Overall comparison (Mann-Whitney U test)

Right; Paired comparison (Paired *t*-test)

RBBP8 was a candidate gene selected based on ChIP-seq data. Its expression was further verified by IHC staining in HCC tissues. Forty-three cases of HCC tissues and 15 cases of noncancerous tissues were stained for RBBP8. The IHC results showed that RBBP8 was significantly increased in HCC tissues (IHC score = 6.51 ± 1.70) ($p < 0.0001$) compared with noncancerous tissues (IHC score = 4.17 ± 1.07) ($p = 0.0006$). Based on IHC staining, RBBP8 was particularly expressed in cytoplasmic part, and in some cancerous tissues it was found in nuclei (Figure 47-48).

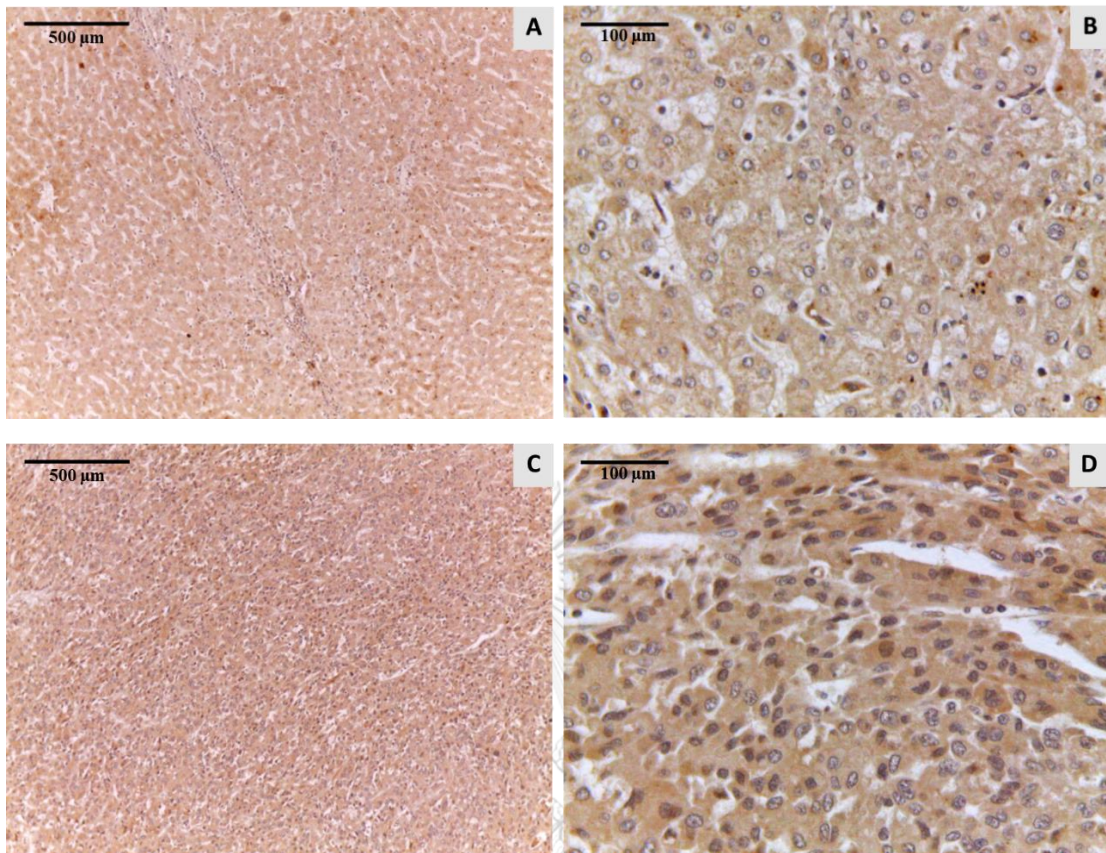


Figure 47 RBBP8 expression in HCC tissues

RBBP8 expression in HCC tissues (C, D) was higher than that in noncancerous tissues (A, B). Magnification; 100x (A, C), 400x (B, D)

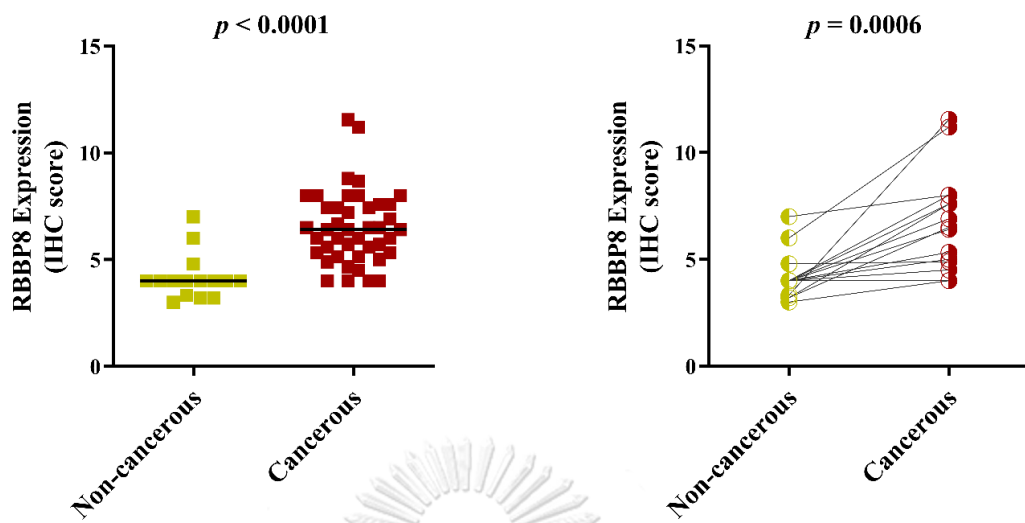


Figure 48 RBBP8 expression in HCC tissues quantitatively compared with noncancerous tissues. The expression of RBBP8 was significantly increased in HCC tissues (light green) compared with noncancerous liver tissues (dark red).

Left; Overall comparison (Mann-Whitney U test)

Right; Paired comparison (Paired *t*-test)

Chapter 5

Discussion and Conclusion

Discussion

Oxidative stress contributes to both carcinogenesis and tumor progression through both genetic and epigenetic mechanisms (10). We previously demonstrated that oxidative stress was increased in patients with HCC, and ROS promoted tumor progressiveness in HCC cell lines (6). In this study, we confirmed that ROS provoked oxidative stress and enhanced progressive phenotypes, specifically EMT, in HepG2 and Huh7 cells. Our new findings were that ROS upregulated expression of H3K4me3, H3K9me3 and H4K20me3, and their corresponded histone modifying enzymes (SMYD3, SUV39H1 and SUV420H2) suggested that ROS could remodel chromatin structures through changes in histone methylation patterns. ChIP-seq analysis was performed to identify genes that were potentially regulated by H4K20me3 and H3K4me3. The ChIP-seq data demonstrated that genes with low enrichment for inactive chromatin mark H4K20me3 in ROS-treated HCC cells were those involved in DNA repair (e.g., MRE11, BRCA2, MMS22L and RBBP8) and telomere maintenance (e.g., DCLER1B, TERF1 and TERF2). On the other side, genes with high enrichment for active chromatin mark H3K4me3 in ROS-treated HCC cells were those related to EMT and cytoskeleton change (SOS1 and RHOA). For validation, the transcript expression of the mentioned genes (those with low H4K20me3 enrichment and those with high H3K4me3 enrichment) were increased in the ROS-treated HCC cells. For validation in human HCC tissues, H4K20me3, H3K9me3, H3K4me3, RBBP8 were overexpressed in HCC tissues relative to the noncancerous liver tissues. Importantly, the high expression of H4K20me3 was associated with tumor recurrence and poor survival.

The present *in vitro* study was performed in HepG2 and Huh7 cell lines to investigate oxidative stress induction by H₂O₂, a ROS representative. The concentration of H₂O₂ in human body is about 20 - 50 μM depending on tissues or cell types (86). Cell viability of HCC cells against H₂O₂ showed that cells were response to H₂O₂ in

dose-dependent manner. Increasing concentrations of H₂O₂ (40 - 200 μM for HepG2 and 70 - 200 μM for Huh7) were progressively toxic to cells subsequently leading to cells death. Concentrations of H₂O₂ at sub-lethal doses (30 μM for HepG2 and 60 μM for Huh7) were used for further experiments. To induce oxidative stress, cells were treated with H₂O₂ at sub-lethal concentrations for 72 hours. The result showed increased intracellular ROS production and protein carbonyl contents. Cells co-treated with antioxidant (H₂O₂ + TA) showed decreased intracellular ROS production and oxidized protein compared to cell treated with only H₂O₂. Moreover, genes responded to oxidative stress, NRF2 and NQO1, were examined. NRF2 is a transcription factor to regulate expression of antioxidants and detoxification enzymes. NQO1 is the one of promoter region that can be activated by NRF2 (87). Under oxidative stress condition, high level of NRF2 is advantage to cancer cells to induce oncogenic process (88). The present results showed that both NRF2 and NQO1 in H₂O₂ treated cells were up-regulated compared with untreated control. It may suggest that increase in NRF2 and NQO1 expression in HCC cells under oxidative stress condition may be the one important factor to initiate tumor progression. Likewise, H₂O₂-induced oxidative stress in Huh7 showed higher than HepG2 cells, whereas NQO1 exhibited a lower level than that in HepG2 cells. As mentioned above, H₂O₂ concentration that used in Huh7 treatment was higher than in HepG2. It might be implied that Huh7 had higher antioxidative capacity than HepG2 to protect cells from oxidative stress. It could be a reason for the use of higher H₂O₂ concentration in Huh7 cells. In addition, total antioxidant capacity was evaluated by DPPH assay. Co-treatment with TA showed increased level of total antioxidant capacity compared with H₂O₂ alone. Our previous studies reported that H₂O₂ provoked oxidative stress in HepG2 and bladder cancer cells, and antioxidants (TA and N-acetylcysteine) successfully attenuated the oxidative stress, as indicated by increased total antioxidant levels (5, 6, 40, 89). These results indicated that H₂O₂ at sub-toxic concentration induced oxidative stress, whereas antioxidant could reduce the ROS-induced oxidative stress in HCC cells.

It is well recognized that oxidative stress caused by elevated ROS can promote cell proliferation, resistance to cell death, and cell survival (7). ROS also activate oncogene and inactivate tumor suppressor genes in cancer cells leading to cancer

progression through the enhancement of malignant phenotype and EMT regulating (41). We experimentally investigated the role of ROS in HCC progression through EMT. Cells exposed to H₂O₂ showed decreased E-cadherin, but increased α -SMA compared with untreated control. On the other hand, co-treatment with TA restored E-cadherin expression and inhibited α -SMA up-regulation compared with the cells treated with H₂O₂ alone. Previous studies revealed that ROS activated TGF- β leading to EMT promoting via NRF2 signaling (90, 91). According to the current results, we also found increased NRF2 expression under oxidative stress exposure. It might suggest that EMT activated by oxidative stress in HCC cells was partly mediated through NRF2 signaling. However, ROS-induced EMT was known to be regulated through epigenetic regulation. Study by Lim et al. demonstrated that ROS activated hypermethylation of E-cadherin promoter by up-regulation of SNAIL (92). To investigate further aggressiveness of cancer cells, cell migration, invasion and colony formation were investigated in HCC cells. The results showed that ROS promoted cell migration, invasion and colony formation in HCC cells. In contrast, cells co-treated with TA reduced the cell migration, invasion and colony number compared with H₂O₂-treated cells. Based on the present results, Huh7 cells had α -SMA expression, migrated activity and invaded capacity higher than HepG2 cells. Huh7 cells were more aggressive than HepG2 suggesting having higher ability of metastasis than HepG2 cells. These finding clearly indicated that ROS triggered aggressive capability of tumor progression via EMT regulation in HCC cells and antioxidant could inhibit cancer progression in HCC cells. According to literature, elevated ROS has been associated with cancer progression via epigenetic regulation, and most studies investigate that DNA methylation (10). The mechanism of how ROS altered the aberration of histone modifications was not fully understood. Therefore, it is interesting to explore the mechanism of ROS-induced cancer progression in HCC cells through histone remodeling.

The effect of ROS on histone methylations was investigated in HCC cells. Histone methylation mainly occurs in arginine and lysine residues of histone tails, and it is catalyzed by histone methyltransferases. However, lysine methylation is more stable and complex modification of gene expression regulation and it is largely

modified on histone H3 and histone H4 (93). The present results showed that H4K20me3 and H3K9me3, inactive heterochromatin marks, were up-regulated in HCC cells exposed to H₂O₂ compared with untreated control. In the same way, active chromatin H3K4me3 was also up-regulated in HCC cells treated with H₂O₂ compared with untreated control cells. Whongsiri et al. demonstrated that ROS enhanced to chromatin alteration such as H3K9me3, H3K27me3, and H3K4me3 in bladder cancer cells (51). Another study revealed that the levels of H3K27me3 and H3K4me3 were up-regulated by oxidative stress in malignant transforming renal cells (29). Not only ROS affected to histone methylation, but also histone acetylation. Nui et al. found that H₂O₂ increased acetylation of histone H4 proteins in lung cancer A549 cells (31). These data suggested that histone methylation was responsible to oxidative stress in HCC cells. In this study, expression of histone methyltransferase for each chromatin mark (SUV420H for H4K20me3, SUV39H1 for H3K9me3, and SMYD3 for H3K4me3) were investigated. All these histone methyltransferases were elevated in HCC cells exposed to H₂O₂ compared with untreated control. When co-treatment with antioxidant, level of histone methylations and histone modifying enzymes was decreased when compared to H₂O₂ treatment alone. Alteration of histone modifying enzymes was associated with tumor progression in various cancers. Increased SUV420H2 expression was directly related to advanced stage of pancreatic cancer (24). Up-regulated SUV39H1 and H3K9me3 was an important role in HCC development and progression (14). Furthermore, elevated SMYD3 was associated with HCC development in HBV patients (94). The alteration of histone modifying enzymes after exposure to ROS was associated with tumorigenesis and cancer progression in various cancers including lung and renal cancers (29, 30). They demonstrated that oxidative stress provoked transfer of methyl groups to histones enzyme 1 (HMT1) (29). Our data suggested that oxidative stress also enhanced histone modifying enzymes. These results obviously indicated that oxidative stress could activate histone methyltransferase leading to up-regulation of histone methylations while antioxidant could inhibit histone methylation process.

To further clarify the mechanism of ROS-induced histone methylation in HCC cells, ChIP-seq was investigated in both HepG2 and Huh7 cells by immunoprecipitating

H4K20me3 (inactive chromatin) and H3K4me3 (active chromatin). Histone methylation is important part of histone modification that involves in various biological processes including chromatin organization, transcriptional regulation, and DNA damage repair. Alteration of methylation plays an important role in tumor initiation and progression (95). We designed ChIP experiment in two conditions, untreated control and H₂O₂ treatment. According to ChIP-seq analysis, we focused on the protein-coding genes that were associated with H4K20me3 and H3K4me3 enrichments. The enrichments of these H4K20me3 and H3K4me3 marks were largely located at promoter or transcription start site (TSS) of protein-coding genes. The results showed that more than 40% were located at promoter site. On the other hand, less than 5% were located at transcription terminal site (TTS). Then, the identified genes were compared and combined between untreated control and H₂O₂ condition in both HepG2 and Huh7 cells for further analysis. The criteria for selecting genes were followed: ratio of peak score of H₂O₂ to control ≤ 0.5 for H4K20me3 and ratio ≥ 2 for H3K4me3 in both HepG2 and Huh7 cell lines, these genes were chosen for GO analysis and KEGG pathway. Then, genes with significant level of $p < 0.05$ and fold enrichment > 1.5 were grouped.

Genes with less enrichment for H4K20me3 under oxidative stress were predominantly associated with DNA repair pathway and telomere maintenance. MRE11, BRCA2, MMS22L, RBBP8, DCLRE1B, TERF1, and TERF2 were selected to verify by qPCR in H₂O₂-treated HCC cells. Not only these seven genes were investigated, but their complexes or correlated genes in the same signaling cascade were also examined. MRE11 (Meiotic recombination 11) is a subunit of MRE11-RAD50-NBS1 (MRN) complex that has an important role in DNA damage response (96). TP53BP1 (Tumor suppressor p53-binding protein 1) is a key regulator of DNA double-strand break (DSB) repair process, it can bind to damaged chromatin to recruit DSB signaling and repair proteins to the site of DNA damage (97). TP53BP1 is recruited to chromatin surrounding DSB by reading the histone methylation, particularly the recognition of H4K20me2 by its tandem tudor domain (98). Our results showed that the expression levels of MRE11 and TP53BP1 mRNA were increased following H₂O₂ treatment compared with untreated control. MRE11 has been established as a predictive biomarker for muscle-invasive bladder cancer (99). MRE11 expression was elevated in

oral cancer, and it showed positive correlation with tumor size, cancer stages and lymph node metastasis. MRE11 also promoted cell proliferation, migration and invasion (100). Furthermore, Elevation of ROS caused by cisplatin increased MRE11 expression in MDA-AM-231 cells (101). Previous study revealed that TP53BP1 expression, particularly in nucleus, was higher in the high grade of urothelial cancer than that in the low grade (102). Similarly, in esophagus carcinoma, TP53BP1 level was increased in advanced grade of tumors. Furthermore, elevation of TP53BP1 was associated with tumor progression and increased genome instability (103). BRCA1 (Breast-cancer susceptibility gene 1) and BRCA2 are tumor suppressor gene involved in multiple functions including DNA repair, transcription, and cell cycle control (104). This study found that ROS enhanced expression of BRCA1 and BRCA2 in HCC cells. Previous studies have shown that the up-regulation of BRCA1 and BRCA2 was found in tumor with breast, ovarian and brain cancers, and the positive correlation between BRCA1 and BRCA2 expression and survival rate were observed (105-107).

MMS22L (Methyl methanesulfonate-sensitivity protein 22-like) and its complex, TONSL, so called MMS22L-TONSL. The MMS22L-TONSL complex is required to maintain genome integrity during DNA replication by promoting homologous recombinant (HR) repair (108). Our current study demonstrated that H₂O₂ promoted expression of MMS22L and TONSL mRNA in HCC cells. Nguyen and colleagues exhibited that MMS22L-TONSL complex may act as an upstream molecule of anti-apoptosis factors and DNA repair factors, especially p53, and targeting MMS22L-TONSL could be clinically beneficial to avoid the therapeutic resistance of cancer cells (109). MMS22L is highly expressed in lung, esophageal and cervical cancers (110). Furthermore, elevated TONSL was significantly up-regulated in HCC tissues compared to normal liver tissues, and high level of TONSL expression was correlated with advance stage, vascular invasion, elevated serum alpha-fetoprotein expression and worse prognosis (111).

RBBP8 (Retinoblastoma-binding protein 8) is involved in transcription, DNA repair, and a key checkpoint of G1 and G2 phase in cell cycle. RBBP8 plays a role in HR repair, has impairment of which reduces DNA repair fidelity and may promote

genome instability. RBBP8 interacts with MRN complex to initiate HR repair (112, 113). Additionally, RBBP8 is also formed complex with BRCA1 to regulate CHEK1 activation and cell cycle G2/M checkpoint under DNA damage (114). RBBP8 also identified as an candidate oncogene participated in regulating cell cycle (111). Our study found that H₂O₂ can enhance expression of RBBP8 in HCC cells. Recent study demonstrated that up-regulated RBBP8 promoted gastric cancer cell growth and cell migration which might be associated with decreased β -catenin function (112). The other study focused on relation between histone modification and RBBP8. The results showed that RBBP8 recruited histone modifying enzymes to control gene transcription and promote oncogenesis (115). These evidences suggested that RBBP8 can be used as a potential biomarker for assessing cancer prognosis. However, RBBP8 has not been reported in HCC, it is interesting to demonstrate RBBP8 expression in HCC tissues.

p53 is a major tumor suppressor gene and acts as a transcription factor that is activated in response to multiple processes to regulate gene expression that control cell proliferation, senescence, cell death and DNA repair. p53 is the single most altered gene in human cancers, and mutation of p53 presents in approximately 50% of all invasive tumors (116). p21 is a cyclin-dependent kinase regulator, inhibits cell cycle G1/S phase and retinoblastoma protein phosphorylation. p21 is the one of major tumor suppressor genes, but it also promotes oncogenesis (117). p21 has been involved in multiple cellular functions including G1/S cell cycle progression, cell growth, cell stemness and DNA damage (117). Our study demonstrated that p53 and p21 were elevated in HCC cells following H₂O₂ treatment. Elevated p21 expression was induced by p53 under DNA damage or oxidative stress (118). p21 acts as the downstream of p53, and p21 expression was induced by wild-type p53, and it was not associated with mutant p53 (119).

It is obvious that ROS triggered genes associated with DNA repair process including MRE11, BRCA2, MMS22L and RBBP8. It might imply that oxidative stress decreased formation of H4K20me3 on DNA repair pathway in HCC cells. Interestingly, up-regulated RBBP8 might be associated with HCC tumor progression according to the previous studies. The present study is the first study to demonstrate the effect of oxidative stress on RBBP8 in HCC cells. Therefore, RBBP8 was selected

as a candidate gene to further validate using IHC staining in human HCC tissues relative to the noncancerous liver tissues.

DCLRE1B (DNA cross-link repair 1B) plays an important role in protecting telomeres by interacting with the shelterin complex to inhibit DNA damage after replication. Our study demonstrated that H₂O₂ promoted DCLRE1B expression in HCC cells. Depletion of DCLRE1B in mouse fibroblast and human lymphoma cells decreased cell viability after cisplatin (120). Furthermore, decreased DCLRE1B enhanced the response of cisplatin in colorectal cancer cells through epigenetic regulation of lysine-specific demethylase KDM1B (121). Shelterin complex consists of six proteins including TERF1, TERF2, POT1, RAP1, TIN2 and TPP1. Shelterin complex is known as a capping to protect and regulate telomerase (122). This study, TERF1, TERF2 and POT1 was investigated, and the results presented that H₂O₂ provoked TERF2, TERF2 and POT1. In consistence with previous study, oxidative stress activated telomerase in HCC cells leading to elevated proliferation and apoptotic resistance in HCC tissues (58). Elevation of shelterin complex may activate telomerase to protect telomere shortening. However, telomerase activity was not measured in this study. Another study mentions that telomere shortening is contributed to hepatocarcinogenesis and it is presented in the early stages, while telomerase is reactivated in the advanced stages of HCC (123). Nevertheless, the role of epigenetic regulation of telomere has been studied in mouse. Knockout of HMTs such as SUV39H1/2 and SUV420H1/2 led to defective telomere function leading to elevated telomere length and chromosomal instability (124). It is obvious that ROS up-regulated genes associated with telomere maintenance, DCLRE1B, TERF1 and TERF2 in HCC cells. It might imply that oxidative stress decreased formation on telomere maintenance leading to elevated telomere maintenance-associated genes that could preserve telomere length in HCC cells.

According to ChIP-seq data of genes highly enriched for H3K4me3 under oxidative stress condition, biological processes included positive regulation of GTPase activity, regulation of RHO protein signal transduction, cell-cell adhesion, cytoskeleton organization, and cell migration were chosen. SOS1, RHOA and genes related to their signaling pathway were validated using qRT-PCR method.

EMT can be regulated by many growth and differentiation factors including TGF- β , growth factors that act via receptor tyrosine kinases, such as fibroblast growth factor, hepatic growth factor and platelet derived growth factor, and Wnt and Notch proteins. TGF- β has been found to activate both SMAD and non-SMAD pathways that includes both SOS and RHOA cascades. SOS1 is well known to participate in family of guanine nucleotide exchange factors (GEFs) and it is a key regulator of RAS signaling pathway. SOS1 binds to SH3 domain that induces Ras/Raf activation and consequently affects to MEK/ERK transduction in cancer development and progression (125). MEK/ERK might activate activity of MMP2 and MMP9 that leads to break through extracellular matrix and promotes malignancy of tumor (126). The current study found that expression of SOS1 and its downstream, JNK2, c-JUN, and MMP9, were induced by oxidative stress in HCC cells. Consistence with the study by Timofeeva et al, they showed that SOS1 was overexpressed in prostate cancer cells, and it was associated with increased cell migration and invasion (127). These data suggested that elevated SOS1 may be linked to enhanced aggressiveness of tumor cells.

The activation of RHOA in response to TGF- β in turn results in activation of ROCK1, and then ROCK1 activates LIM kinase (LIMK) and radixin, downstream targets of ROCK1, resulting in actin cytoskeletal changes. LIMK has been found to trigger actin polymerization of cofilin (128). Our study showed that H₂O₂ up-regulated RHOA, ROCK1, LIMK and radixin expression in HCC cells. RHOA is up-regulated in a variety of human cancer types and stimulates tumor progression. Wang et al. reported that knockdown of RHOA expression had an antitumor effect in ovarian cancer cells and nude mice (129). Study by Jeong et al. found that RHOA was highly expresses in metastasis colorectal cancer cells and it was associated with invasion of lymph nodes and blood vessels in patients with colorectal cancer (130). Ko et al exhibited that NRF2 regulated cell motility via RHOA-ROCK1 signaling in non-small-cell lung cancer cells (82). Moreover, RHOA was up-regulated in HCC tissues, and RHOA expression was associated with poor prognosis (131).

EMT induced by SMAD signaling has been explored. EMT induced by TGF- β is mediated via activation of SMAD2 and SMAD3. Our data revealed that ROS enhanced expression of SMAD2, SMAD3 and SNAIL. SNAIL, a master transcription

factor of EMT, was induced by TGF- β through SMAD and NF- κ B to promote cancer cells survival, proliferation and EMT in HCC cells (132). As mentioned above, we found that E-cadherin was decreased in HCC cells exposed to ROS, it may be repressed by SNAIL. The study exhibited that SNAIL could demethylate H3K4me₂ at E-cadherin promoter leading to down-regulated E-cadherin (66). Furthermore, previous studies suggested that genes associated with H3K4me₃ were identified during EMT process in prostate cells and activation of H3K4me₃ promoted TGF- β -induced EMT leading to tumorigenesis and progression in prostate cancer cells (133, 134). However, the protein expression of genes associated with SMAD signaling was not evaluated in this study.

Our present evidence supported that increased ROS enhanced SOS1, RHOA and SMAD pathway. It may suggest that oxidative stress increased formation of H3K4me₃ at EMT-related genes that could promote EMT and matrix metalloproteinase via both non-SMAD and SMAD pathway that further led to cancer progression in HCC cells. In this study, it is indicated that ROS-induced EMT in HCC cells could also be regulated by the non-SMAD pathway through the H3K4me₃ regulation.

According to *in vitro* study, the results suggested that inactive (H4K20me₃ and H3K9me₃) and active (H3K4me₃) chromatin were elevated in ROS exposed HCC cells. Moreover, RBBP8, a gene with low enrichment for H4K20me₃ following H₂O₂ treatment based on using ChIP-seq, was found to be obviously up-regulated in H₂O₂-treated cells. There is no report about RBBP8 in HCC before. It was interesting to evaluate the expression of RBBP8 in HCC tissues.

H4K20me₃ expression was significantly increased in HCC tissues, mainly labeled in nuclei, compared with non-cancerous liver tissues ($p = 0.0003$). Previous studies reported that H4K20me₃ were elevated in brain cancer (135), whereas declined in breast (136), lung (137), and colorectal cancers (138). Association between H4K20me₃ and disease progressions, relapse, and overall survival, was explored. High expression of H4K20me₃ (IHC score ≥ 7.3) was significantly associated with tumor relapse ($p = 0.0259$). In addition, association between H4K20me₃ and overall survival was assessed, and patients with high expression of H4K20me₃ (IHC score ≥ 11) had significantly shorter survival than those with low expression of H4K20me₃ (IHC score

< 11) ($p = 0.0306$). These data indicated that overexpressed H4K20me3 was associated with tumor recurrence and poor prognosis in patients with HCC.

The level of H3K9me3, heterochromatin mark, showed significantly increased in HCC tissues compared with noncancerous tissues ($p < 0.0001$). Most of cancers showed increased H3K9me3 expression including brain (139), gastric (140), and colon cancer (141). Increased H3K9me3 expression had been shown in Japanese HCC patients (14). Wang and colleagues revealed that elevated H3K9me3 was induced by hepatitis B virus resulting in HCC development (142). Moreover, the other study exhibited that H3K9me3 were positively correlated with the degree of tumor differentiation and the patients' prognosis (143). For H3K4me3, the IHC results showed that it was significantly overexpressed in HCC tissues compared with noncancerous liver tissues ($p = 0.0001$). In HCC studies, the elevated H3K9me3 and H3K4me3 expression were associated with short survival in HCC patients and with HCC development (14, 35).

To verify the level of RBBP8 expression in HCC tissues, IHC staining was performed. The results showed that RBBP8 was significantly up-regulated in HCC tissues compared with noncancerous liver tissues ($p < 0.0001$). RBBP8 is involved in variety of cancers, but evidence is still controversial regarding its expression. RBBP8 was overexpressed in gastric cancer cells and tissues compared with normal gastric cells and adjacent tissues, respectively (112). In contrast, depletion of RBBP8 expression was associated with poor prognosis in ovarian and breast cancers (144, 145). Furthermore, advanced stage of bladder cancer was associated with the deletion of nuclear RBBP8 protein (146).

Previous studies exhibited that protein carbonyl, oxidized protein, content in plasma from HCC patients was higher than healthy control and oxidative stress indicated by increased expression of 8-OHdG, oxidized DNA, was elevated in HCC tissues relative to noncancerous tissues (6, 40). These results suggested that elevated histone methylations and up-regulation of RBBP8 could be associated with elevated oxidative stress in HCC tissues. These data supported by the study of Whongsiri et al. that showed that expression of histone methylation was correlated with increased

oxidative DNA lesions (51). Therefore, these data may indicate that oxidative stress regulated RBBP8 expression through H4K20me3 regulation.

Conclusion

This *in vitro* study exhibited that H₂O₂, ROS representative, at sub-toxic concentration was able to induce oxidative stress in HCC cells. Oxidative stress provoked the HCC aggressiveness indicated by increases in EMT, migration and invasion. Expression of H4K20me3, H3K9me3, H3K4me3, and histone modifying enzymes in HCC cells were enhanced by oxidative stress. Furthermore, co-treatment with antioxidant inhibited progressiveness of HCC cells, and reversed histone methylation pattern. Expression of H4K20me3 was associated with tumor recurrence and short survival in HCC patients.

Genes lowly enriched for H4K20me3 and genes highly enriched for H3K4me3 in HCC cells under oxidative stress were identified by ChIP-seq. Most of the genes lowly enriched for H4K20me3 identified in H₂O₂-treated HCC cells were genes related to DNA repair (MRE11, BRCA2, MMS22L and RBBP8) and telomere maintenance (DCLER1B, TERF1 and TERF2). In contrast, most of genes highly enriched for H3K4me3 in H₂O₂-treated HCC cells were genes involved in EMT and cytoskeleton change (SOS1 and RHOA). All of the mentioned genes were verified to be up-regulated in the H₂O₂-treated HCC cells. RBBP8 was selected to verify its expression in HCC tissues, and its expression was significantly higher in HCC tissues than the noncancerous liver tissues. Our data suggested that ROS decreased formation of H4K20me3 in DNA repair and telomere maintenance genes, and triggered formation of H3K4me3 in EMT-related genes. These resulted in increased progressivity of HCC under the oxidative stress condition.

Limitation of this study should be mentioned. Only one ChIP-seq experiment was carried out. Validation of selected gene by ChIP-qPCR was not performed. The sample size for IHC staining was relatively small, especially for the paired cases. Only one candidate gene associated with less enrichment for H4K20me3 was selected for validation by IHC staining. Gene associated with the more enrichment for H3K4me3

was not selected for validation. The mechanistic insight into the role of RBBP8 to contribute to ROS-induced HCC progression should be explored in further studies.

Taken together, oxidative stress provoked tumor progression and histone methylation change in HCC. Increased RBBP8 expression in HCC cells exposed to ROS was, at least in part, regulated through a decreased formation of H4K20me3. Histone methylation might be a promising target for HCC prognosis and therapy in the future.



References

1. Hanahan D, Weinberg RA. Hallmarks of cancer: the next generation. *Cell*. 2011;144(5):646-74.
2. Reuter S, Gupta SC, Chaturvedi MM, Aggarwal BB. Oxidative stress, inflammation, and cancer: how are they linked? *Free Radical Biology and Medicine*. 2010;49(11):1603-16.
3. Kryston TB, Georgiev AB, Pissis P, Georgakilas AG. Role of oxidative stress and DNA damage in human carcinogenesis. *Mutation Research/Fundamental and Molecular Mechanisms of Mutagenesis*. 2011;711(1):193-201.
4. Fang J, Seki T, Maeda H. Therapeutic strategies by modulating oxygen stress in cancer and inflammation. *Advanced Drug Delivery Reviews*. 2009;61(4):290-302.
5. Whongsiri P, Pimratana C, Wijitsettakul U, Jindatip D, Sanpavat A, Schulz WA, et al. LINE-1 ORF1 Protein Is Up-regulated by Reactive Oxygen Species and Associated with Bladder Urothelial Carcinoma Progression. *Cancer Genomics-Proteomics*. 2018;15(2):143-51.
6. Ma-on C, Sanpavat A, Whongsiri P, Suwannasin S, Hirankarn N, Tangkijvanich P, et al. Oxidative stress indicated by elevated expression of Nrf2 and 8-OHdG promotes hepatocellular carcinoma progression. *Medical Oncology*. 2017;34(4):57.
7. Gorrini C, Harris IS, Mak TW. Modulation of oxidative stress as an anticancer strategy. *Nature Reviews Drug Discovery*. 2013;12(12):931.
8. Storz P. Reactive oxygen species in tumor progression. *Frontiers in Bioscience*. 2005;10(1-3):1881-96.
9. Giampieri F, Afrin S, Forbes-Hernandez TY, Gasparrini M, Cianciosi D, Reboledo-Rodriguez P, et al. Autophagy in human health and disease: novel therapeutic opportunities. *Antioxidants & Redox Signaling*. 2018.
10. Ziech D, Franco R, Pappa A, Panayiotidis MI. Reactive Oxygen Species (ROS)—Induced genetic and epigenetic alterations in human carcinogenesis. *Mutation Research/Fundamental and Molecular Mechanisms of Mutagenesis*. 2011;711(1-2):167-73.
11. Kanwal R, Gupta K, Gupta S. Cancer epigenetics: an introduction. *Cancer Epigenetics*: Springer; 2015. p. 3-25.
12. Sharma S, Kelly TK, Jones PA. Epigenetics in cancer. *Carcinogenesis*. 2010;31(1):27-36.
13. Cai M-Y, Hou J-H, Rao H-L, Luo R-Z, Li M, Pei X-Q, et al. High expression of H3K27me3 in human hepatocellular carcinomas correlates closely with vascular invasion and predicts worse prognosis in patients. *Molecular Medicine*. 2011;17(1):12-20.
14. Chiba T, Saito T, Yuki K, Zen Y, Koide S, Kanogawa N, et al. Histone lysine methyltransferase SUV39H1 is a potent target for epigenetic therapy of hepatocellular carcinoma. *International Journal of Cancer*. 2015;136(2):289-98.
15. He L-R, Liu M-Z, Li B-K, Rao H-L, Liao Y-J, Guan X-Y, et al. Prognostic impact of H3K27me3 expression on locoregional progression after chemoradiotherapy in esophageal squamous cell carcinoma. *BMC Cancer*. 2009;9(1):461.
16. Kondo Y, Shen L, Issa J-PJ. Critical role of histone methylation in tumor suppressor gene silencing in colorectal cancer. *Molecular and Cellular Biology*. 2003;23(1):206-15.

17. Seligson DB, Horvath S, McBrien MA, Mah V, Yu H, Tze S, et al. Global levels of histone modifications predict prognosis in different cancers. *The American Journal of Pathology*. 2009;174(5):1619-28.
18. Yokoyama Y, Matsumoto A, Hieda M, Shinchi Y, Ogihara E, Hamada M, et al. Loss of histone H4K20 trimethylation predicts poor prognosis in breast cancer and is associated with invasive activity. *Breast Cancer Research*. 2014;16(3):R66.
19. Yu J, Yu J, Rhodes DR, Tomlins SA, Cao X, Chen G, et al. A polycomb repression signature in metastatic prostate cancer predicts cancer outcome. *Cancer Research*. 2007;67(22):10657-63.
20. Sawan C, Herceg Z. Histone modifications and cancer. *Advances in genetics*. 70: Elsevier; 2010. p. 57-85.
21. Pei H, Zhang L, Luo K, Qin Y, Chesi M, Fei F, et al. MMSET regulates histone H4K20 methylation and 53BP1 accumulation at DNA damage sites. *Nature*. 2011;470(7332):124-8.
22. Gong F, Clouaire T, Aguirrebengoa M, Legube G, Miller KM. Histone demethylase KDM5A regulates the ZMYND8–NuRD chromatin remodeler to promote DNA repair. KDM5A promotes DNA repair via ZMYND8–NuRD. *The Journal of Cell Biology*. 2017;216(7):1959-74.
23. McDonald OG, Wu H, Timp W, Doi A, Feinberg AP. Genome-scale epigenetic reprogramming during epithelial-to-mesenchymal transition. *Nature Structural & Molecular Biology*. 2011;18(8):867-74.
24. Viotti M, Wilson C, McClelland M, Koeppen H, Haley B, Jhunjhunwala S, et al. SUV420H2 is an epigenetic regulator of epithelial/mesenchymal states in pancreatic cancer. *Journal of Cell Biology*. 2018;217(2):763-77.
25. Antosova M, Bencova A, Mikolka P, Kosutova P, Mokrá D, Rozborilová E. The markers of oxidative stress in patient with lung cancer. *European Respiratory Society*; 2015.
26. Jo M, Nishikawa T, Nakajima T, Okada Y, Yamaguchi K, Mitsuyoshi H, et al. Oxidative stress is closely associated with tumor angiogenesis of hepatocellular carcinoma. *Journal of Gastroenterology*. 2011;46(6):809-21.
27. Kennedy CH, Mitchell JB. Identification of molecular markers of oxidative stress in human prostate cells. *AACR*; 2004.
28. Sanjyoti B, Melinkeri R. Oxidative stress and antioxidant status in patients of ovarian cancer. *Biomedical Research*. 2011;22(2).
29. Mahalingaiah PKS, Ponnusamy L, Singh KP. Oxidative stress-induced epigenetic changes associated with malignant transformation of human kidney epithelial cells. *Oncotarget*. 2017;8(7):11127.
30. Moodie FM, Marwick JA, Anderson CS, Szulakowski P, Biswas SK, Bauter MR, et al. Oxidative stress and cigarette smoke alter chromatin remodeling but differentially regulate NF- κ B activation and proinflammatory cytokine release in alveolar epithelial cells. *The FASEB Journal*. 2004;18(15):1897-9.
31. Niu Y, DesMarais TL, Tong Z, Yao Y, Costa M. Oxidative stress alters global histone modification and DNA methylation. *Free Radical Biology and Medicine*. 2015;82:22-8.
32. Chitapanarux T, Phornphutkul K. Risk factors for the development of hepatocellular carcinoma in Thailand. *Journal of Clinical and Translational Hepatology*. 2015;3(3):182.

33. Tang A, Hallouch O, Chernyak V, Kamaya A, Sirlin CB. Epidemiology of hepatocellular carcinoma: target population for surveillance and diagnosis. *Abdominal Radiology*. 2018;43(1):13-25.
34. Allaire M, Nault JC. Advances in management of hepatocellular carcinoma. *Current Opinion in Oncology*. 2017;29(4):288-95.
35. He C, Xu J, Zhang J, Xie D, Ye H, Xiao Z, et al. High expression of trimethylated histone H3 lysine 4 is associated with poor prognosis in hepatocellular carcinoma. *Human Pathology*. 2012;43(9):1425-35.
36. Zhang Y, Takahashi S, Tasaka A, Yoshima T, Ochi H, Chayama K. Involvement of micro RNA-224 in cell proliferation, migration, invasion, and anti-apoptosis in hepatocellular carcinoma. *Journal of Gastroenterology and Hepatology*. 2013;28(3):565-75.
37. Bigarella CL, Liang R, Ghaffari S. Stem cells and the impact of ROS signaling. *Development*. 2014;141(22):4206-18.
38. Azad MB, Chen Y, Gibson SB. Regulation of autophagy by reactive oxygen species (ROS): implications for cancer progression and treatment. *Antioxidants & Redox Signaling*. 2009;11(4):777-90.
39. Ha H-L, Shin H-J, Feitelson MA, Yu D-Y. Oxidative stress and antioxidants in hepatic pathogenesis. *World Journal of Gastroenterology*. 2010;16(48):6035.
40. Pongpaiboj P, Whongsiri P, Suwannasin S, Khlaiphuengsin A, Tangkijvanich P, Boonla C. Increased oxidative stress and RUNX3 hypermethylation in patients with hepatitis B virus-associated hepatocellular carcinoma (HCC) and induction of RUNX3 hypermethylation by reactive oxygen species in HCC cells. *Asian Pacific Journal of Cancer Prevention*. 2015;16(13):5343-8.
41. Kumar B, Koul S, Khandrika L, Meacham RB, Koul HK. Oxidative stress is inherent in prostate cancer cells and is required for aggressive phenotype. *Cancer Research*. 2008;68(6):1777-85.
42. Kouzarides T. Chromatin modifications and their function. *Cell*. 2007;128(4):693-705.
43. Jenuwein T, Allis CD. Translating the histone code. *Science*. 2001;293(5532):1074-80.
44. Au SL-K, Ng IO-L, Wong C-M. Epigenetic dysregulation in hepatocellular carcinoma: focus on polycomb group proteins. *Frontiers of Medicine*. 2013;7(2):231-41.
45. Rodríguez-Paredes M, Esteller M. Cancer epigenetics reaches mainstream oncology. *Nature Medicine*. 2011;17(3):330.
46. Kanwal R, Gupta S. Epigenetics and cancer. *Journal of Applied Physiology*. 2010;109(2):598-605.
47. Ning B, Li W, Zhao W, Wang R. Targeting epigenetic regulations in cancer. *Acta Biochimica et Biophysica Sinica*. 2015;48(1):97-109.
48. Fraga MF, Ballestar E, Villar-Garea A, Boix-Chornet M, Espada J, Schotta G, et al. Loss of acetylation at Lys16 and trimethylation at Lys20 of histone H4 is a common hallmark of human cancer. *Nature Genetics*. 2005;37(4):391.
49. Schneider AC, Heukamp LC, Rogenhofer S, Fechner G, Bastian PJ, von Ruecker A, et al. Global histone H4K20 trimethylation predicts cancer-specific survival in patients with muscle-invasive bladder cancer. *BJU International*. 2011;108(8b):E290-E6.

50. Benard A, Goossens-Beumer IJ, van Hoesel AQ, de Graaf W, Horati H, Putter H, et al. Histone trimethylation at H3K4, H3K9 and H4K20 correlates with patient survival and tumor recurrence in early-stage colon cancer. *BMC Cancer*. 2014;14(1):1-9.
51. Whongsiri P, Pimratana C, Wijitsettakul U, Sanpavat A, Jindatip D, Hoffmann MJ, et al. Oxidative stress and LINE-1 reactivation in bladder cancer are epigenetically linked through active chromatin formation. *Free Radical Biology and Medicine*. 2019;134:419-28.
52. Soares LM, He PC, Chun Y, Suh H, Kim T, Buratowski S. Determinants of histone H3K4 methylation patterns. *Molecular Cell*. 2017;68(4):773-85. e6.
53. Ahuja N, Sharma AR, Baylin SB. Epigenetic therapeutics: a new weapon in the war against cancer. *Annual Review of Medicine*. 2016;67:73-89.
54. Ferlay J, Soerjomataram I, Dikshit R, Eser S, Mathers C, Rebelo M, et al. Cancer incidence and mortality worldwide: sources, methods and major patterns in GLOBOCAN 2012. *International Journal of Cancer*. 2015;136(5).
55. Boyle DA. Hepatocellular Carcinoma: Implications for Asia-Pacific Oncology Nurses. *Asia-Pacific Journal of Oncology Nursing*. 2017;4(2):98.
56. Marquardt JU, Andersen JB, Thorgeirsson SS. Functional and genetic deconstruction of the cellular origin in liver cancer. *Nature Reviews Cancer*. 2015;15(11):653.
57. Machida K, Cheng KT-H, Sung VM-H, Lee KJ, Levine AM, Lai MM. Hepatitis C virus infection activates the immunologic (type II) isoform of nitric oxide synthase and thereby enhances DNA damage and mutations of cellular genes. *Journal of Virology*. 2004;78(16):8835-43.
58. Nishikawa T, Nakajima T, Katagishi T, Okada Y, Jo M, Kagawa K, et al. Oxidative stress may enhance the malignant potential of human hepatocellular carcinoma by telomerase activation. *Liver International*. 2009;29(6):846-56.
59. Ito Y, Sasaki Y, Horimoto M, Wada S, Tanaka Y, Kasahara A, et al. Activation of mitogen-activated protein kinases/extracellular signal-regulated kinases in human hepatocellular carcinoma. *Hepatology*. 1998;27(4):951-8.
60. Zhang P, Li K, Shen Y, Gao P, Dong Z, Cai J, et al. Galectin-1 induces hepatocellular carcinoma EMT and sorafenib resistance by activating FAK/PI3K/AKT signaling. *Cell Death & Disease*. 2016;7(4):e2201.
61. Du H, Yang W, Chen L, Shen B, Peng C, Li H, et al. Emerging role of autophagy during ischemia-hypoxia and reperfusion in hepatocellular carcinoma. *International Journal of Oncology*. 2012;40(6):2049-57.
62. Ha T-Y, Hwang S, Moon K-M, Won Y-J, Song G-W, Kim N, et al. Sorafenib inhibits migration and invasion of hepatocellular carcinoma cells through suppression of matrix metalloproteinase expression. *Anticancer Research*. 2015;35(4):1967-76.
63. Zhang Y, Huang J, Li Q, Chen K, Liang Y, Zhan Z, et al. Histone methyltransferase SETDB1 promotes cells proliferation and migration by interacting with Tiam1 in hepatocellular carcinoma. *BMC Cancer*. 2018;18(1):539.
64. Chen Y, Lin MC, Yao H, Wang H, Zhang AQ, Yu J, et al. Lentivirus-mediated RNA interference targeting enhancer of zeste homolog 2 inhibits hepatocellular carcinoma growth through down-regulation of stathmin. *Hepatology*. 2007;46(1):200-8.
65. Lee HS, Jung W, Lee E, Chang H, Choi JH, Kim HG, et al. SIRT7, H3K18ac, and ELK4 immunohistochemical expression in hepatocellular carcinoma. *Journal of Pathology and Translational Medicine*. 2016;50(5):337.

66. Lin T, Ponn A, Hu X, Law BK, Lu J. Requirement of the histone demethylase LSD1 in Snai1-mediated transcriptional repression during epithelial-mesenchymal transition. *Oncogene*. 2010;29(35):4896.
67. Pathil A, Armeanu S, Venturelli S, Mascagni P, Weiss TS, Gregor M, et al. HDAC inhibitor treatment of hepatoma cells induces both TRAIL-independent apoptosis and restoration of sensitivity to TRAIL. *Hepatology*. 2006;43(3):425-34.
68. Whongsiri P, Phoyen S, Boonla C. Oxidative Stress in Urothelial Carcinogenesis: Measurements of Protein Carbonylation and Intracellular Production of Reactive Oxygen Species. *Urothelial Carcinoma*: Springer; 2018. p. 109-17.
69. Chen J, Yu Y, Ji T, Ma R, Chen M, Li G, et al. Clinical implication of Keap1 and phosphorylated Nrf2 expression in hepatocellular carcinoma. *Cancer Medicine*. 2016;5(10):2678-87.
70. Hamamoto R, Silva FP, Tsuge M, Nishidate T, Katagiri T, Nakamura Y, et al. Enhanced SMYD3 expression is essential for the growth of breast cancer cells. *Cancer Science*. 2006;97(2):113-8.
71. Mahalingaiah PKS, Ponnusamy L, Singh KP. Chronic oxidative stress leads to malignant transformation along with acquisition of stem cell characteristics, and epithelial to mesenchymal transition in human renal epithelial cells. *Journal of Cellular Physiology*. 2015;230(8):1916-28.
72. Pasadi S, Muniyappa K. Evidence for functional and regulatory cross-talk between Wnt/ β -catenin signalling and Mre11–Rad50–Nbs1 complex in the repair of cisplatin-induced DNA cross-links. *Oncotarget*. 2020;11(44):4028.
73. Guo G, Li L, Song G, Wang J, Yan Y, Zhao Y. miR-7/SP1/TP53BP1 axis may play a pivotal role in NSCLC radiosensitivity. *Oncology Reports*. 2020;44(6):2678-90.
74. Sibuh BZ, Khanna S, Taneja P, Sarkar P, Taneja NK. Molecular docking, synthesis and anticancer activity of thiosemicarbazone derivatives against MCF-7 human breast cancer cell line. *Life Sciences*. 2021;273:119305.
75. Wang S, Wang H, Sun B, Li D, Wu J, Li J, et al. Acetyl-11-keto- β -boswellic acid triggers premature senescence via induction of DNA damage accompanied by impairment of DNA repair genes in hepatocellular carcinoma cells in vitro and in vivo. *Fundamental & Clinical Pharmacology*. 2020;34(1):65-76.
76. Wang H, Ni J, Guo X, Zhou T, Ma X, Xue J, et al. Shelterin differentially respond to oxidative stress induced by TiO₂-NPs and regulate telomere length in human hepatocytes and hepatocarcinoma cells in vitro. *Biochemical and Biophysical Research Communications*. 2018;503(2):697-702.
77. Xing F, Zhao D, Wu S-Y, Tyagi A, Wu K, Sharma S, et al. Epigenetic and Posttranscriptional Modulation of SOS1 Can Promote Breast Cancer Metastasis through Obesity-Activated c-Met Signaling in African-American Women. *Cancer Research*. 2021;81(11):3008-21.
78. Sun S, Zhu L, Lai M, Cheng R, Ge Y. Tanshinone I inhibited growth of human chronic myeloid leukemia cells via JNK/ERK mediated apoptotic pathways. *Brazilian Journal of Medical and Biological Research*. 2021;54.
79. Kobelt D, Zhang C, Clayton-Lucey IA, Glauben R, Voss C, Siegmund B, et al. Pro-inflammatory TNF- α and IFN- γ promote tumor growth and metastasis via induction of MACC1. *Frontiers in Immunology*. 2020;11:980.

80. Chen R, Cui J, Xu C, Xue T, Guo K, Gao D, et al. The significance of MMP-9 over MMP-2 in HCC invasiveness and recurrence of hepatocellular carcinoma after curative resection. *Annals of Surgical Oncology*. 2012;19(3):375-84.
81. Friel AM, Curley M, Ravikumar N, Smith TJ, Morrison JJ. Rho A/Rho kinase mRNA and protein levels in human myometrium during pregnancy and labor. *The Journal of the Society for Gynecologic Investigation: JSGI*. 2005;12(1):20-7.
82. Ko E, Kim D, Min DW, Kwon S-H, Lee J-Y. Nrf2 regulates cell motility through RhoA–ROCK1 signalling in non-small-cell lung cancer cells. *Scientific Reports*. 2021;11(1):1-9.
83. Wang W, Yang C, Nie H, Qiu X, Zhang L, Xiao Y, et al. LIMK2 acts as an oncogene in bladder cancer and its functional SNP in the microRNA-135a binding site affects bladder cancer risk. *International Journal of Cancer*. 2019;144(6):1345-55.
84. Kobori T, Tameishi M, Tanaka C, Urashima Y, Obata T. Subcellular distribution of ezrin/radixin/moesin and their roles in the cell surface localization and transport function of P-glycoprotein in human colon adenocarcinoma LS180 cells. *PLoS One*. 2021;16(5):e0250889.
85. Zhong F-J, Sun B, Cao M-M, Xu C, Li Y-M, Yang L-Y. STMN2 mediates nuclear translocation of Smad2/3 and enhances TGF β signaling by destabilizing microtubules to promote epithelial-mesenchymal transition in hepatocellular carcinoma. *Cancer Letters*. 2021;506:128-41.
86. Halliwell B, Clement MV, Long LH. Hydrogen peroxide in the human body. *FEBS Letters*. 2000;486(1):10-3.
87. Zhang H, Davies KJ, Forman HJ. Oxidative stress response and Nrf2 signaling in aging. *Free Radical Biology and Medicine*. 2015;88:314-36.
88. Gañán-Gómez I, Wei Y, Yang H, Boyano-Adánez MC, García-Manero G. Oncogenic functions of the transcription factor Nrf2. *Free Radical Biology and Medicine*. 2013;65:750-64.
89. Kloypan C, Srisa-art M, Mutirangura A, Boonla C. LINE-1 hypomethylation induced by reactive oxygen species is mediated via depletion of S-adenosylmethionine. *Cell Biochemistry and Function*. 2015;33(6):375-84.
90. Hiraga R, Kato M, Miyagawa S, Kamata T. Nox4-derived ROS signaling contributes to TGF- β -induced epithelial-mesenchymal transition in pancreatic cancer cells. *Anticancer Research*. 2013;33(10):4431-8.
91. Ryu D, Lee J-H, Kwak M-K. NRF2 level is negatively correlated with TGF- β 1-induced lung cancer motility and migration via NOX4-ROS signaling. *Archives of Pharmacal Research*. 2020;43(12):1297-310.
92. Lim S-O, Gu J-M, Kim MS, Kim H-S, Park YN, Park CK, et al. Epigenetic changes induced by reactive oxygen species in hepatocellular carcinoma: methylation of the E-cadherin promoter. *Gastroenterology*. 2008;135(6):2128-40. e8.
93. Qin J, Wen B, Liang Y, Yu W, Li H. Histone modifications and their role in colorectal cancer. *Pathology & Oncology Research*. 2020;26(4):2023-33.
94. Binh MT, Hoan NX, Giang DP, Van Tong H, Bock C-T, Wedemeyer H, et al. Upregulation of SMYD3 and SMYD3 VNTR 3/3 polymorphism increase the risk of hepatocellular carcinoma. *Scientific Reports*. 2020;10(1):1-8.
95. Meyers RA. *Epigenetic regulation and epigenomics*: John Wiley & Sons; 2012.

96. Bian L, Meng Y, Zhang M, Li D. MRE11-RAD50-NBS1 complex alterations and DNA damage response: implications for cancer treatment. *Molecular Cancer*. 2019;18(1):1-14.
97. Panier S, Boulton SJ. Double-strand break repair: 53BP1 comes into focus. *Nature Reviews Molecular Cell Biology*. 2014;15(1):7-18.
98. Pellegrino S, Michelena J, Teloni F, Imhof R, Altmeyer M. Replication-coupled dilution of H4K20me2 guides 53BP1 to pre-replicative chromatin. *Cell Reports*. 2017;19(9):1819-31.
99. Choudhury A, Nelson LD, Teo MT, Chilka S, Bhattarai S, Johnston CF, et al. MRE11 expression is predictive of cause-specific survival following radical radiotherapy for muscle-invasive bladder cancer. *Cancer Research*. 2010;70(18):7017-26.
100. Wang Y-Y, Chen Y-K, Lo S, Chi T-C, Chen Y-H, Hu SC-S, et al. MRE11 promotes oral cancer progression through RUNX2/CXCR4/AKT/FOXA2 signaling in a nuclease-independent manner. *Oncogene*. 2021;40(20):3510-32.
101. Cheng SM, Lin T-Y, Chang Y-C, Lin I-W, Leung E, Cheung CHA. YM155 and BIRC5 downregulation induce genomic instability via autophagy-mediated ROS production and inhibition in DNA repair. *Pharmacological Research*. 2021;166:105474.
102. Matsuda K, Kawasaki T, Akazawa Y, Hasegawa Y, Kondo H, Suzuki K, et al. Expression pattern of p53-binding protein 1 as a new molecular indicator of genomic instability in bladder urothelial carcinoma. *Scientific Reports*. 2018;8(1):1-9.
103. Ueki N, Akazawa Y, Miura S, Matsuda K, Kurohama H, Imaizumi T, et al. Significant association between 53 BP1 expression and grade of intraepithelial neoplasia of esophagus: alteration during esophageal carcinogenesis. *Pathology-Research and Practice*. 2019;215(11):152601.
104. Yoshida K, Miki Y. Role of BRCA1 and BRCA2 as regulators of DNA repair, transcription, and cell cycle in response to DNA damage. *Cancer Science*. 2004;95(11):866-71.
105. Hedau S, Batra M, Singh UR, Bharti AC, Ray A, Das BC. Expression of BRCA1 and BRCA2 proteins and their correlation with clinical staging in breast cancer. *Journal of Cancer Research and Therapeutics*. 2015;11(1):158.
106. Wang Z, Zhang J, Zhang Y, Deng Q, Liang H. Expression and mutations of BRCA in breast cancer and ovarian cancer: Evidence from bioinformatics analyses. *International Journal of Molecular Medicine*. 2018;42(6):3542-50.
107. Meimand SE, Pour-Rashidi A, Shahrabak MM, Mohammadi E, Meimand FE, Rezaei N. The prognostication potential of BRCA genes expression in gliomas: a genetic survival analysis study. *World Neurosurgery*. 2021.
108. Piwko W, Mlejnkova LJ, Mutreja K, Ranjha L, Stafa D, Smirnov A, et al. The MMS22L-TONSL heterodimer directly promotes RAD51-dependent recombination upon replication stress. *The EMBO Journal*. 2016;35(23):2584-601.
109. Nguyen MH, Ueda K, Nakamura Y, Daigo Y. Identification of a novel oncogene, MMS22L, involved in lung and esophageal carcinogenesis. *International Journal of Oncology*. 2012;41(4):1285-96.
110. Daigo Y, Nakamura Y. From cancer genomics to thoracic oncology: discovery of new biomarkers and therapeutic targets for lung and esophageal carcinoma. *General Thoracic and Cardiovascular Surgery*. 2008;56(2):43-53.

111. Ciriello G, Cerami E, Sander C, Schultz N. Mutual exclusivity analysis identifies oncogenic network modules. *Genome Research*. 2012;22(2):398-406.
112. Yu Y, Chen L, Zhao G, Li H, Guo Q, Zhu S, et al. RBBP8/CtIP suppresses P21 expression by interacting with CtBP and BRCA1 in gastric cancer. *Oncogene*. 2020;39(6):1273-89.
113. Sartori AA, Lukas C, Coates J, Mistrik M, Fu S, Bartek J, et al. Human CtIP promotes DNA end resection. *Nature*. 2007;450(7169):509-14.
114. Yu X, Chen J. DNA damage-induced cell cycle checkpoint control requires CtIP, a phosphorylation-dependent binding partner of BRCA1 C-terminal domains. *Molecular and Cellular Biology*. 2004;24(21):9478-86.
115. Chinnadurai G. CtBP, an unconventional transcriptional corepressor in development and oncogenesis. *Molecular Cell*. 2002;9(2):213-24.
116. Kruiswijk F, Labuschagne CF, Vousden KH. p53 in survival, death and metabolic health: a lifeguard with a licence to kill. *Nature reviews Molecular cell biology*. 2015;16(7):393-405.
117. Xiao B-D, Zhao Y-J, Jia X-Y, Wu J, Wang Y-G, Huang F. Multifaceted p21 in carcinogenesis, stemness of tumor and tumor therapy. *World Journal of Stem Cells*. 2020;12(6):481.
118. Rong J-J, Hu R, Song X-M, Ha J, Lu N, Qi Q, et al. Gambogic acid triggers DNA damage signaling that induces p53/p21Waf1/CIP1 activation through the ATR-Chk1 pathway. *Cancer Letters*. 2010;296(1):55-64.
119. El-Deiry WS, Tokino T, Velculescu VE, Levy DB, Parsons R, Trent JM, et al. WAF1, a potential mediator of p53 tumor suppression. *Cell*. 1993;75(4):817-25.
120. Demuth I, Digweed M, Concannon P. Human SNM1B is required for normal cellular response to both DNA interstrand crosslink-inducing agents and ionizing radiation. *Oncogene*. 2004;23(53):8611-8.
121. Lee YK, Lim J, Yoon SY, Joo JC, Park SJ, Park YJ. Promotion of cell death in cisplatin-resistant ovarian cancer cells through KDM1B-DCLRE1B modulation. *International Journal of Molecular Sciences*. 2019;20(10):2443.
122. Bhari VK, Kumar D, Kumar S, Mishra R. Shelterin complex gene: Prognosis and therapeutic vulnerability in cancer. *Biochemistry and Biophysics Reports*. 2021;26:100937.
123. Oh B-K, Kim H, Park YN, Yoo JE, Choi J, Kim K-S, et al. High telomerase activity and long telomeres in advanced hepatocellular carcinomas with poor prognosis. *Laboratory Investigation*. 2008;88(2):144-52.
124. Blasco MA. The epigenetic regulation of mammalian telomeres. *Nature Reviews Genetics*. 2007;8(4):299-309.
125. Downward J. Targeting RAS signalling pathways in cancer therapy. *Nature Reviews Cancer*. 2003;3(1):11-22.
126. Brown GT, Murray GI. Current mechanistic insights into the roles of matrix metalloproteinases in tumour invasion and metastasis. *The Journal of Pathology*. 2015;237(3):273-81.
127. Timofeeva OA, Zhang X, Ransom HW, Varghese RS, Kallakury BV, Wang K, et al. Enhanced expression of SOS1 is detected in prostate cancer epithelial cells from African-American men. *International Journal of Oncology*. 2009;35(4):751-60.
128. Xu J, Lamouille S, Derynck R. TGF- β -induced epithelial to mesenchymal transition. *Cell Research*. 2009;19(2):156-72.

129. Wang X, Jiang W, Kang J, Liu Q, Nie M. Knockdown of RhoA expression alters ovarian cancer biological behavior in vitro and in nude mice. *Oncology Reports*. 2015;34(2):891-9.
130. Jeong D, Park S, Kim H, Kim C-J, Ahn TS, Bae SB, et al. RhoA is associated with invasion and poor prognosis in colorectal cancer. *International journal of oncology*. 2016;48(2):714-22.
131. Bai Y, Xie F, Miao F, Long J, Huang S, Huang H, et al. The diagnostic and prognostic role of RhoA in hepatocellular carcinoma. *Aging (Albany NY)*. 2019;11(14):5158.
132. Franco DL, Mainez J, Vega S, Sancho P, Murillo MM, de Frutos CA, et al. Snail1 suppresses TGF- β -induced apoptosis and is sufficient to trigger EMT in hepatocytes. *Journal of Cell Science*. 2010;123(20):3467-77.
133. Ke X-S, Qu Y, Cheng Y, Li W-C, Rotter V, Øyan AM, et al. Global profiling of histone and DNA methylation reveals epigenetic-based regulation of gene expression during epithelial to mesenchymal transition in prostate cells. *BMC Genomics*. 2010;11(1):1-15.
134. Naik A, Dalpatraj N, Thakur N. Global Histone H3 Lysine 4 Trimethylation (H3K4me3) Landscape Changes in Response to TGF β . *Epigenetics Insights*. 2021;14.
135. Sepsa A, Levidou G, Gargalionis A, Adamopoulos C, Spyropoulou A, Dalagiorgou G, et al. Emerging role of linker histone variant H1x as a biomarker with prognostic value in astrocytic gliomas. A multivariate analysis including trimethylation of H3K9 and H4K20. *PLoS One*. 2015;10(1):e0115101.
136. Yokoyama Y, Matsumoto A, Hieda M, Shinchi Y, Ogihara E, Hamada M, et al. Loss of histone H4K20 trimethylation predicts poor prognosis in breast cancer and is associated with invasive activity. *Breast Cancer Research*. 2014;16(3):1-13.
137. Van Den Broeck A, Brambilla E, Moro-Sibilot D, Lantuejoul S, Brambilla C, Eymin B, et al. Loss of histone h4k20 trimethylation occurs in preneoplasia and influences prognosis of non-small cell lung cancer. *Clinical Cancer Research*. 2008;14(22):7237-45.
138. Özgür E, Keskin M, Yörüker EE, Holdenrieder S, Gezer U. Plasma histone H4 and H4K20 trimethylation levels differ between colon cancer and precancerous polyps. *In Vivo*. 2019;33(5):1653-8.
139. Venneti S, Felicella MM, Coyne T, Phillips JJ, Gorovets D, Huse JT, et al. Histone 3 lysine 9 trimethylation is differentially associated with isocitrate dehydrogenase mutations in oligodendrogliomas and high-grade astrocytomas. *Journal of Neuropathology & Experimental Neurology*. 2013;72(4):298-306.
140. Xu J, Wang W, Wang X, Zhang L, Huang P. Expression of SIRT1, H3K9me3, H3K9Ac and E-cadherin and its correlations with clinicopathological characteristics in gastric cancer patients. *International Journal of Clinical and Experimental Medicine*. 2016;9(9):17219-31.
141. Yokoyama Y, Hieda M, Nishioka Y, Matsumoto A, Higashi S, Kimura H, et al. Cancer-associated upregulation of histone H3 lysine 9 trimethylation promotes cell motility in vitro and drives tumor formation in vivo. *Cancer Science*. 2013;104(7):889-95.
142. Wang D-Y, An S-H, Liu L, Bai S-S, Wu K-X, Zhu R, et al. Hepatitis B virus X protein influences enrichment profiles of H3K9me3 on promoter regions in human hepatoma cell lines. *Oncotarget*. 2016;7(51):84883.

143. Qian Y, Li Y, Zheng C, Lu T, Sun R, Mao Y, et al. High methylation levels of histone H3 lysine 9 associated with activation of hypoxia-inducible factor 1 α (HIF-1 α) predict patients' worse prognosis in human hepatocellular carcinomas. *Cancer Genetics*. 2020;245:17-26.
144. Quaye L, Dafou D, Ramus SJ, Song H, Maharaj AG, Notaridou M, et al. Functional complementation studies identify candidate genes and common genetic variants associated with ovarian cancer survival. *Human Molecular Genetics*. 2009;18(10):1869-78.
145. Soria-Bretones I, Sáez C, Ruíz-Borrego M, Japón MA, Huertas P. Prognostic value of CtIP/RBBP 8 expression in breast cancer. *Cancer Medicine*. 2013;2(6):774-83.
146. Mijnes J, Veeck J, Gaisa NT, Burghardt E, de Ruijter TC, Gostek S, et al. Promoter methylation of DNA damage repair (DDR) genes in human tumor entities: RBBP8/CtIP is almost exclusively methylated in bladder cancer. *Clinical Epigenetics*. 2018;10(1):1-20.



Appendix



Reagents used in this study

1. 10X PBS, pH 7.4

- 80 g/L NaCl
- 2 g/L KCl
- 14.4 g/L Na₂HPO₄

- 2.4 g/L KH_2PO_4

2. RIPA buffer, pH 7.4

- 6 g/L Tris
- 8.7 g/L NaCl
- 1 g/L SDS
- 1% Triton X-100
- Store at 4°C

3. Reagents for protein carbonyl assay

- 2 N HCl
- 10 mM DNPH in 2 N HCl
- 20% w/v Trichloroacetic acid (TCA)
- Ethanol: Ethyl acetate (1:1 V/V)
- 6 M Guanidine hydrochloride in 0.5 M potassium phosphate, pH 2.5

4. DCFH-DA

- 50 mM DCFH-DA in DMSO
- Store at -20°C
- Working DCFH-DA: 0.5 mM DCFH-DA in serum-free media

5. MTT reagent

- 5 mg/mL MTT in PBS
- Store at -20°C
- Working MTT: 0.5 mg/mL MTT in serum-free media

6. 10X sodium citrate buffer (0.1 M), pH 6.0

- 29.41 g/L Sodium citrate dihydrate
- Store at 4°C
- Working citrate buffer: 1X sodium citrate buffer + 0.05% Tween 20

7. Reagent for western blot analysis

7.1 Separating gel (12% acrylamide for 10 mL)

- H₂O 3.55 mL
- 40% Polyacrylamide 3.75 mL
- 1.5 M Tris pH 8.8 2.5 mL
- 10% SDS 0.1 mL
- 10% APS 0.1 mL
- TEMED 0.005 mL

7.2 Stacking gel (2.5% acrylamide for 5 mL)

- H₂O 3.61 mL
- 40% Polyacrylamide 0.62 mL
- 1 M Tris pH 6.8 2.5 mL
- 10% SDS 0.05 mL
- 10% APS 0.05 mL
- TEMED 0.005 mL

7.3 1X Running buffer

- 3 g/L Tris
- 14.41 g/L Glycine
- 0.1% SDS

7.4 10X Transfer buffer

- 30.3 g/L Tris
- 144 g/L Glycine
- Store at 4°C
- Working transfer buffer: 100 mL 10X transfer buffer + 200 mL methanol
+ 700 mL distilled waster

7.5 10X TBS (Tris-buffered saline), pH 7.6

- 60.6 g/L Tris
- 87.6 g/L NaCl
- Store at 4°C
- Working TBS-T: 1X TBS + 0.1% Tween 20



REFERENCES

จุฬาลงกรณ์มหาวิทยาลัย
CHULALONGKORN UNIVERSITY



จุฬาลงกรณ์มหาวิทยาลัย
CHULALONGKORN UNIVERSITY

VITA

NAME	Miss Suchitra Phoyen
DATE OF BIRTH	30 September 1992
PLACE OF BIRTH	Angthong, Thailand
INSTITUTIONS ATTENDED	Bachelor Degree in Medical Sciences, Naresuan University
HOME ADDRESS	9 Moo. 3 Phosa, Muang District, Angthong Province, Thailand, 14000
PUBLICATION	Whongsiri P, Phoyen S and Boonla C: Oxidative Stress in Urothelial Carcinogenesis: Measurements of Protein Carbonylation and Intracellular Production of Reactive Oxygen Species. <i>Methods Mol Biol.</i> 2018;1655:109-117.
AWARD RECEIVED	Outstanding student of Faculty of Medicine, Chulalongkorn University in the academic year of 2018